TURNER, JACOB R., Ph.D. Geophysical Remote Sensing of North Carolina's Historic Cultural Landscapes: Studies at House in the Horseshoe State Historic Site. (2017) Directed by Dr. Roy S. Stine. 119pp.

This dissertation is written in accordance with the three article option offered by the Geography Department at UNC Greensboro. It contains three manuscripts to be submitted for publication. The articles address specific research issues within the remote sensing process described by Jensen (2016) as they apply to subsurface geophysical remote sensing of historic cultural landscapes, using the buried architectural features of House in the Horseshoe State Historic Site in Moore County, North Carolina.

The first article compares instrument detection capabilities by examining subsurface structure remnants as they appear in single band ground-penetrating radar (GPR), magnetic gradiometer, magnetic susceptibility and conductivity images, and also demonstrates how excavation strengthens geophysical image interpretation.

The second article examines the ability of GPR to estimate volumetric soil moisture (VSM) in order to improve the timing of data collection, and also examines the visible effect of variable moisture conditions on the interpretation of a large historic pit feature, while including the relative soil moisture continuum concepts common to geography/geomorphology into a discussion of GPR survey hydrologic conditions.

The third article examines the roles of scientific visualization and cartography in the production of knowledge and the presentation of maps using geophysical data to depict historic landscapes. This study explores visualization techniques pertaining to the private data exploration view of the expert, and to the simplified public facing view.

GEOPHYSICAL REMOTE SENSING OF NORTH CAROLINA'S HISTORIC CULTURAL LANDSCAPES: STUDIES AT HOUSE IN THE HORSESHOE STATE HISTORIC SITE

by

Jacob R. Turner

A Dissertation Submitted to
the Faculty of The Graduate School at
The University of North Carolina at Greensboro
in Partial Fulfillment
of the Requirements for the Degree
Doctor of Philosophy

Greensboro
2017

Approved by

_____
Committee Chair

APPROVAL PAGE

This dissertation written by Jacob R. Turner has been approved by the following committee of the Faculty of The Graduate School at The University of North Carolina at Greensboro.

Committee Chair_____
Roy S. Stine

Committee Members_____
P. Daniel Royall

_____
Zhi-Jun Liu

_____
Christopher Moore

_____
Date of Acceptance by Committee

_____
Date of Final Oral Examination

ACKNOWLEDGMENTS

Many individuals have contributed time, funding, expertise and moral support toward the completion of this work. At the top of the list is Roy Stine, whose guidance was essential. Roy introduced me to geophysical remote sensing, both in concept and practice. He recognized early that application is key to becoming versed in these methods, and provided many opportunities to work with ground-penetrating radar (GPR) and gradiometer. Roy also made Geography department funds available for the rental of an electromagnetic induction (EMI) meter which was essential to this work. Linda Stine contributed her time, essential equipment (total station, Global Positioning System (GPS) and gradiometer) and archaeological expertise to my scholarly pursuits. Access to House in the Horseshoe and other sites was possible due to the positive relationship that Roy and Linda have with the North Carolina Office of State Archaeology, and North Carolina Historic Sites.

My committee members Dan Royall, Z.J. Liu and Chris Moore also deserve special mention. Each have spent focused time with me, thoughtfully fielding my questions and offering key suggestions for better research and writing that have undoubtedly improved the quality of the articles herein. North Carolina Deputy State Archaeologist John Mintz was also a tireless supporter and informal advisor. John provided access to many of North Carolina's state managed Historic Sites and the state archives, and has given a highly positive profile to my research by arranging public forums, press exposure, and publication in *North Carolina Archaeology*. Fellow

Geography graduate students Stacy Johnson, Ari Lukas, Doug Gallaway, Megan Peters, and Michael Enoch were all key players in helping with fieldwork during all seasons, sometimes with very little notice. Shawn Patch and Sarah Lowry at New South Associates were excellent technical advisors when I was first learning to conduct geophysical surveys, and de-mystified much of the practice, both in the field and in data processing stages. Shawn and Sarah are where the rubber meets the road when it comes to the use of geophysical mapping methods in the world of Cultural Resource Management (CRM). Bruce Young provided much needed assistance reproducing the "Swoopy" diagram in Illustrator. I was granted permission to use the diagram by David DiBiase, whom I would also like to thank here.

Finally, I most gratefully acknowledge the support of my wife, Sandra Kathleen Ziegler Turner. Sandy has been there every step of the way with me through the process of earning this degree, and kept me going when I thought that I was not going to make it to the finish line. Sandy introduced me to the wisdom of the Wood Brothers, and the work of "mysterious forces", often reminding me that "…I am the luckiest man". I am indeed.

TABLE OF CONTENTS

Page

LIST OF TABLES vii

LIST OF FIGURES viii

CHAPTER

I. INTRODUCTION 1

II. A COMPARISON OF GROUND-PENETRATING RADAR, MAGNETIC GRADIOMETER AND ELECTROMAGNETIC INDUCTION SURVEY TECHNIQUES AT HOUSE IN THE HORSESHOE STATE HISTORIC SITE 6

2.1 Introduction 6
2.2 Literature Review 9
2.3 Methods 15
2.4 Results 20
2.5 Discussion 35
2.6 Conclusion 40

III. ESTIMATING VOLUMETRIC SOIL MOISTURE WITH GROUND-PENETRATING RADAR TO IMPROVE SURVEY TIMING AND CULTURAL FEATURE REPRESENTATION IN SLICE MAPS 43

3.1 Introduction 43
3.2 Previous Work 44
3.3 Study Area 52
3.4 Methods 53
3.4.1 Field Methods 53
3.4.2 Lab Methods 57
3.5 Results 59
3.5.1 Excavation 59
3.5.2 Direct Volumetric Soil Moisture Measurements 59
3.5.3 Interpretations of Slice Maps and Vertical Profiles 61
3.5.4 GPR Soil Moisture Estimation 65

3.6 Discussion 70
3.6.1 Different Moisture Conditions and Effects Upon Feature Appearance in Slice Maps 70
3.6.2 Study Limitations and Issues to Overcome for Future Work 72
3.7 Conclusion 75

IV. REPRESENTING THE HIDDEN CULTURAL LANDSCAPE AT HOUSE IN THE HORSESHOE USING GEOPHYSICAL REMOTE SENSING, SCIENTIFIC VISUALIZATION AND CARTOGRAPHIC METHODS 77

4.1 Introduction 77
4.1.1 Geophysical Sensors 78
4.1.2 Scientific Visualization and Cartographic Representation of Survey Data 83
4.2 Previous Work 86
4.3 Methods 87
4.4 Results/Discussion 90
4.5 Conclusion 102

V. CONCLUSION 107

REFERENCES 113

LIST OF TABLES

Page

Table 3.1 Range Gain Settings....56

Table 3.2 Summary Results....62

Table 3.3 Difference in Topp VSM and Directly Measured Average to Depth VSM with Distance From Reflector to Soil Sample....67

Table 4.1 Threshold Values Denoting Anomaly Ranges for Each Sensor....98

LIST OF FIGURES

Page

Figure 2.1 House in the Horseshoe Physiographic and Topographic Context 12

Figure 2.2 Alston House Proposed Kitchen Locations, Baroody (1978) and Hairr (2013) 15

Figure 2.3 House in the Horseshoe Geophysical Survey Area 16

Figure 2.4 Geophysical Survey Results (Turner and Lukas 2016) 21

Figure 2.5 Structure One Rubble from Foundation Identified Within Conductivity and Magnetic Susceptibility Images 22

Figure 2.6 Structure Two Geophysical Results With GPR Vertical Profile and Coinciding Shovel Test Profile Walls 24

Figure 2.7 Structure Three Geophysical Survey Results With GPR Vertical Profiles and Coinciding Test Unit Wall 29

Figure 2.8 Structure Three Test Unit West Wall Profile Showing Historic Pit Zones 31

Figure 2.9 Green Salt Glazed Stoneware In Context at Base of Pit 32

Figure 2.10 Edward or Chester Webster Sherd Confirmed With Known Examples 34

Figure 3.1 House in the Horseshoe Physiographic and Topographic Context 52

Figure 3.2 The Alston House Today 54

Figure 3.3 GPR Survey Area With Soil Core Sample Locations 55

Figure 3.4A. Volumetric Soil Moisture Content of GPR Survey Area Soils Per Given Survey Date 60

Figure 3.4B. Field Capacity (Blue) and Wilting Point (Orange) Values for Different Soil Textures....60

Figure 3.5 All Survey Dates at .50 m Beneath the Surface, GPR Profiles Traverse the Long Axis of the Pit....63

Figure 3.6 All Survey Dates at .50 m Beneath the Surface, GPR Profiles Traverse the Short Axis of the Pit....64

Figure 4.1 The Range of Functions of Visual Methods in an Idealized Research Sequence 84

Figure 4.2 House in the Horseshoe Geophysical Survey Area....88

Figure 4.3 Stages in the Scientific Visualization Process....91

Figure 4.4 Geophysical Survey Results....94

Figure 4.5 House in the Horseshoe Graphical Fusion, Semitransparent Conductivity Over GPR 95

Figure 4.6 Discrete Fusion Example, Binary Sum 97

Figure 4.7 Binary Threshold Example Using Conductivity 100

Figure 4.8 House in the Horseshoe Standing Structures and Buried Structural Remnants....103

CHAPTER I
INTRODUCTION

Traditional remote sensing studies in geography utilize airborne or satellite platforms that most often identify phenomena at the surface of the earth based upon how they reflect incoming solar energy or emit long wave radiation. These works are sometimes include orbital and sub orbital radar, but are mainly constrained to visible and infrared portion of the electromagnetic spectrum. Ground based geophysical remote sensing methods such as ground-penetrating radar (GPR), magnetic gradiometer, and electromagnetic induction (EMI) offer methods of "seeing beneath the soil" in a way that traditional methods do not, using physical properties of the earth, such as magnetic or electrical characteristics, as they vary in the shallow subsurface (Clark 2000).

While the physical characteristics of space recorded in geophysical imagery differ from imagery produced by optical sensors, they are similarly displayed in georeferenced raster images for processing, interpretation, and analysis with other spatial data. The subsurface view makes geophysical sensors a highly useful and complementary source of information for historic landscape research. This includes research topics in historical geography, historical Geographic Information Systems (GIS), or any other geographic work that needs to determine the distribution of something as it appears otherwise unseen beneath the surface. The utility of geophysical subsurface mapping has long been recognized by archaeological researchers and Cultural Resource Management (CRM)

professionals who are using the tools with increasing frequency to detect areas of the subsurface that have been modified by human activity, in recent history and in the distant past. The increasing use of geophysical mapping methods is creating a demand for professionals who are knowledgeable in different survey techniques, interpretation abilities, and who have the skills to present interpretive information in maps and images.

With such a natural fit between the disciplines of geographic remote sensing, Geographic Information Science (GIScience), historical geography and historical GIS, and intense interest within the sister discipline of archaeology, it is perhaps no surprise that interest in geophysical remote sensing is also growing within the discipline of geography. This is most recently evidenced by the interest of the editors of *Southeastern Geographer* in planning a special issue in 2017 featuring studies that use these techniques (Danielle Haskett. Editorial Assistant for Southeastern Geographer. 2016. Personal communication: conversation at SEDAAG annual meeting in Columbia, South Carolina).

While unmanned aircraft systems (UAS) are currently revolutionizing optical remote sensing, a great deal of satellite imagery for geographic research is acquired online, or purchased from the commercial vendors who produce it. Geophysical sensor based research requires planning and data collection effort on the part of those conducting the study to build an image. This means that researchers who want to get a subsurface glimpse using these tools must have access to the instruments, have knowledge of how to conduct controlled data collection efforts with a particular sensor or combination, know how to select appropriate instruments for a particular feature type and environment, and must know the effects of environmental conditions on the output of

surveys. Geophysical remote sensors must also have data interpretation knowledge prior to data collection and processing, so that important information is not missed or removed, and must know how to effectively visualize the results from these sensors so that a variety of non-specialist audiences can understand what the surveys are designed to detect. The prior knowledge of survey techniques and planning that is required of the geophysical remote sensor is far more critical to the outcome of the results than remote sensing using optical imagery not acquired by UAS.

The overarching purpose of this dissertation is to bring subsurface geophysical remote sensing methods into the previously established remote sensing and GIScience research paradigms, by connecting current research issues with the remote sensing process offered by Jensen (2016). This will be accomplished by examining issues in data collection, processing, image interpretation and information presentation as it pertains to using geophysical methods to understanding the buried architectural landscape at House in the Horseshoe State Historic Site, in Moore County, North Carolina.

Jensen (2016) illustrates that the remote sensing process roughly mirrors the scientific method, and is executed in four basic steps, each with different decisions to be made in order to produce information relevant to the project's hypothesis or goals: Statement of the Problem, Data Collection, Data-to-Information Conversion, and Information Presentation. This dissertation is divided into three research articles designed to address issues within the data collection, data to information conversion, and information presentation stages.

The first article compares instrument detection capabilities at House in the Horseshoe by examining subsurface structure remnants as they appear in single band GPR, magnetic gradiometer, magnetic susceptibility and conductivity images, and also demonstrates how excavation strengthens geophysical image interpretation. Each instrument's response to four types of historic structure features and the objects that make the features visible are examined, which contributes to the interpretive knowledge of those who would use these tools to understand historic sites, as well as understanding which instruments are most effective, and in what combination in similar scenarios. In terms of stages in the remote sensing process, the article examines the use of multiple sensors for geophysical data collection, what each records, and how results of geophysical surveys can be interpreted in conjunction with the historical record of a site. This emphasizes the role of ground truthing and interpretation in the data-to-information conversion stage.

The second article is designed to explore data collection issues and potential abilities of a single sensor, GPR. GPR measures subsurface contrasts in relative dielectric permittivity, which is known to vary based upon the amount of water present in the soil during a given survey (Conyers 2012, Conyers 2013a, Conyers 2013b). Differences in water holding capacity between features of interest and surrounding soil are known to play a role in determining what is visible to GPR, which indicates that timing of GPR surveys according to optimal soil moisture conditions can be critical to getting interpretable results (Conyers 2004, Rogers et al. 2012). Despite this, no previous works attempt to indicate the actual volume of water in the soil when cultural features are the

focus of the work. Soil hydrology studies using GPR have explored the instrument's potential for measuring soil moisture conditions directly. This study explores the effectiveness of estimating soil moisture using hyperbolic reflections in GPR data under highly varying soil moisture conditions, from wilting point to soils approaching saturation. In addition, the study observes the effect of the varying volumetric soil moisture conditions on the appearance of a large historic pit feature in GPR profiles and horizontal slice maps. These questions are examined to determine the proper timing of GPR surveys following rainfall in similar contexts for imaging historic pit features, and to determine the effectiveness of using GPR to estimate soil moisture for other non-cultural works as well.

The third article examines the process of creating information about the former locations of historic structures by interactively visualizing raw geophysical data, and the effective presentation of data to multiple audiences. This article illustrates the processing chain of geophysical data from GPR, magnetic gradiometer, magnetic susceptibility, and conductivity survey, the role of interactive visualization and classification, side by side interpretation and presentation, fusion into a single image using the GIS based Boolean combination and semitransparent overlay methods of Kvamme (2006), so that all building remnants can be visualized in the same image. Finally this article explores how the interactive interpretation of a sensor's data distribution curve makes possible the creation of cartographic objects that can be used to identify historic buildings in a traditional map that is intended for both expert and non-expert viewers.

CHAPTER II

A COMPARISON OF GROUND-PENETRATING RADAR, MAGNETIC GRADIOMETER AND ELECTROMAGNETIC INDUCTION SURVEY TECHNIQUES AT HOUSE IN THE HORSESHOE STATE HISTORIC SITE

This chapter is a manuscript prepared for submission to *Journal of Archaeological Science: Reports*

2.1 Introduction

In the spring of 2013, the University of North Carolina at Greensboro (UNCG) Geography and Anthropology faculty were invited by officials at the North Carolina Department of Natural and Cultural Resource to lead fieldwork at House in the Horseshoe State Historic Site. A mutually beneficial partnership formed between institutions as a result, with the overarching goals of learning noninvasive geophysical techniques to understand cultural landscapes of the past, while serving site specific management and academic research needs. In a pre-fieldwork consultation, the site manager informed the UNCG remote sensing team of specific questions that might be answered with noninvasive geophysical methods. It has long been surmised that the site contains burials associated with an American Revolution skirmish that occurred there in 1781 (Caruthers 1854). The manager also indicated that the former location of the main house external kitchen was in question, as well as the locations of many other structures

associated with the site's history as an agricultural plantation. Previous archaeological work and historical studies at House in the Horseshoe provided a background upon which geophysical survey and ground truthing could build (Baroody 1978, Harper 1984, Willcox 1999)

The research tested ground-penetrating radar (GPR), and magnetic gradiometer, in addition to magnetic susceptibility and conductivity images produced using an electromagnetic induction meter. The surveys offered an opportunity to evaluate how each instrument resolves structural remnants, supported by ground truthing confirmation. It was anticipated that the evaluation of effective sensor combinations used in a fine sandy loam would allow the determination of how many instruments are necessary, and which to select for future work in similar contexts where a map of the buried architectural landscape is sought.

GPR transmits electromagnetic energy into the ground in the MHz to GHz range, recording the returning signal time in nanoseconds, and its amplitude within a given observation time window. The velocity of transmitted energy changes at interfaces in the subsurface where materials vary in their ability to allow the incoming energy to pass (Conyers 2013a). The changes in velocity generate a return wave, recorded in the time window, and delineate objects where the water holding capacity or soil compactness is different from the surrounding soil matrix (Conyers 2013b).

A gradiometer is a specially configured type of magnetometer that measures variation in magnetism in the shallow subsurface, in units of nanoTesla (nT) (Clay 2001, Aspinall et al. 2009). The measurement is achieved with two magnetometers vertically

separated by a given distance, in which the difference between the surface detector and the upper detector is calculated. When the values approach zero, there is no local difference in magnetic field strength. Quantifiable differences in local magnetism that are of interest to archaeological mapping occur where objects or soils contain iron (Clark 2001, Dalan 2006, Aspinall et al. 2009). Objects are potentially visible where a permanent, persistent and independent magnetic field exists (refined iron objects in manmade materials, or thermoremnant bricks and soils magnetized by exposure to intense heat), or where soils with iron compounds display a greater temporarily induced magnetism (magnetic susceptibility) than their surrounding matrix (pits, trenches, ditches, heat-exposed soils) that would not otherwise exist without the presence of the earth's magnetic field (Clark 2001, Dalan 2006, Kvamme 2008, Aspinall et al. 2009).

The latest generation of EMI instruments with close coil spacing (~1 m) are able to measure two quantities simultaneously: soil electrical conductivity (in milisiemens per meter or ms/m), and magnetic susceptibility (ratio of primary to secondary field, in parts per thousand or ppt) (Doolittle and Brevik 2014, Geonics Limited 2015). This is accomplished via sending and receiving coils horizontally separated by a given distance (0.5 to 1 m). An electromagnetic field is generated in the sending coil which penetrates the ground, which in turn, induces a secondary electrical current in the subsurface that varies spatially in intensity based on the conductive properties of soil and the objects within it. Variations in soil conductivity are largely driven by the amount of water present, which is mostly determined by the amount of available pore space and recent rainfall history (Grisso et al. 2009). Due to this relationship, the instrument can be used to

measure both horizontal and vertical variations in soil texture (Geonics Limited 2015). It is a useful tool for archaeological sites where earthworks are, or were, a dominant feature on the landscape, or where structural underpinnings or other large solid objects create discontinuity in the ability of soil to conduct electricity (Clay 2006). The magnetic susceptibility of soils measured by this instrument is derived from a directly induced magnetic field, rather than utilizing the earth's ambient magnetic field as the gradiometer described does. Also, EMI measured magnetic susceptibility reveals only contrasts in the temporarily induced magnetic qualities of the subsurface, and is not sensitive to objects that present permanent magnetic fields (Dalan 2006). As such, it is able to detect the same magnetic susceptibility contrast features that appear to the gradiometer, but does not respond to objects with permanent magnetic fields. While each sensor discussed has a proven record of success when used by itself to identify archaeological features (Johnson 2006), Clay (2001) wrote that two instruments are always better than one.

2.2 Literature Review

Different sensors complement one another because they measure different physical characteristics, or dimensions of the subsurface (Clay 2001, Kvamme et al. 2006, Ernenwein 2009). Johnson (2006:12) explains further, stating that in terms of archaeological feature detection abilities, "Not only do the different instruments detect different things, but often they see the same things differently." This basic wisdom pertaining to archaeological geophysics is evident in current research efforts (Stine and Stine 2014, Patch 2016, Thompson et al. 2016).

Archaeological feature type and site conditions determine geophysical visibility of features, and therefore suggest which sensor or sensor combination is likely to perform best in a given context, but economic factors and instrument availability also often play a dominant role in choosing instruments for subsurface imaging (Clay 2001, Thompson et al. 2016). Gradiometer and GPR are often chosen as an instrument pair (Stine et al. 2013, Patch 2016), as are conductivity and magnetometer (Clay 2001), ultimately because of their complementary nature in a wide variety of contexts. Magnetic susceptibility surveys display only induced magnetism, and can be used in conjunction with magnetometer or gradiometer surveys to determine which features are displaying temporary magnetic characteristics and which are permanent (Dalan 2006, Ernenwein 2009). Kvamme's (2006) work that placed emphasis on integrating several geophysical datasets into a single image pushed the number of instruments to include EMI (yielding conductivity and magnetic susceptibility), GPR, magnetic gradiometer, resistivity, and thermal infrared photography. His study utilized more datasets than most prospection work because of its fusion method testing goals.

Thompson et al. (2016) observe that geophysical remote sensing is most often applied to the understanding of prehistoric sites, with fewer examples of peer reviewed historic site studies, but also notes that the volume of literature in this area is growing. While this may be the case, multiple instrument geophysical research and workshops on multi-period American historic sites have been funded in the past by the National Park Service (Stine et al. 2013), and the affiliated National Center for Preservation Technology and Training (Watters 2012). The ultimate goals of these works are site preservation,

landscape research and training in geophysical and 3D research methods, while contributing new knowledge to site managers about the layout and history of a site (Stine and Stine 2014, Curry et al. 2016). The multi-agency collaboration and multiple instrument survey at House in the Horseshoe is similar in its broadest goals of education and historic landscape research, and to contribute to the literature by examining which instruments best detect historic site features in a fine sandy loam soil textural context, and in what combination.

The House in the Horseshoe is a state-managed Colonial/Antebellum period historic site located at the southern edge of the Piedmont in Moore County, North Carolina (35.466667 N, 79.383333 W) (Figure 2.1). The house sits on the edge of a hill in the center of a great horseshoe-shaped bend in the Deep River, 56 km above its confluence with the Haw River at Mermaid Point. The house is approximately 26.5 m above the river channel due west (97.5 m above mean sea level), overlooking wide floodplains which historically and currently are used for agricultural purposes (Willcox 1999). Soils within the flat, open hilltop geophysical survey area are generally classified as Masada fine sandy loam, two to eight percent slopes. Soils within this series typically display 0.23 m of fine sandy loam at the surface, immediately underlain by a thick clay horizon down to 1.14 m, followed by gravelly sandy clay loam down to 2.03 m beneath the surface. Depth to the water table and restrictive natural features are reported by the survey as deeper than 2.03 m (USDA NRCS 2017).

The House in the Horseshoe, also known as the Alston House, is perhaps most notable as a historic landmark that bears the scars of the American Revolution.

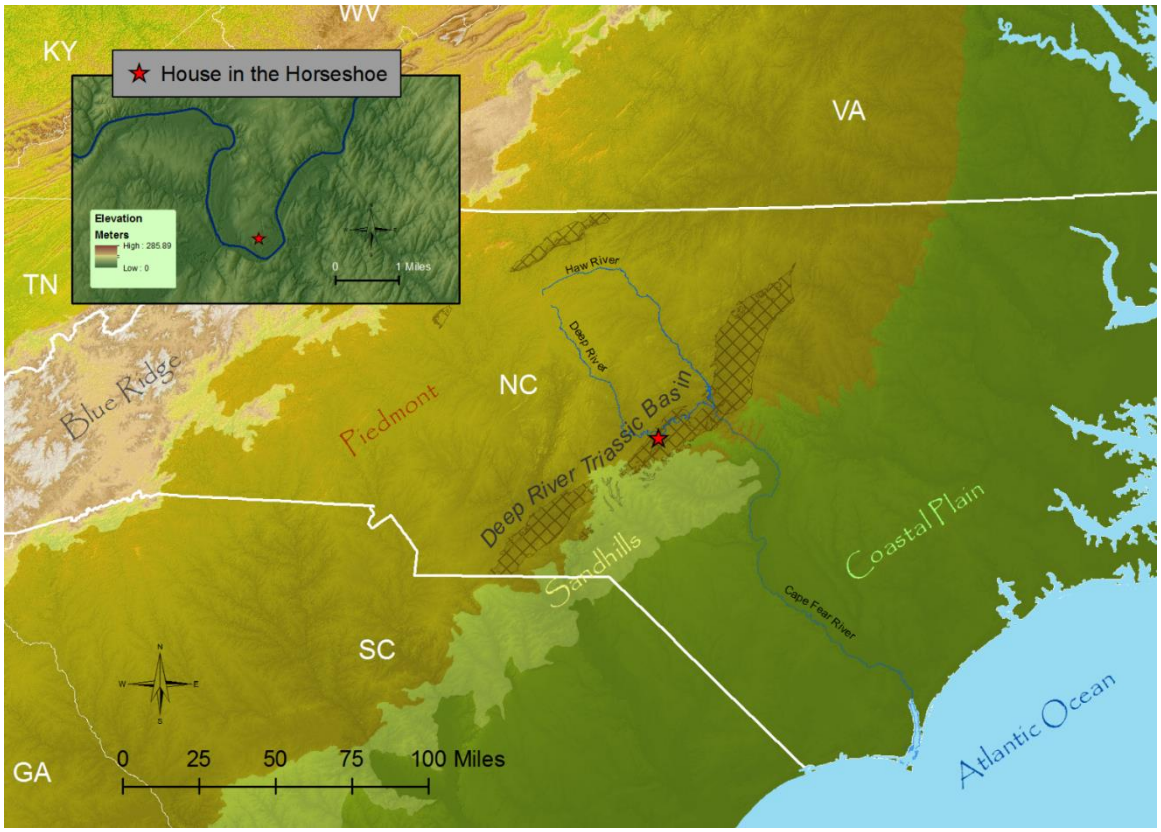

Figure 2.1. House in the Horseshoe Physiographic and Topographic Context

The house was built in 1772 or 1773 for Patriot militia colonel Philip Alston (Willcox 1999). Colonel Alston was very active and forceful in gathering support for the Whig movement in the Deep River counties of the North Carolina Piedmont. He was attacked while inside the house with his wife, children and a small group of his militiamen present on Sunday July 29th 1781, by a small rival Loyalist group lead by Colonel David Fanning (NC Historic Sites 2017). While the Alston family survived the confrontation unscathed, oral history states that eight individuals were buried "…on the brow of the hill, a few rods from the house" the day following (Caruthers 1854:189). Today, evidence of the

confrontation still exists, but only in the form of musket ball holes visible in the structure's wooden siding and interior. The location of the buried soldiers is not known.

While its association with the American Revolution may be the largest attraction to the site, the historical research of Willcox (1999) explains that the Alston House has also served as the center of a slave managed agricultural plantation throughout the occupation of many of its early owners. Alston was a major landowner in the Deep River region in 1780 (2,500 acres) and operated from the house as a planter with a group of twenty slaves as did his successor, Thomas Perkins. North Carolina multi-term Governor Benjamin Williams bought the house and lands from Perkins in 1798, remarking in his correspondence that Perkins had run a successful plantation for many years with as many as eighty slave hands. Governor Williams's tenure as owner of House in the Horseshoe was the "pinnacle" of the house's existence (Willcox 1999:314), expanding the original structure with additional wings and outbuildings, and pushing the productivity of the surrounding lands to their optimal agricultural potential. Such productivity was only possible through the use of enslaved laborers, which the United States Federal Census suggests were 103 in number at the plantation in 1810 (HeritageQuest 2017).

Emily Burke noted that southern plantations have "…as many roofs as rooms" (Burke 1850, Vlach 1993:77). The most detailed record of such structures built at House in the Horseshoe are written in Governor Williams' correspondence, which describe the partial construction and dimensions of a granary, stable, weaving house, smokehouse, and carriage house, as well as the intent to build two other houses, two gardens, a cotton house, and a platform for loading wagons (Willcox 1999, Baroody 1978). However, no

map of his constructions, or those of Alston are known to exist (Harper 1984). Further, none of the Horseshoe plantation descriptions in the exhaustive work of Willcox (1999) describe the location of slave housing that must have existed nearby. Other families have lived on the grounds throughout the years, each altering, building, or dismantling the outbuildings surrounding the house, and altering the house itself, according to their needs (Baroody 1978, Willcox 1999).

Baroody (1978) conducted an archaeological survey to increase the knowledge of the historic architectural landscape at House in the Horseshoe. The work included the use of oblique infrared aerial photography of the site, in conjunction with powered auger tests and systematic probe survey. The results of this investigation produced two sets of maps: one displaying positive auger tests, and the other depicting characteristics of the physical resistance met (e.g. crunchy area) as a metal probe was pushed into the ground at a given location. The field report and maps indicate that two likely locations for a granary were discovered at the northern edge of the survey area via probing, as well as a buried gravel walkway that in part suggests the previous location of a building, possibly a privy. A possible kitchen location was discovered west of the house, marked by subsurface charcoal layering and the presence of brick rubble. The report states that a kitchen building burned to the ground in 1804, but with no historical sources to support this claim, or any other discussion of details. The report also states that most outbuildings probably existed outside of the state managed grounds, and are very likely to have been disturbed by industrial farming equipment.

Figure 2.2. Alston House Proposed Kitchen Locations, Baroody (1978) and Hairr (2013)

2.3 Methods

The site manager in 2013, John Hairr, suggested that the UNCG research team survey the open area northwest of the house in search of the eight individuals who may be buried there, while simultaneously gathering information about any buried architectural features associated with the plantation. Additionally, Hairr surmised that the Alston House kitchen may have existed on the side of the house facing east, away from the river, not in the area proposed by Baroody in 1978 shown in Figure 2.2.

Figure 2.3. House in the Horseshoe Geophysical Survey Area

With these goals in mind, the UNCG geophysical research team established a survey grid with 10 m^2 data collection units in the northeast and eastern portion of the yard, as well as a smaller detached survey area established to investigate the kitchen area proposed by Hairr, totaling 2840 m^2 (Figure 2.3). UTM co-ordinate solutions were obtained by static Global Positioning Systems (GPS) data collection for two points onsite, using a Topcon GR3 GPS antenna in conjunction with The National Geodetic

Survey Online Position User Service (OPUS). These points were used to tie the data collection grid and total station mapping to the NAD 83 (2011) horizontal datum and elevations to NAVD88. These methods allowed all geophysical surveys to be georeferenced with a high degree of positional accuracy, and enabled the resulting images to be viewed in a Geographic Information System (GIS) with other spatial data.

Geophysical survey instruments included a GSSI SIR 3000 GPR equipped with a three wheel survey cart, 400 MHz antenna and survey encoder for distance and depth calculation, a Bartington 601 dual sensor gradiometer, and a Geonics EM38 MK 2 electromagnetic induction meter. The EM 38 collected conductivity and magnetic susceptibility data simultaneously using the 1 m coil separation in vertical dipole mode. Transect lines were placed at 0.5 m intervals with a density of 8 samples/m for gradiometer and EMI data, and 50 traces/m for GPR data collection.

Following surveys, raw data from each sensor were processed using software designed to address data collection issues and processing needs unique to each instrument. Gradiometer data was processed in TerraSurveyor v3.0.29.1 (DW Consulting, Barneveld, The Netherlands), and included a contrast stretch to two standard deviations, zero mean traverse to match the background values for each grid square, destaggering to correct transects for variations in operator pace, destripe to color balance adjacent transect lines not corrected by the zero mean function, resample to 0.125 m to match the data collection density, and a low pass filter to smooth the image. The processed composite was then exported to ASCII raster format for import and georeferencing in ArcGIS v 10.3.1 (Environmental Systems Research Institute, Redlands California)

All GPR profiles were processed and interpreted using RADAN v7.3.13.1227 (Geophysical Survey Systems Inc. Nashua, New Hampshire) software, which links vertical profile data of the subsurface with a horizontal slice view, also forming a 3D data cube for on-screen interpretation. Processes used to correct and clarify radar profiles included time zero adjustment to determine the location of the surface, background removal to remove antenna ringing, estimation of signal velocity for each collection date using hyperbolic reflectors, conversion of profile vertical scale from time to depth using the average velocity determined for each date, and a band pass filter that retained all frequencies between 200 to 600 MHz. A depth slice of 0.30 m was determined by interactively adjusting the visible depth of the combined GPR data collection areas, so that modern reflective debris, roots, or rodent burrows in the plow zone would be excluded as much as possible, and the clearest view of all potential structural features and other areas of interest could be presented in the same image. The composite slice was then exported to a comma separated values (.CSV) file for interpolation via ordinary kriging in Surfer v 10.7.972 (Golden Software Inc. Golden, Colorado), where a 0.125 m pixel resolution was imposed, as well as a low pass filter to remove small spikes in the data before importing and georeferencing in ArcGIS.

All raw EMI data were first processed using DAT38MK2 v1.12 (Geonics Limited, Mississauga, Ontario, Canada), which allowed the files to be converted to a text file, bad transect lines to be removed, line limits set, and data to be split into separate magnetic susceptibility and conductivity ASCII raster grids. Both data sets were then processed in Surfer using ordinary kriging interpolation, with a 0.125 m pixel resolution

set to match the instrument data density settings of 8 samples/m, also matching the resolution of the other images, and receiving the same low pass filter. Both images were then exported to ASCII raster, and were then imported and georeferenced in ArcGIS.

All data layers were interpreted together in ArcGIS, where they were examined for evidence of the Alston House kitchen, other outbuildings, and for potential burial locations. Several spatial data sources were used to aid in the interpretation of geophysical imagery, including historic aerial photography from the Moore County North Carolina GIS website, scanned and georeferenced map documents on file at the North Carolina Historic Sites Division of Archives created by Baroody (1978), oblique infrared aerial photography captured during the Baroody investigation in September of 1978, oblique aerial infrared photography captured in 1987, as well as the written report of Baroody's field work (Baroody 1978), and site history written by Willcox (1999).

A selection of anomalies visible within the images were chosen for investigation in the field. The co-ordinate position of each anomaly was noted while displayed in ArcGIS, and was subsequently marked on the lawn using a total station and plastic pin flag markers. The locations were investigated using a metal detector with assistance from Mac McAtee of Old North State Detectorists, metal probe, bucket auger, one 0.5 m^2 controlled shovel test excavated by natural levels, and two contiguous 1 m^2 excavation units also excavated by natural levels. All shovel test and test unit excavation data were recorded in level forms, profile drawings and photographs. Soil textures were determined by feel, and colors were assigned from moist samples taken from excavation levels and profiles using Munsell Soil Color Charts (2013). Ceramic artifacts were identified and

assigned a date range according to those used by the North Carolina Office of State Archaeology laboratory, which was compiled from Miller et al. (2000) and the Florida Museum of Natural History digital type collection (Emily McDowell, Research Laboratory Supervisor, Office of State Archaeology Research Center. 2016. Personal communication: email). Assistance with local stoneware identification and dating was given by Hal Pugh of New Salem Pottery. Mean ceramic dates were calculated according to the method established by South (2002). Nails were evaluated using the typology and date ranges established by Nelson (1968).

2.4 Results

The surveys revealed the location of four areas where structures were potentially located (Figure 2.4) (Turner and Lukas 2016). Of the four structures, field investigation by probe and auger revealed that remnants of structures one and four were contained within the plow zone, close to the surface. Shovel test excavation of Structure Two and test unit excavation of Structure Three revealed intact archaeological deposits, with the Structure Three anomalies appearing in the area indicated by Hairr to be a possible kitchen site (2013 personal communication). Evidence of a mass burial excavation or individual shafts were not evident in any of the four images of the total survey area, or in radar vertical profiles. Structure One was visible to all sensors used in the study as a 7.16 m sided square shed or small house foundation. Probing revealed brick and stone foundation fragments at the surface just beneath the grass (Figure 2.5).

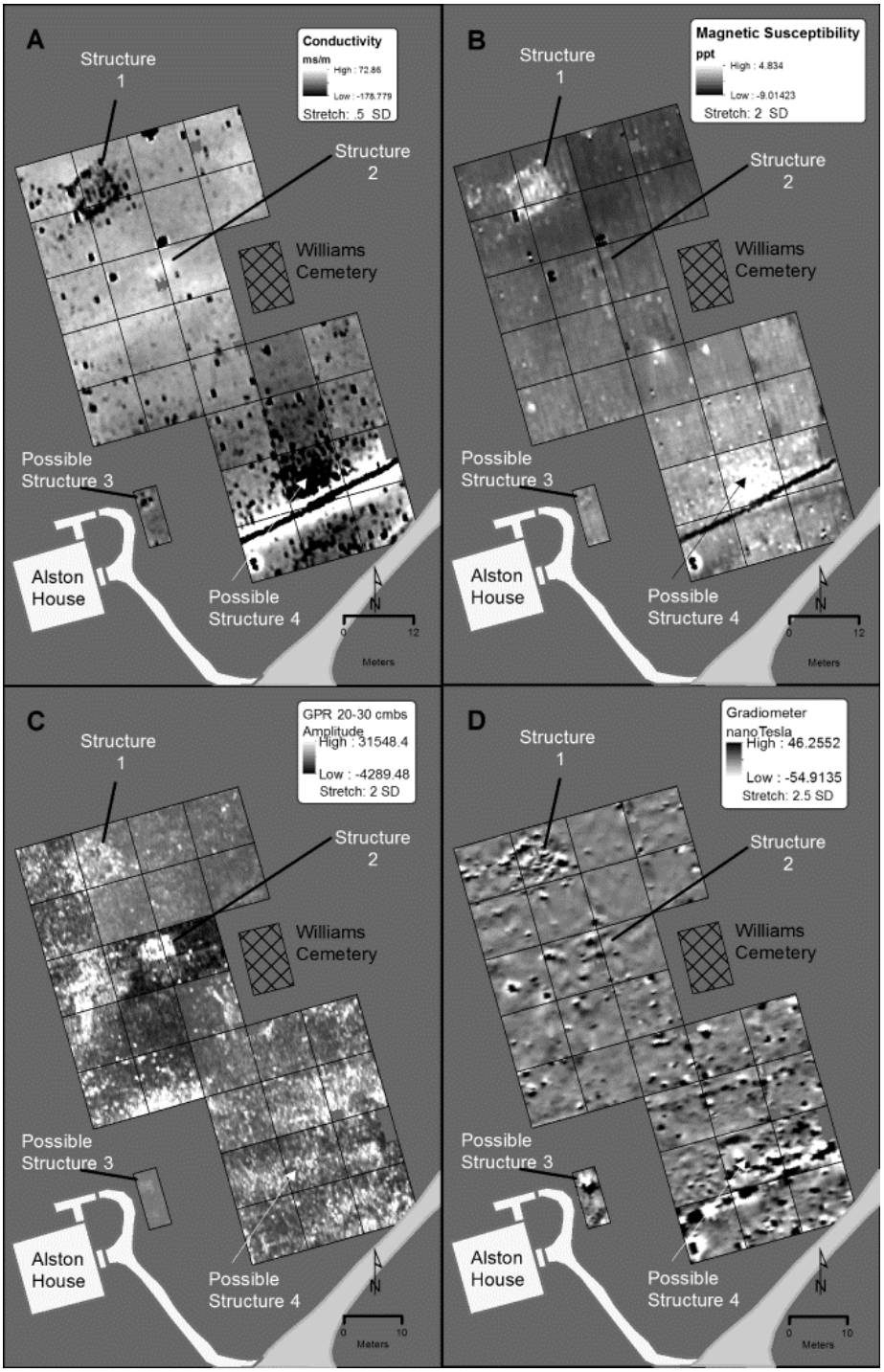

Figure 2.4. Geophysical Survey Results (Turner and Lukas 2016).
A. Conductivity B. Magnetic Susceptibility C. GPR D. Magnetic Gradiometer

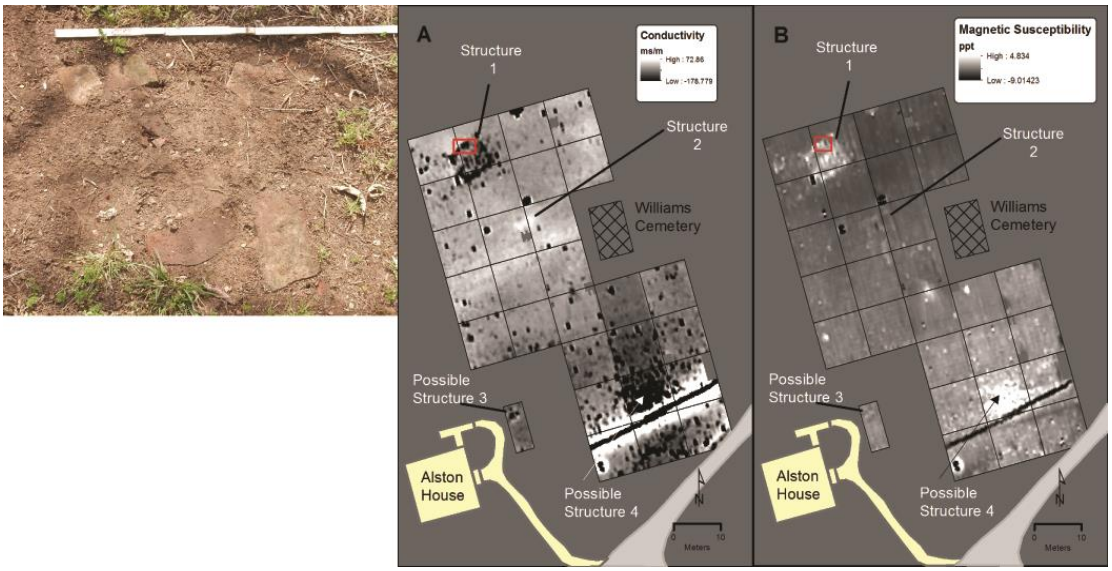

Figure 2.5. Structure One Rubble From Foundation Identified Within Conductivity and Magnetic Susceptibility Images

The brick and stone were lower in conductivity than the matrix in which they were buried, causing the meter to record slightly negative values (0 to -10 millisiemens per meter (ms/m)) compared to the range of background values (4 to 6 ms/m) for the surrounding soils (Figure 2.4A and Figure 2.5A). The rectangular pattern of foundation material as it appeared in magnetic susceptibility readings was indicated by high values (approx. 1.15 to 1.9 parts per thousand (ppt)) compared to the surrounding matrix (0.77 to 0.90 ppt) (Figure 2.4B and Figure 2.5B). The pattern of higher magnetic susceptibility associated with the foundation was due to the presence of decomposing bricks, and likely small metal objects decomposing in the area soils. GPR was also able to image the brick rubble, capturing the general shape of the foundation as a pattern of reflective objects forming a square (Figure 2.4C). The gradiometer displayed a linear dipolar region at the structures northern boundary with an intensity that may have been caused by the

concentration and shallow burial of the brick materials, or may indicate that a portion of the house burned (Figure 2.4D) although no charcoal was apparent at the surface. A building was visible in in 1939 and 1950 aerial photos, and absent during the 1966 series. This suggests that it was removed during the restoration of the house that began sometime in 1954 (Willcox 1999).

Structure Two was discovered primarily due to its appearance in the GPR slice map as a high amplitude rectangle shape, approximately 5.79 by 3.35 m. The distinct shape is visible in the 0.2 to 0.3 m depth slice of the GPR survey results (Figure 2.4C), and is displayed in greater detail in Figure 2.6A (GPR depth slice zoom with color) and Figure 2.6A-1 (GPR vertical profile). No structural remains were evident in this area of the yard during the review of historic aerial photography, archival oblique infrared imagery, the maps of Baroody's (1978) investigation, or during the time of the UNCG geophysical fieldwork. Baroody (1978) indicated that this area was not probed or tested at the time of his investigation because it was thought to be the previous location of a pond. The gradiometer data complemented the GPR maps, displaying five post or pier-like magnetic dipoles appearing along the structure boundary, as well as a slight positive increase in values in the 5 to 11 nT range in contrast with the near zero background (Figure 2.6B). This rise in nanoTesla values was coincident with the edges of the feature as displayed in the GPR image (Figure 2.6A). Conductivity maps of Structure Two indicated a slight increase in values in the center of the structure (8 to 9.5 ms/m) compared to the surrounding values (~6 ms/m)(Figure 2.6C), likely due to the increased

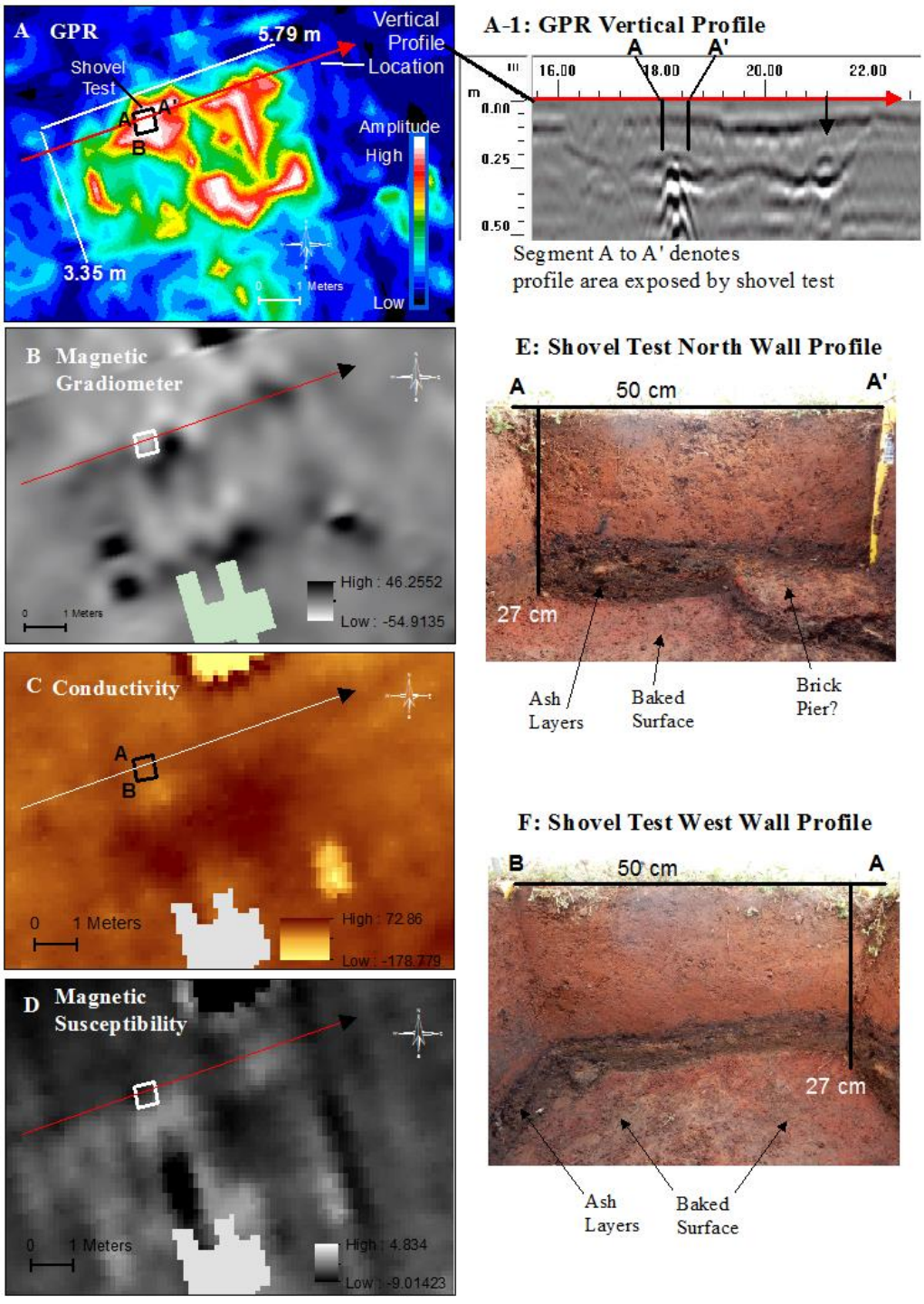

Figure 2.6. Structure Two Geophysical Results With GPR Vertical Profile and Coinciding Shovel Test Profile Walls

thickness (0.24 m) of clayey soil over the depression as shown in the south wall profile photo of Figure 2.6F. Additionally, slightly lower conductivity readings (~5 ms/m) appeared to correspond well with the central most pier-like dipoles visible in the gradiometer data. Magnetic susceptibility maps agreed with the gradiometer readings, confirming slightly higher magnetic susceptibility values (1.13 to 1.20 ppt, compared to .8 to .95 ppt background) coincident with the pier or post- like underpinning features (Figure 2.6D). It is noteworthy that while the magnetic susceptibility and conductivity datasets added helpful complementary information when used with the other instruments, it would be difficult to determine that a feature is present in this location at House in the Horseshoe with this dataset alone.

A single 0.5 by 0.5 m shovel test was excavated by natural levels at the edge of the northernmost central dipole that appeared in the gradiometer map, also coincident with the largest area of high amplitude GPR returns. The shovel test location is presented in all horizontal geophysical maps in Figure 2.6, and also in GPR vertical profile, with the shovel test exposed area indicated by line segment A to A'. (Figure 2.6A-1). The shovel test excavation profiles are presented in Figure 2.6E (North Wall) and Figure 2.6F (West Wall), also displaying the A to A' line segment corresponding with same notation in other vertical and horizontal displays in the figure, as well as line segment A to B , which is discussed below in conjunction with the conductivity image. Measurements were reported according to their thickness in the northwest corner.

The shovel test excavation revealed intact archeological deposits beginning at the base of Level 1, which was 17 cm thick, and consisted of a 2.5 YR 4/6 red clay loam.

Level 1 had only a single piece of buckshot associated that likely came from the abrupt and highly visible transition to Level 2. Level 2 was identified as a layer of charcoal 3 cm thick, with four square nails found in association. Level 3 also presented as a distinct and abrupt change at the base of Level 2. Level 3 displayed a layer of ash and charcoal 4 cm in thickness, which was intermixed with 2.5 YR 2.5/3 dark reddish brown sticky clay/ash. Level 3 artifacts revealed only nails (n=19), with several types present (52.6% = hand wrought, 10.5 % = early machine cut with handmade heads, 15.8% = completely machine cut, 21.1% unidentified). Removal of Level 3 revealed a single brick in the northern profile wall, likely to be the edge of a brick pier (Figure 2.6E). Level 4 was a 3 cm thick, wet, slick 7.5 YR 3/2 dark brown soil that was probably pure ash, its color altered by water flowing downward from the overlying soils over time. Level 4 had only a single wrought nail tip present, along with possible tiny brick fragments or baked clay bits. The bottom of Level 4 presented a reddened (2.5 YR 3/6 dark red) and hardened baked clay floor at 27 cm beneath the surface which, along with superimposed ash layering, indicating prolonged exposure to heat. The baked clay surface was left intact as a clear point of reference or floor that would clearly tie the excavation reported here with future work, and so that the reflective surface imaged with GPR would remain intact until the broader area could be investigated by excavation.

The baked and hardened surface at the base of Level 4, combined with the burned brick pier were the source of the geophysical anomalies visible in the survey results. GPR profiles displayed the baked clay surface as a low to moderate amplitude, concave reflective surface, approximately 6 m in length, and approximately 0.30 to 0.35 m in

maximum depth (Figure 2.6A-1). The distinct hard and fused nature of the surface created a moisture barrier which produced the radar reflections visible in profile and slice maps. The intensely heated surface appeared in the gradiometer map (Figure 2.6B) and to a lesser degree in the magnetic susceptibility map (Figure 2.6D) along the structure's edge due to its enhanced magnetic susceptibility. The exposed brick in the northern profile (Figure 2.6E) suggests that the interpretation of the magnetic dipoles present in the gradiometer data are highly likely to represent the remnants of piers that have been exposed to intense heat. The pier remnant noted in the exposed excavation profile was also visible as a high amplitude, somewhat inarticulate or overlapping point source reflection within the GPR vertical profile (Figure 2.6A-1) located within the dashed exposure area at approximately 0.20 m in depth. A similar, but slightly weaker feature was visible at approximately the same depth at the 20.20 m surface mark, also lending evidence that a similar underpinning may exist 3 m northeast. The piers were also very weakly visible within the magnetic susceptibility map as slightly higher magnetic susceptibility values in contrast with the darker background, having this characteristic strengthened by heat exposure. Conductivity data revealed the fire hardened area near the structures central piers as regions slightly lower in conductivity (4.79 to 5.42 ms/m) than the central fill (~10 ms/m) and the external matrix (~ 6 ms/m). The area of lower values did not display a well-defined border or shape. Darker positive areas of conductivity values in the center of the structure area likely represent the thickening red clay rich topsoil or overburden that were visible in the western profile (Figure 6F), which may have been placed over the area in the past to fill the spot if it appeared upon the landscape

as a depression, as the GPR profile suggests. Potential dates of use for Structure Two relied upon the analysis of nails, which was nearly the only artifact type recovered from the shovel test. Nails recovered from Level 3 (n=19) were mostly hand wrought (n=10, 17^{th} - 19^{th} century), with fewer, slightly later nail types present, such as early machine cut with handmade heads (n= 2,mid 1790s to c.1803), completely machine cut (n=3,c. 1810 to present) and unidentified(n = 4), all of which were well preserved, showing only moderate corrosion (Nelson 1968). Structure Two likely functioned as a smokehouse, dating to the era of Philip Alston (1772/73 to 1790/91), Thomas Perkins (1790/91 to 1798), or possibly Governor Williams (1798 to 1814) (Willcox 1999). The lack of wire nails is notable, but no firm identification of function or date can be reported here beyond possible colonial through post bellum, given the limited exposure of the shovel test and the broad range of dates associated with hand wrought and cut nail types.

Structure Three was most distinctly revealed by GPR data, which displayed a large cellar like feature, approximately 2.5 m by 1.5 m in depth slice (Figure 2.7A), with an estimated depth of 0.9 m as shown in GPR vertical profiles (Figure 2.7A-1 and Figure 2.7A-2). The moderate to high amplitude reflections displayed in slice maps represented the feature as roughly rectangular in shape.

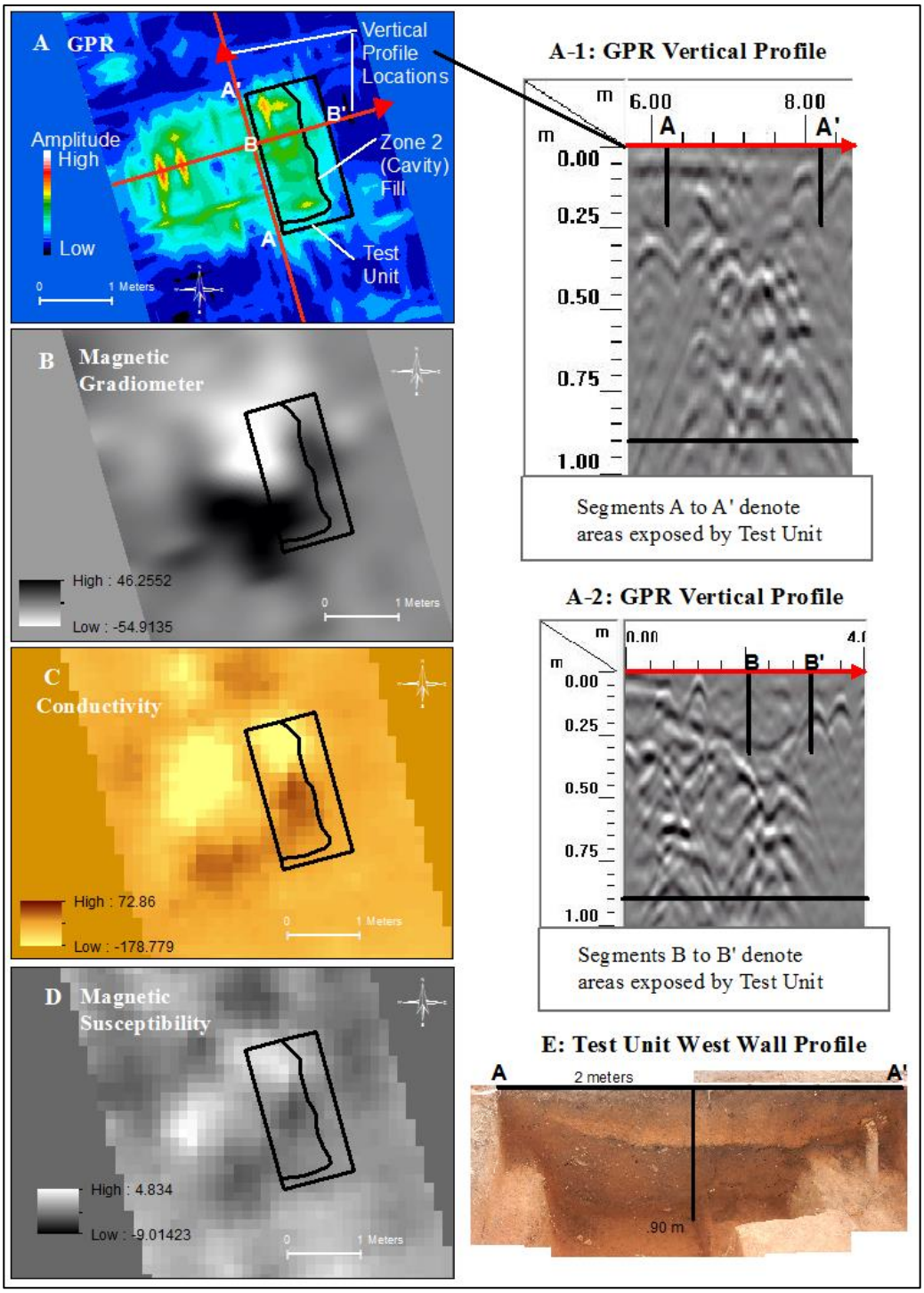

Figure 2.7. Structure Three Geophysical Survey Results With GPR Vertical Profiles and Coinciding Test Unit Wall

Vertical profiles indicated a weak transitional zone 0.10 to 0.30 m beneath the surface, dipping downward toward the eastern end along the long axis of the feature, with many complex overlapping reflections beneath, which suggested the presence of many small reflective objects (Figure 2.7A-2). The gradiometer data revealed a single large dipole (Figure 2.7B) in association with the rectangular feature visible in the GPR depth slice and profiles, but did not conform to the GPR estimated boundary. The dipole was associated with the highest (46.26 nT) and lowest (-54.91 nT) values of the entire processed image, which suggested that a large iron object was near the surface, or that the area had been exposed to intense heat. The pit like feature was displayed in conductivity maps as well (Figure 2.7C), roughly conforming to the feature extent as imaged by the GPR. The northern portion of the conductivity anomaly was dominated by negative values (-2 to -7.3 ms/m) compared to the surrounding soil matrix (2.5 to 3.6 ms/m). The southern half was marked by higher positive conductivity values (5.4 to 6.9 ms/m), which suggested that the southern portion of the shaft imaged by the radar may be filled with a soil of greater conductivity than the matrix. Corresponding magnetic susceptibility values for the feature were far less organized, and only roughly conformed to the fill extent as imaged by the other instruments, most closely corresponding with the conductivity image. The magnetic susceptibility image displayed the feature as having indistinct northern and southern differences in values, with the northern half vaguely indicated by slightly higher values (1.33 to 1.45 ppt) than the matrix (1.18 to 1.2 ppt), and with the southern half showing slightly lower values (1.00 to 1.06 ppt) than the surrounding soils.

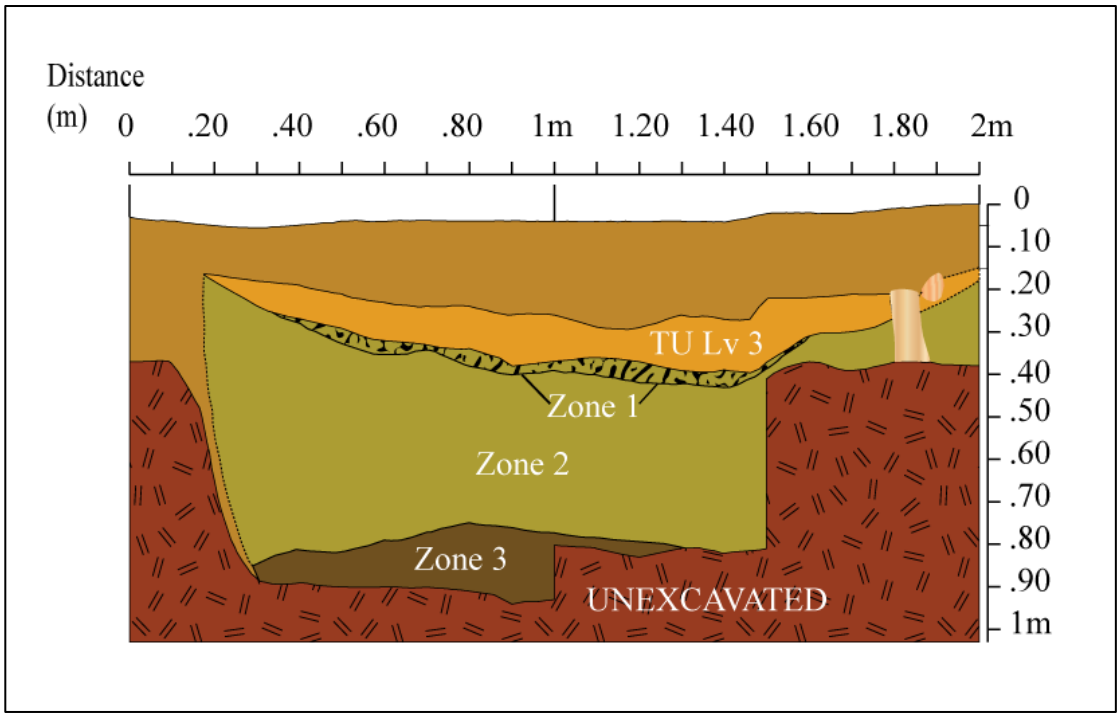

Figure 2.8. Structure Three Test Unit West Wall Profile Showing Historic Pit Zones

Test unit excavations confirmed the feature as a large historic pit, very closely matching the dimensions estimated from the GPR data shown in Figure 2.7. The 1 by 2 m test unit is depicted by a solid black line forming a rectangle at the eastern end of the anomaly as it appears in Figures 2.7A, 2.7B, 2.7C, and 2.7D, with the internal line representing the horizontal boundary of the infilled pit cavity. The historic pit displayed vertical zonation as shown in the unlabeled photo of Figure 2.7E and as labeled in the profile drawing of Figure 2.8. Measurements are reported from the center of the excavation unit. The floor layer Zone 3 was a distinct, 5 YR ¾ dark reddish brown sandy loam, 17 cm in thickness, ending at 90 cmbs.

Figure 2.9. Green Salt Glazed Stoneware In Context at Base of Pit

Zone 3 displayed a thin distribution of artifacts resting on its surface, including bricks (n=3), brick fragments (n=3), stoneware (green salt glazed jug (Figure 2.9) and gray salt glazed crock rim = 2), porcelain (=1), opaque white glass (n=2), and window glass (n=2). Zone 3 was overlain by Zone 2, which was a 5 YR ¾ dark brown layer of sandy loam, 38 cm in thickness, which was deposited in a single episode into the cavity

above the floor layer. Immediately above Zone 2 was Zone 1: a 2 cm thick, single layer of charcoal mixed with Zone 2 soils, which was the source of the dipping low amplitude surface visible in GPR vertical profile shown in Figure 2.7A-2 and the large magnetic dipole in Figure 2.7B. Above the charcoal lens, test unit excavation Level 3 presented an overlying layer of 5 YR 5/6 yellowish red, compact sandy loam, 11 cm in thickness. The very compact, heat reddened soil of test unit Level 3 was used to smother the single episode fire at the buried surface of the feature, and was the source of low conductivity and high magnetic susceptibility anomalies, also contributing to the intensity of the large dipole in the gradiometer map. While the fire smothering layer presented a historically disturbed context, it revealed a jar rim or pitcher fragment displaying incisions attributed to the stoneware pottery decorations of Edward or Chester Webster (Figure 2.10)(Hal Pugh, Ceramics author, potter and owner of New Salem Pottery, 2015, Personal communication: email and conversation; Scarborough 1984). Bricks within the floor layer and within the pit fill, as well as large cast iron artifacts (pot/pan base, waffle iron, and plow blade) were confirmed as the sources of high amplitude radar returns. While soil moisture variation plays a role in the intensity and shape of pit features in GPR slice maps and profiles (Conyers 2013b, Turner 2015) the feature is primarily visible to the radar due to the presence of reflective objects within the Zone 3 floor and the backfilled cavity of Zone 2.

Figure 2.10. Edward or Chester Webster Sherd Confirmed With Known Examples

Ceramic artifacts resting on or just beneath the surface of Zone 3 included a gray salt-glazed stoneware flared jar or crock rim sherd (1826-1905, Date: Office of State Archaeology Lab 2016), several (n=7) pieces of porcelain (1830-1900, Date: Florida Museum of Natural History 2017), and a green salt glazed stoneware jug shown in Figure 2.9, missing its base and applied handle (1850-1900, Date: Pugh 2015 personal communication). The jug was likely turned in the Piedmont of North Carolina, having a squared spout and applied handle that may indicate the Craven family of potters, but not with certainty (Pugh 2015, personal communication). The later ranges of the ceramic

dates from the base layer surface demonstrate that this pit/basement postdate the construction of the house in 1772 or 1773 (Willcox 1999) by approximately 100 years, revealing that the pit is not contemporaneous with the original construction of the house, ruling out the possibility that the pit served as an 18th century kitchen root cellar. The feature was likely used as a basement, root cellar, or privy, and was last in use during the years immediately following the American Civil War, with a mean ceramic date of 1866.17 (n=9) (South 2002).

2.5 Discussion

The geophysical work at House in the Horseshoe is consistent with the assertion of Johnson (2006): the sensors in use see different objects because they measure different physical properties of the subsurface, and see the same objects differently for the same reason. In Structure One, all instruments respond well to the presence of shallowly buried brick and rocks of the foundation. The brick rubble forms a mass close to the surface that is close to the passing sensors. The foundation appears as a robust anomaly within the conductivity dataset also because the brick mass is less electrically conductive than the soil matrix (Figure 2.5). While conductivity appears to perform best at defining the shallow foundation elements of Structure One, GPR also articulates the same features very well, responding to the compactness of the bricks near the surface compared to surrounding soils (Figure 2.4C). The foundation feature appears very similar in shape in magnetic susceptibility data (Figure 2.4B and Figure 2.5B) when compared with the conductivity data set (Figure 2.5A). However, the values associated with nonconductive bricks trend negative (0 to -10 ms/m, compared to a 4 to 6 ms/m matrix background),

while the same materials display a magnetic response nearly twice as high as the inducing field (1.15 to 1.9 ppt). The northern extremity of Structure One appears to the gradiometer as a mostly linear dipole, which suggests that the formerly independent and randomly oriented magnetic fields that are associated with singular bricks are consolidated into a single linear dipole, by intense heat. The induced magnetism visible in the magnetic susceptibility dataset may not only be because of the fired bricks present then, but also may have been enhanced by fire as well. While the gradiometer does not define the structure boundary in the discrete, precise way the other data sets do, it does indicate that the structure may have burned, which cannot be detected by the GPR. If evidence of this structure were not visible at the surface, GPR alone would have been sufficient to locate it. The gradiometer complements the GPR best in this instance because it suggests the fate that this shed ultimately met, while the radar articulates the actual shape of the buried foundation.

While Structure Two is visible within all data sets, the fire hardened, fused smokehouse subfloor and piers are best imaged by the GPR and gradiometer combo, with both EMI based datasets offering far less articulate information (Figure 2.6). The GPR profiles indicate precisely the depth below surface to the hardened floor (Figure 2.6A-1). Because the bricks are refired along with the clay floor, they become somewhat less visible to the GPR in slice maps, although they are present in vertical profile as weak point source reflectors (Figure 2.6A-1). The piers themselves become most visible within the gradiometer, which again shows the strengthening, consolidating and orienting thermoremnant effect that fire has upon the magnetic qualities of iron rich bricks (Figure

2.6B). These observations suggest a highly complementary relationship between gradiometer and GPR in which different portions of the feature are revealed. While conductivity and magnetic susceptibility do coincide and complement the GPR and gradiometer with information, they only subtly indicate that a feature exists (Figure 2.6C and Figure 2.6D). This is in part due to the 10 cm height that the EMI meter was carried during the survey. While instrument height has little effect on the conductivity data, it directly affected the shallower depth of measurement of magnetic susceptibility using the EM38 MK2. As such, the magnetic susceptibility data very weakly indicate that the floor and piers are present (Figure 2.6D), and also vaguely indicate the same increased susceptibility associated with the floor that the gradiometer shows (Figure 2.6B). Even if the EMI instrument readings were taken directly at the surface they would not indicate the presence of the piers as well as the gradiometer, which responded to their permanenet thermoremnant magnetic characteristics as well as the increased magnetic susceptibility of the floor. GPR shows the feature in the most discrete, readily identifiable way, and would have identified this structure without the assistance of the other sensors, but is most effectively combined with the gradiometer.

The large historic pit, Structure Three, is most readily visible to the GPR and gradiometer, which distinctly reveal different characteristics of the same feature (Figure 2.7A and Figure 2.7B). The GPR accurately defines the vertical (Figure 2.7A-1 and Figure 2.7A-2) and horizontal (Figure 2.7A) dimensions of the pit largely due to the concentration of reflective objects buried within its fill. Under the right soil moisture conditions and gain settings, the zone transition between the burning episode and the fire

smothering cap are also visible (Figure 2.7A-2), demonstrating that when soil moisture conditions allow, zones or surfaces within historic pit features are visible to this instrument. The GPR is unable to detect whether or not the fill has been exposed to intense heat, but the gradiometer easily detects this with a large amorphous magnetic dipole (Figure 2.7B). Excavation is required in this instance to confirm the age and to discern how the pit was used, but the appearance of reflective objects occurring in the cavity, in conjunction with the shape in horizontal slice maps suggest with a high level of confidence that a pit or basement exists in this location without excavation. This information is useful to site managers who need to be able to protect cultural resources when site improvements are made, and who are interpreting a sites history, and telling the story to the visiting public. The conductivity image of the Structure Three area indicates that the large rectangular pit is present (Figure 2.7C), but in a far less precise way than radar (Figure 2.7A). Magnetic susceptibility values for this feature do not suggest a consolidated signal source, likely because of the uneven heating of the smothering cap (Figure 2.7D), and due to the height at which the EMI meter was carried during the survey (~0.10 m).

Of all the possible features identified via geophysical methods on site, Structure Four presents the most ambiguous case. The slice maps of the GPR do not indicate that any intact foundation or piers exist in this location, or any other obvious foundation pattern (Figure 2.4C). The gradiometer detects at least one large iron object near the surface that obscures much of the surrounding terrain (Figure 2.4D). Conductivity (Figure 2.4A) and magnetic susceptibility (Figure 2.4B) data for the area however, offer

information that is obscured by the metal object distorting the gradiometer, and not visible to the radar. The most extreme and anomalous positive readings (2 to 4.84 max ppt) of the entire magnetic susceptibility survey and erratically low readings (~ -116 to -149 ms/m) of the conductivity survey are concentrated in this area, coinciding with a position in the yard where Baroody (1978) reports many nails exist. This is also confirmed by metal detection in the general area that indicates the widespread presence of metal. A bucket auger test in the area of the most intense conductivity values does not reveal visible charcoal chunks or burned objects, but does also reveal the presence of metal objects in the plow zone. The EMI sensors excel in the case of Structure Four, articulating the concentration and distribution of decomposing metal in the plow zone (Figure 2.4A and Figure 2.4B). The concentration of nails demonstrated by Baroody (1978) suggests that a workshop or barn once stood in this part of the yard, which is vaguely consistent with the historical record of Willcox (1999), who states that an old barn and other structures were removed during the restoration of House in the Horseshoe. While the debris associated with Structure Four does not as clearly indicate the presence of a structure as the other examples given here, it does provide site management with a specific area that needs further testing prior to alteration of the landscape, while also precisely indicating the presence of an underground transmission line to be avoided by earth disturbing activities onsite.

The best single instrument for prospection of historic structures at House in the Horseshoe is the GPR. Radar precisely located intact archaeological deposits, proving to be an excellent estimator of position and depth to buried features. The historic features at

House in the Horseshoe such as brick supports and deep basement like pits, and intensely heated soils are typical features that are likely to exist on any number of sites making this sensor highly applicable in many historic contexts. The gradiometer is also a highly useful sensor that can be employed alone to detect many types of features. While survey completion times were not recorded during the work at Horseshoe, generally speaking, the gradiometer survey technique was the fastest method employed in the study. The work at House in the Horseshoe illustrates that it is an excellent tool to use in tandem with GPR because it is able to often image features that the GPR cannot, and has the potential to indicate whether historic features have been exposed to intense heat, or if iron objects are present. Conductivity and magnetic susceptibility did not prove to be as useful at House in the Horseshoe, only vaguely suggesting the presence of the larger historic features, and most sharply defining objects near or at the surface that are not likely to be of historic interest, deposited in the uppermost layer of soils onsite. It must be stated however, that its lackluster performance at this study site is not indicative of its overall usefulness as a prospection tool on historic sites. Many have found EMI to be a useful, and even preferred method (Bevan 1994, Clay 2001). It may be more usefully employed in the context of other sites with different features than those observed here.

2.6 Conclusion

The geophysical surveys of House in the Horseshoe provide excellent examples of historic site features as imaged by three commonly utilized sensors. The structural anomalies within the images were exposed, providing interpretive details that reveal what features may look like when using GPR gradiometer and EMI instruments in Masada

soils and in similar contexts. The interpretations and images of buried structural features can be used by state officials at House in the Horseshoe to avoid these locations in accordance with cultural resource management duties, and offer new information about the historic landscape of the site. Other historic site managers benefit from these results as well, by following these detailed examples to identify what buried historic site features look like in geophysical imagery, and to gain an appreciation of the potential that non-destructive geophysical methods have for increasing knowledge pertaining to the history of a site.

These results concur with the interpretation work of Conyers (2012), finding that GPR is an excellent choice by itself for exploring historic pit features, buried surfaces, and foundation elements. It readily identified the historic features of interest with precision. It was observed that GPR is very usefully employed with magnetic gradiometer, which identified portions of the historic features on site that were not clearly visible within the conductivity and magnetic susceptibility maps. The gradiometer was also able to see permanently magnetized thermoremnant features, in addition to those expressing temporary magnetic response in the presence of the earths field in the smokehouse subfloor of Structure Two. The magnetic susceptibility data supplemented and confirmed the temporary magnetic component of the baked floor of Structure Two, indicating that it may usefully be applied to determine which coincident features in gradiometer maps are likely to be expressed due to thermoremnance as noted by Dalan (2006).

The images produced by the sensors provided a precise guide indicating where important features were located on site, but did not themselves indicate the cultural associations of the structures imaged. At House in the Horseshoe, ground truthing investigation was required to determine the cultural relevance of each structure. This is likely to be the case for many sites, and these methods should almost always be used in tandem with excavations that determine cultural relevance based on artifact based evidence. Excavation also plays a critical role in building the interpretive knowledge base of those who use the instruments, and for site managers, state officials, and others who will in the future be required to make decisions or understand the buried cultural landscape based upon the images that result from the growing practice of archaeological geophysics.

CHAPTER III

ESTIMATING VOLUMETRIC SOIL MOISTURE WITH GROUND-PENETRATING RADAR TO IMPROVE SURVEY TIMING AND CULTURAL FEATURE REPRESENTATION IN SLICE MAPS

3.1 Introduction

Ground Penetrating Radar (GPR) is recognized in the fields of agricultural science and hydrology as a viable method of estimating the amount of water in soil at a given time (Vellidis et al. 1990, Huisman et al. 2003, Lunt et al. 2005, Weihermüller et al. 2007). This is possible due to GPR's primary function as a tool for mapping contrasts in relative dielectric permittivity (RDP), which has a strong correlation to volumetric soil moisture (VSM). The relationship was described by Topp et al. (1980) in an equation that is commonly used to convert RDP to VSM. Soil water content is also the dominant factor affecting the appearance of cultural features in GPR slice maps and vertical profiles of archaeological sites (Conyers 2012). Given this sensitivity, survey planning should consider the timing or seasonality of precipitation for optimal image results and better archaeological site interpretations (Rogers et al. 2012). This is often ignored and such work proceeds as time permits (Rogers et al. 2012), often leaving the analyst only with general clues as to the quality of survey results affected by soil water levels. Although precipitation records and dielectric values are valuable ways of explaining soil moisture levels, few studies examining the effects of soil moisture on slice maps report the actual

amount of moisture present in the soil when imaging archaeological features. This paper tests the use of naturally occurring reflectors, recorded by a commonly used, monostatic ground coupled, 400 MHz antenna and GPR system to estimate soil moisture under a range of conditions across the soil moisture continuum of the vadose zone on a historic site in North Carolina.

3.2 Previous Work

GPR is often used in hydrology and soil science studies to estimate soil water content. Survey areas typically covered by GPR improve the spatial scale gap between coarse measurements by satellite, and point measurements by Time Domain Reflectometry probe (TDR) or direct measurement methods (Huisman et al. 2003). Such studies aid in the understanding of horizontal surface distribution of soil water (Jadoon et al. 2010, Jonard et al. 2011, Minet et al. 2011), depth to water table (Słowick 2012), wetting front movement (Vellidis et al. 1990, Charlton 2000) and are also used to improve hydrologic models (Minet et al. 2011). This is due to GPR's primary function as a tool for mapping vertical and horizontal contrasts in RDP within a given space, which is correlated with soil water (Topp et al. 1980). RDP is defined by Conyers (2013a:48) and Davis and Anaan (1989) as,

$$K = \left(\frac{C}{V}\right)^2$$

where *K* is equal to the relative dielectric permittivity (RDP) of the material through which the radar energy passes, *C* is the speed of light, (0.2998 meters per nanosecond, m/ns), and *V* is the velocity of radio waves passing through a given material, in m/ns (Conyers 2013a).

The equation presents RDP as a ratio: the speed of light in free space *relative* to the velocity of electromagnetic energy as it passes through a given medium (Huisman et al. 2003, Conyers 2013a). While RDP has a formal definition known as complex dielectric permittivity that factors in the potential effects of magnetic permeability, conductivity of soils, and antenna central frequency (Topp et al. 1980, Huisman et al. 2003), it is common for basic mapping applications to use the simplified formula given here. Typical permittivity values for dry soils are around three to five, regardless of texture, while the RDP of water is around eighty (Conyers 2012, Conyers 2013a). When water is introduced to dry soils, RDP values increase, depending upon the amount of available pore space and the volume of water added (Conyers 2012, Conyers 2013a). Topp et al. (1980) assert that water content is the dominant factor affecting differences in RDP for many mineral soils, independent of type, density, temperature, and soluble salt.

The velocity factor in the RDP equation represents the speed at which radar energy travels through the soil, to objects or interfaces and back to the antenna, and is directly related to the amount of moisture present on a given date. With increasing water in soil pores, radio wave velocity slows, resulting in a higher observed average RDP value within GPR profiles (Conyers 2013a). Additionally, reflections that delineate the boundaries of objects visible in typical mapping surveys are also due to differences in the

amount of water present in the object and the surrounding matrix of soil, and the associated contrast in radio wave velocity, which result in observed differences in RDP (Conyers 2013b). Conyers (2012) asserts that water distribution may be the only factor affecting the visibility of objects imaged in GPR horizontal slice maps and vertical profiles.

When the velocity of radar energy traveling through a material is known, the RDP of the material can then be calculated, also allowing signal return times to be converted to depth measurements. Estimating velocity is therefore an essential part of creating accurate GPR profiles and slice maps. Radar wave velocity can be estimated by an unreflected ground wave traveling between two antenna separated by a known distance, or by the reflection of waves from buried objects or interfaces (Conyers and Lucius 1996, Huisman et al. 2003). In the latter case, if the depth to a horizontal reflection or interface is known, the two way travel time recorded in radar profiles is easily converted to velocity, and RDP down to the reflective surface (Lunt et al. 2005). Similarly, it is common to excavate a hole and place a solid metal object in the undisturbed soil profile at a known depth, followed by GPR data collection and velocity measurement from two way travel time and depth over the reflective object (Sternberg and McGill 1995, Conyers and Lucius 1996). Hyperbolic shaped reflections of radar energy from point source objects can also be used to measure average velocity and permittivity without knowing depth (Huisman et al. 2003, Rogers et al. 2012, Conyers 2013a). This is done with computer software that utilizes an adjustable hyperbolic arc to fit over similarly shaped objects visible in vertical profiles. If visible hyperbolic reflectors are present, this method

is an accurate way to estimate average soil velocity and RDP above a given point (Conyers 2013a), which can then be converted to soil moisture measurements using an equation derived by Topp et al. (1980), known as the Topp equation (Huisman et al. 2003). While the Topp equation has been used in early GPR soil moisture work (Vellidis et al. 1990, Huisman et al. 2003) this simple approach is not usually taken in soil moisture studies due to the lack of control over the number, known depth and spatial distribution of reflectors (Huisman et al. 2003). The formula states that when RDP is known, VSM is estimated by:

$$\Theta = -5.3 * 10^{-2} + 2.92 * 10^{-2} K - 5.5 * 10^{-4} K^2 + 4.3 * 10^{-6} K^3$$

where Θ represents volumetric soil moisture (reported as m^3m^{-3} or as a percent of volume), and K is equal to relative dielectric permittivity.

The Topp equation was developed using TDR in a controlled laboratory setting that sought to measure the relationship between permittivity and soil water content (Topp et al. 1980). The findings for four soils ranging in textural class from sandy loam to clay were that RDP estimates calculated using TDR could be used to closely estimate VSM with an error of estimate at 0.013 m^3m^{-3} (Topp et al. 1980). The Topp equation was independently evaluated with similar results by Jacobsen and Schjønning (1994, as cited by Huisman et al. 2003), who report an accuracy of 0.022 m^3m^{-3}, and more recently by Weihermüller et al. (2007) who compared TDR measurements to volumetric soil samples of silt loam soils with an RMSE of 0.021 m^3m^{-3}. Though these results demonstrate the reproducible nature of the original work, in the years following, others have found that

the equation works better as an estimator in some scenarios than others. The equation is reported to work well with conversions in soils that do not contain salt water, high volumes of bound water, or are not highly porous (Tarantino et al. 2009, Jadoon et al. 2010). Other works report that the equation does not describe the soil water permittivity relationship well in soils that are high in organic matter (Herkelrath,et al. 1991, Jadoon et al. 2010), or are finely textured (Dirksen and Dasberg 1993, Jadoon et al. 2010). Despite these potential limitations, the Topp equation is often used to convert dielectric measurements of TDR probes and the dielectric estimates from GPR reflections to VSM values for comparison.

Recent studies at the FLOWatch test site of Forschungszentrum Jülich GmbH test the ability of GPR to measure soil moisture using the Topp equation to convert both TDR probe reference measurements and GPR signal estimates to VSM. Studies focusing on soil water content at the surface conducted at FLOWatch often utilize off ground monostatic horn antennas, in conjunction with the radar wave surface reflection and computer waveform modeling techniques to derive RDP in order to estimate moisture. TDR derived soil moisture reference measurements are taken within the GPR footprint and compared with radar derived estimates by Jadoon et al. (2010), who determined a RMSE of 0.025 m^3m^{-3} in a silty loam agricultural field, and by Jonard et al. (2011), who report a RMSE of 0.038 m^3m^{-3} in another study at the same site. Weihermüller et al. (2007) also employed an off- ground radar and waveform analysis-derived dielectric values for a portion of their work, and found that RMSE between volumetric sample reference measurements and GPR to be 0.053 m^3m^{-3} and an RMSE of 0.051 m^3m^{-3} when

GPR derived estimates were compared to TDR measurements from the GPR footprint on silty loam soils.

Soil moisture estimates employing bi static ground coupled antenna and groundwave arrival time in conjunction with the Topp equation are also used to derive shallow subsurface to surface soil moisture estimates at FLOWatch. Weihermüller et al. (2007) utilized two 450 MHz antennae spaced 1.2 m apart on silty loam soils, observing a RMSE of 0.076 m^3m^{-3} when comparing GPR to TDR reference measurements, and 0.102 m^3m^{-3} when radar results were compared with direct volumetric sampling of soil moisture.

While soil water content is not often the direct quantity of interest, it is also a critical factor to consider for successful GPR surveys of archaeological sites. Conyers (2004, 2013b) explains that the differences in water content between a cultural feature and the soil matrix may be the most important factor that affects what can be imaged with GPR for archaeological applications. Further, the results of GPR surveys are known to vary based upon seasonal changes in soil water (Conyers 2004). While the visual effect of soil water variability on the visibility of cultural features in GPR slice maps is well documented (Conyers 2004, Conyers 2012, Rogers et al. 2012, Conyers 2013b), general terms such as wet or dry, are often used to communicate the level of soil moisture in these studies. Rogers et al. (2012) describe the general hydrological conditions of their GPR survey of late Bronze Age architecture in a calcareous soil, describing soil water content by reporting the percentage of precipitation at the time of survey compared to a twenty nine year average for the entire island of Cypress, as well as the assumed velocity

for dielectric calculations and the overall dielectric values observed for wet and dry conditions. This study acknowledges other works that have quantified soil moisture using GPR (Lunt et al. 2005, Jacob et al. 2010), but does not report actual soil water volumes. Their intent was to illustrate that the calcareous soils of Cypress often do not hold much water even under wet conditions, but that the mud bricks and plaster that form the features of interest allow water to collect upon surfaces. The pooling potentially causes unwanted reflections that ultimately obscure the architectural objects of interest, indicating that GPR surveys in similar settings that map similar features need to be conducted under dry conditions.

The Topp equation is not typically used to understand soil water and its effect on radar energy in archaeological GPR work. An early exception is the research of Sternberg and McGill (1995) who used neutron probe and TDR instruments to directly measure the level of soil moisture on two archaeological sites imaged with GPR in Arizona. The soil moisture estimates were used to determine the dielectric constant and the corresponding velocity, which was in turn used to appropriately change the GPR signal travel time scale to depth. While their work formally acknowledges the work of Topp et al. (1980) and the conceptual connection of dielectric constant and soil moisture, the formula used for conversions was not explicitly given by Sternberg and McGill (1995). Stating that most soil moisture researchers already have a dielectric value and want to convert to VSM, Topp et al.(1980) also presented a formula that is used to determine RDP when the volume of soil moisture is known for a given sample,

$$K = 3.03 + 9.3\,\Theta + 146.0\,\Theta^2 - 76.7\,\Theta^3$$

where K is relative dielectric permittivity, and Θ is volumetric soil moisture.

Given the working foundation of GPR derived soil moisture estimates, the established effect of soil water content upon the visibility of cultural features in GPR mapping efforts, and the lack of actual reporting of soil water volume in such works, there is fertile and unexplored ground for soil moisture research using common tools and methods familiar to the archaeological geophysicist. The hyperbolic reflection method of measuring velocity in radar profiles described by Conyers (2013a) and Huisman et al. (2003) is a commonly used procedure for determining dielectric values for archaeological mapping efforts. While Huisman et al. (2003) notes that the lack of control over the depth and distribution of reflectors is a large limitation for using hyperbolic shaped objects in radar profiles for VSM estimation for most applications, archaeological mapping efforts are not as strict in their requirements regarding the placement of such reflectors. Archaeological GPR surveys will benefit from the ability to also use noninvasive radar-generated estimates of soil moisture conditions so that survey results may be given better context. This research tests the ability of a monostatic ground coupled, 400 MHz antenna in conjunction with naturally occurring point source reflectors to estimate soil moisture, with the aim of offering a more specific method of reporting moisture conditions at the time of GPR surveys of archaeological sites.

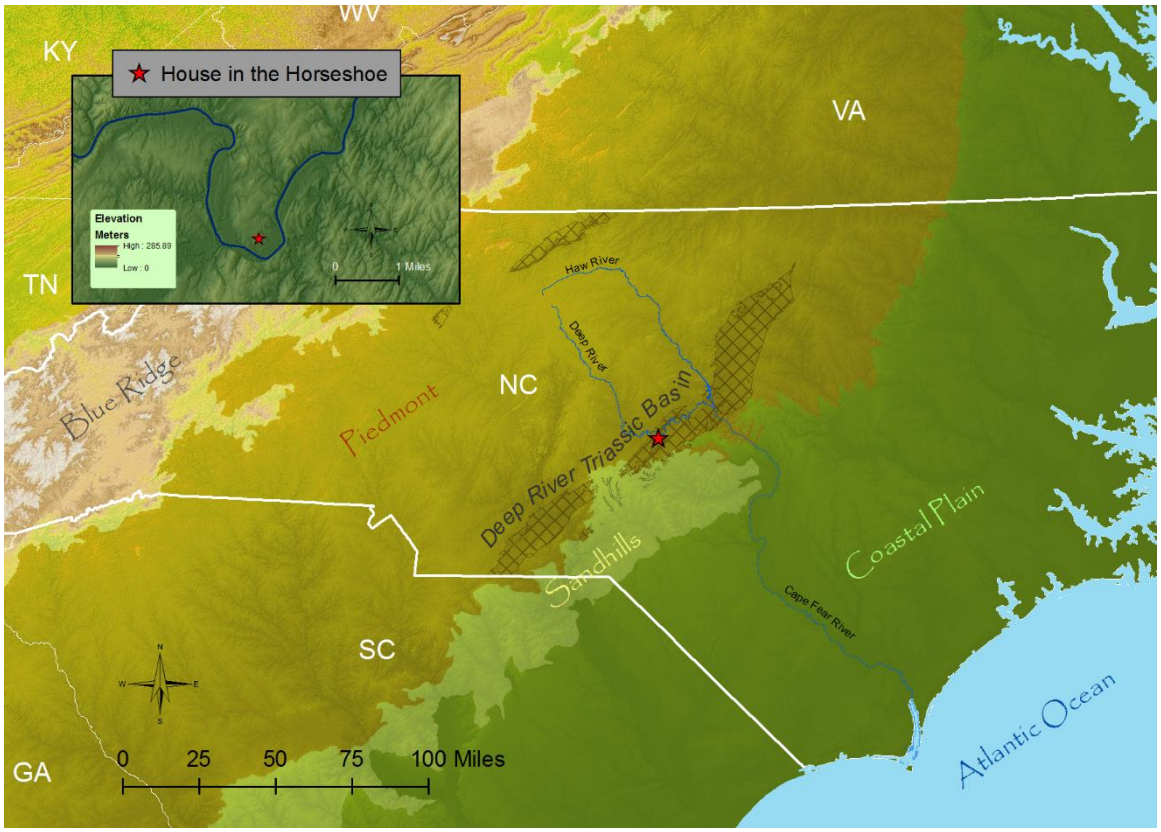

Figure 3.1. House in the Horseshoe Physiographic and Topographic Context

3.3 Study Area

The study area is located in the far northeast corner of Moore County, North Carolina (35.466667 N, 79.383333 W) on a hilltop overlooking wide floodplains that flank the Deep River (Figure 3.1). House in the Horseshoe is named due to its position within a great horseshoe shaped bend in the river. The site is within the Piedmont physiographic province on the northern edge of the Deep River Triassic Basin.

House in the Horseshoe is a state historic site managed by the North Carolina Department of Natural and Cultural Resources. The house was built around 1773 or 1774 for Colonel Philip Alston, who was a planter and Whig militia leader in Moore County

during the American Revolution (Willcox 1999). The site is significant due to a militia confrontation associated with the Revolution as it unfolded in the backcountry, away from the larger, more frequently noted battlegrounds. Alston, his family, and a small group of militiamen were attacked while inside the house in July of 1781, by an opposing Tory militia group led by Colonel David Fanning (Willcox 1999). Also the center of a plantation during the time of Alston and several owners that followed, the house was surrounded by many outbuildings with different functions, the remnants of which are no longer visible at the surface (Willcox 1999). The site management and historical motivation of this research was to investigate a potential location thought to hold the remnants of the original external kitchen that was likely to be in the yard, close to the main house.

3.4 Methods

3.4.1 Field Methods

Initial geophysical prospection surveys on March 15th, 2013 revealed a potential location of the Alston house kitchen root cellar. Slice maps from the initial survey revealed a concentrated area of high amplitude reflections that were rectangular in shape, indicating the presence of a cellar or privy like feature approximately 12 m northeast of the Alston house. Maps generated from the broader area prospection survey were used to guide the placement of a smaller rectangular grid measuring 4 by 10 m, encompassing the boundaries of the rectangular high amplitude feature (**Figures 3.2 and 3.3).**

Figure 3.2. The Alston House Today

The USDA Web Soil Survey identifies the soils within the GPR study area as a Masada fine sandy loam, two to eight percent slopes. Masada fine sandy loam is typically found resting upon "…high stream terraces on Piedmont uplands" (Wyatt 1995:26). According to the Web Soil Survey, a typical Masada soil profile exhibits the following horizons:

0 - 0.23 m: Fine sandy loam
0.23 m- 1.14 m: Clay
1.14 m- 2.03 m: Gravelly sandy clay loam

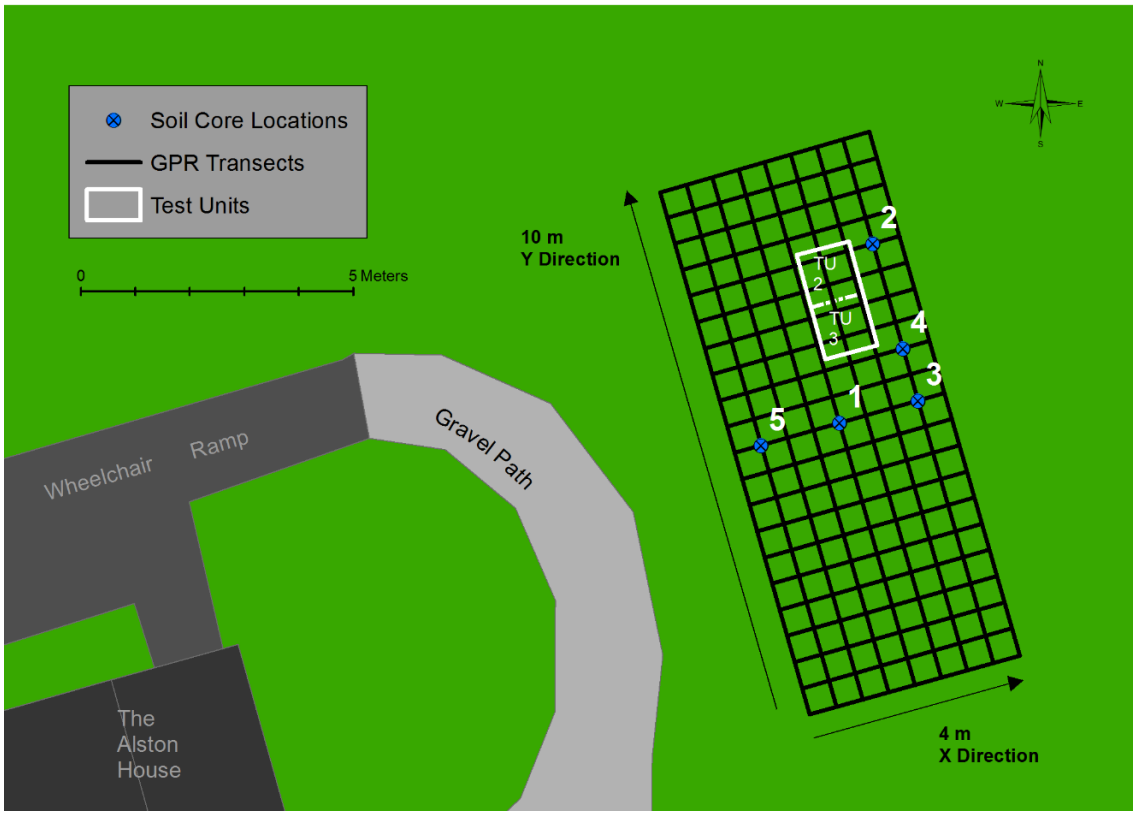

Figure 3.3. GPR Survey Area With Soil Core Sample Locations

However, a more detailed description published in the Moore County soil survey more closely reflects the soils within the area of interest at the study site. The survey describes Masada two to eight percent slope soils as having a potentially different series of horizons in the subsoil (below 0.23 m, down to 1.14 m), with the upper subsoil horizon appearing as a yellowish red clay loam above a red clay horizon with brownish yellow mottles, followed by a red clay loam horizon with strong brown mottles (Wyatt 1995:26). This indicates that Masada two to eight percent slope soil textures can vary slightly in the second and third horizons of the subsoil section, or that the definition of the Masada

series has changed slightly over time. Masada is described as a well-drained soil, with depths to water table and restrictive features deeper than 2.03 m (USDA NRCS 2017).

Table 3.1. Range Gain Settings

Date	**4/8/2014**	**5/24/2014**	**6/7/2014**	**8/8/2014**	**8/22/2014**
Gain 1	-15	-20	-20	-20	-20
Gain 2	17	18	25	13	26
Gain 3	51	52	57	61	56

In order to capture the area of interest with varying levels of water in the soil, the grid was surveyed five times from May to August of 2014. Transect spacing and survey direction were the same for each date, with lines placed at half meter intervals in x and y directions, resulting in a two direction 3D data cube (Figure 3.3). All surveys were conducted with a GSSI SIR 3000 GPR unit, fixed upon a three wheel cart with a survey wheel attached, connected to a 400 MHz antenna. With the exception of range gains, instrument settings were held constant for each date, with the same survey wheel distance calibration, and manufacturer presets for the 400 MHz antenna on a three wheel survey cart in 3D data collection mode. The settings included 120 scans/s, 50 scans/m, and 512 samples/scan. All returning energy was recorded within a 50 ns observation time window, and quantized using sixteen bit signed integers, with the dielectric constant set at eight.

Range gain was optimized for each survey using the auto gain function on the SIR 3000 (Table 3.1). This was accomplished by pushing the antenna over the grid, locating the area where amplitudes were clipping at the most extreme, and then re-initializing the

antenna. This procedure was followed to minimize distortion in radar profiles, which in turn allowed a more clearly interpretable subsurface view.

Immediately following each survey, a 0.8 in. diameter core soil sample was taken from different positions within the GPR grid using a JMC ESP extraction jack (Figure 3.3). The core sample was extracted into plastic sleeves in two sections, reaching 1.6 m in depth. The sample was intended to provide a precise measurement of onsite soil moisture conditions at the time of each survey for comparison with estimates derived from point source reflectors within the same grid.

Once the GPR surveys were complete, a 1 by2 m unit was opened at the east end of the anomaly which was excavated by natural levels down to culturally sterile soil. The excavation allowed the source of the anomaly to be known, real feature dimensions to be measured, and cultural association to be discerned.

3.4.2 Lab Methods

All GPR data was processed using RADAN software (v7.3.13.1227 Geophysical Survey Systems Inc. Nashua, New Hampshire) with time zero correction and background removal functions applied. Following these steps, a mean RDP of survey area soils (Table 3.2) was determined for each date by determining the RDP surrounding individual hyperbolic reflections visible in vertical profiles. During the process, the profile number and locations of each reflector were noted, and a separate set of individual profiles were created so that the depth of each reflector could be assessed individually using its specific RDP and velocity value. Following this, reflector depth and a VSM value down to the reflection was recorded using the formula specified by Topp et al. (1980). In order to

examine the relationship between GPR generated soil moisture estimates and distance from the field sample locations, the horizontal distance between reflectors and the soil sample location was also recorded.

Range gains set in the field were unaltered during lab processing, and no display gain was added to the slice map output. A single horizontal slice depth (0.50 m) was selected for analysis by examining each date to determine which best visually displayed the maximum dimensions of the feature in plan view. As a final step, a band pass filter (High 200 MHz, Low 600 MHz) was also applied to each survey. Each slice was exported to a comma separated values file (.csv) at a 0.20 m thickness, and was gridded using the Kriging interpolation method in Surfer 10, at a 0.10 m pixel resolution. Each grid was saved as a tagged image file (.tif) and was georeferenced for excavation planning and visualization using ArcMap 10.2.2

In order to calculate the actual volume of water in in the soil profile for one location in the survey block, the soil sample tubes from each date were divided into 0.10 m sections, and a 1 cc sample was extracted from each level. The sample was weighed wet, oven dried for 1.5 hours at 100 degrees C, and then weighed again dry. This process determined the mass and the volume of water present in the sample. The results were tabulated and compared to GPR based estimates derived from the Topp equation at other positions within the data collection block.

3.5 Results

3.5.1 Excavation

Excavation revealed the anomaly to be a large historic pit very closely matching the dimensions estimated in the initial survey. The pit displayed (measurements in center) a base layer about 0.17 m thick, terminating at 0.90 m beneath the surface, that was more distinct in color than in texture, with a few large flat lying bricks within it. Above the base was a fine grained homogenous fill within what used to be an open cavity, 0.38 m thick that had many large reflective objects within it, including cast iron cookware, an iron pipe, sheet metal and many large brick fragments. The buried surface of the pit fill was marked by a single 0.02 m thin charcoal layer, beginning at 0.33 m beneath the surface that was the result of a single episode fire. The charcoal layer was capped by a distinctively reddened compact soil approximately 0.11 m in thickness that was used to smother the hot coals. Artifacts resting on or just below the top surface of the base layer roughly date the feature to the time immediately following the American Civil War, postdating the construction of the house by approximately 100 years. This pit was likely the cellar of a small structure or a privy (Turner and Lukas 2016).

3.5.2 Direct Volumetric Soil Moisture Measurements

The soil samples taken from each of the individual GPR survey dates display a range of moisture contents (Figure 3.4A). Variations in water content with depth reflect different soil moisture conditions on the dates of survey. Of the five soil sample dates, August 8th displayed the driest measurements from the study, with the minimum VSM

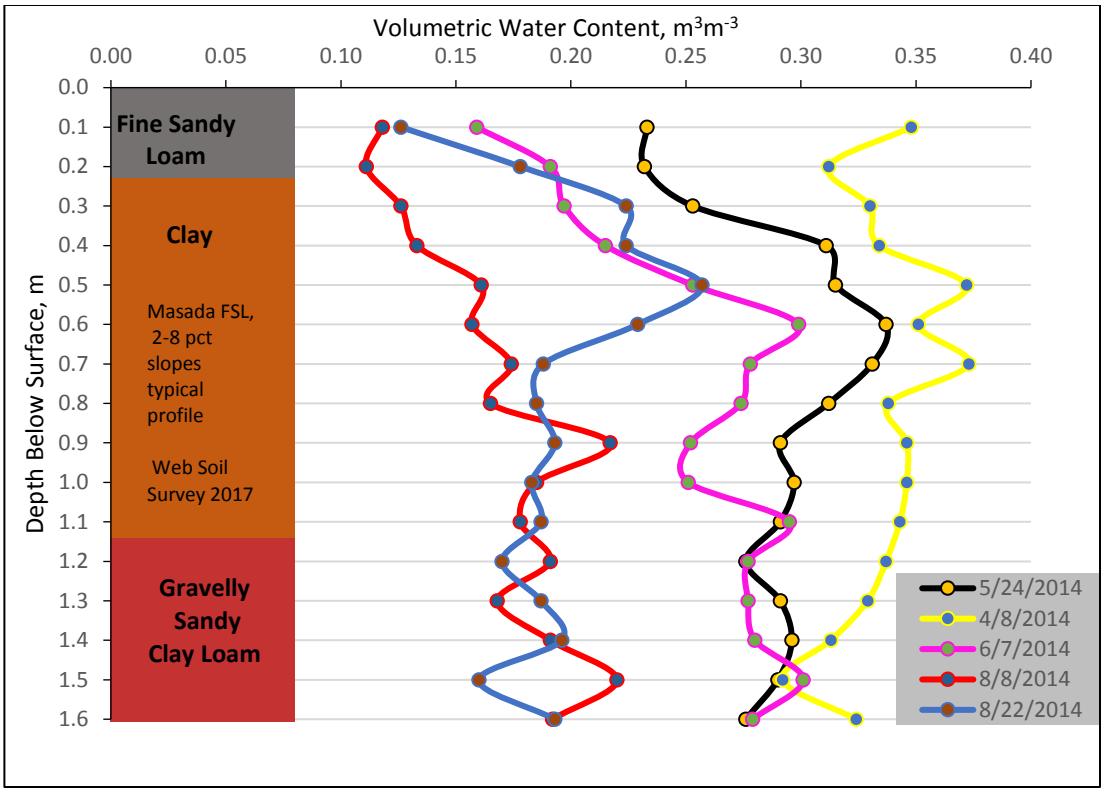

Figure 3.4A. Volumetric Soil Moisture Content of GPR Survey Area Soils Per Given Survey Date

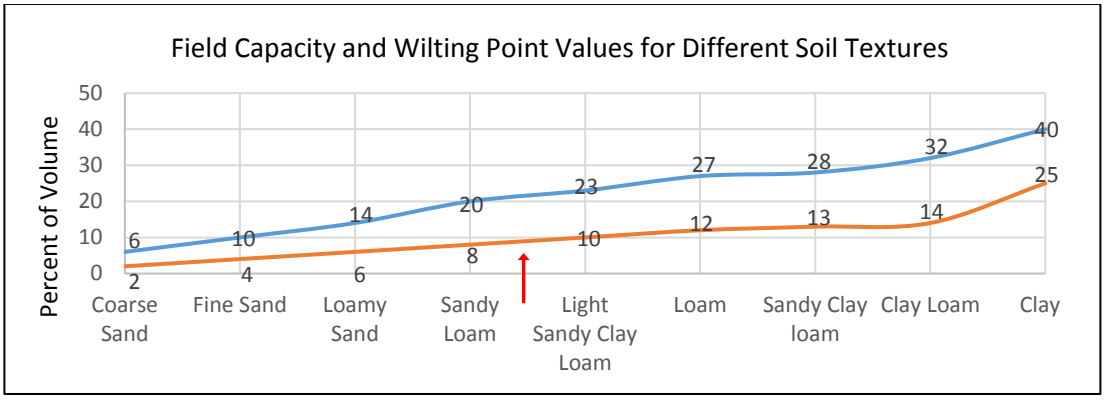

Figure 3.4B. Field Capacity (Blue) and Wilting Point (Orange) Values for Different Soil Textures. Adapted from Hignett and Evett 2008

observed at 0.111 m^3m^{-3} or 11.1 percent of volume at 0.20 m below surface. The wettest survey conditions occurred on April 8th, with a maximum VSM of 0.373 m^3m^{-3} or 37.3 percent of volume recorded at 0.70 m, and a minimum of 0.292 m^3m^{-3} or 29.2 percent at 1.5 m below surface. When placing the measurements within the relative unsaturated zone soil moisture continuum (Figure 3.4B), the upper portions of the soil column on August 8th were likely just above the wilting point, assuming a fine sandy loam down to 0.20 m below surface. Conversely, on April 4th 2014, soil conditions were very wet, with the upper 0.20 m above field capacity for the soil texture class, approaching saturation. Of the five survey dates, June 7th falls into the center of the possible range of soil moisture conditions observed for this study, and is likely to represent the soils at House in the Horseshoe just below field capacity. The soil column displayed in Figure 3.4A is a typical soil profile for Masada Fine Sandy Loam two to eight percent soils as reported by the Web Soil survey, although variation in stratigraphy and soil texture is possible.

3.5.3 Interpretations of Slice Maps and Vertical Profiles

Velocity analysis of the GPR profiles from each of the five survey dates rendered a range of average dielectric values (Table 3.2). The reflectors used to derive RDP in all surveys were all observed at 0.30 m below the surface or less, and therefore represent the average RDP to that depth on a particular date for the survey grid. Figure 5 and Figure 6 display depth slices of all survey dates, showing amplitude values from 0.30 to 0.50 m below surface. Depth slices show the entire GPR grid area and selected vertical profiles that bisect the historic pit feature. The vertical profiles shown correspond with the wettest survey date as calculated by soil sampling, the driest date, and the date that occurs in the

center of the range of possible soil moisture conditions for the study. The white dashed markers visible in the vertical profiles of Figure 3.5 and Figure 3.6 represent area that was exposed by test unit excavations.

Table 3.2 Summary Results

Date	# of Reflectors	Mean RDP	Θ (m^3m^{-3}) Topp with Mean RDP	Θ (m^3m^{-3}) Mean 0-1.6 m, Core Sample	Θ (m^3m^{-3}) Mean 0-.3 m, Core Sample	Θ Min Diff	Θ Max Diff	Θ RMSE
4/8/2014	8	23.25	0.383	0.337	0.330	-0.020	-0.105	0.065
5/24/2014	10	16.39	0.297	0.290	0.239	-0.006	-0.106	0.071
6/7/2014	7	12.92	0.242	0.255	0.182	-0.028	-0.107	0.058
8/8/2014	6	11.75	0.221	0.168	0.118	-0.067	-0.140	0.099
8/22/2014	9	13.53	0.252	0.193	0.176	-0.031	-0.205	0.106

The historic pit feature is visible in the depth slice maps of all surveys, appearing at the northern end of the grid as a rectangular area of moderate to high amplitude reflections. Simple visual comparison between dates indicates that there was very little variation in the shape of the pits midsection with variation of soil moisture conditions at this depth. Under the driest conditions in the study, the pit appears rounded on the westernmost end, but still appears as a vaguely rectangular shape.

The profile views corresponding with the historic pit indicate that the transition between the charcoal layer at the buried surface of the feature and the overlying baked soil cap is best articulated in the June 7th survey in Figure 3.5 as a low to moderate amplitude, sloping, surface-like reflection, angling downward, then suddenly back toward the surface. This transition is also visible in the same profile from August 8th, but is

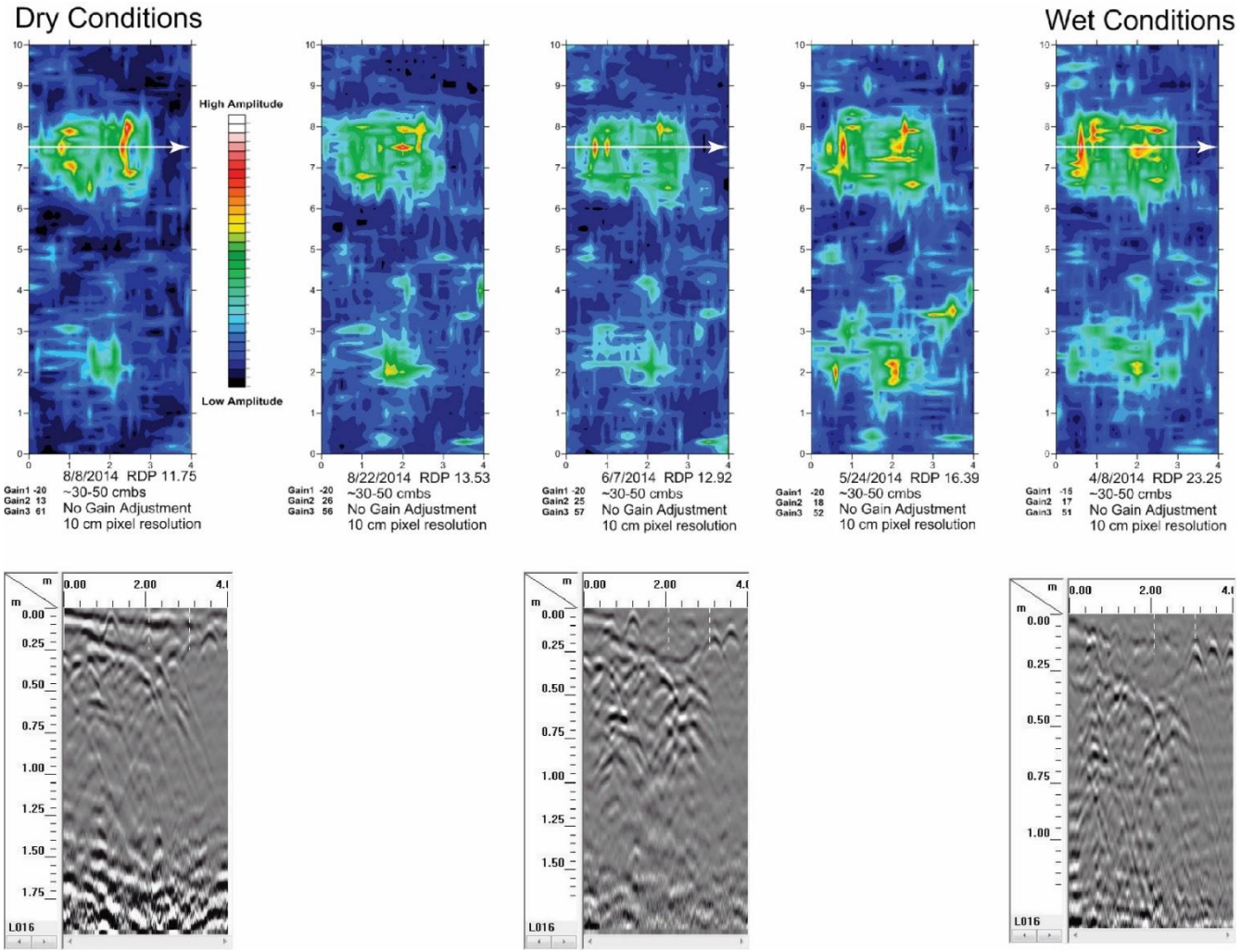

Figure 3.5. All Survey Dates at .50 m Beneath the Surface, GPR Profiles Traverse the Long Axis of the Pit

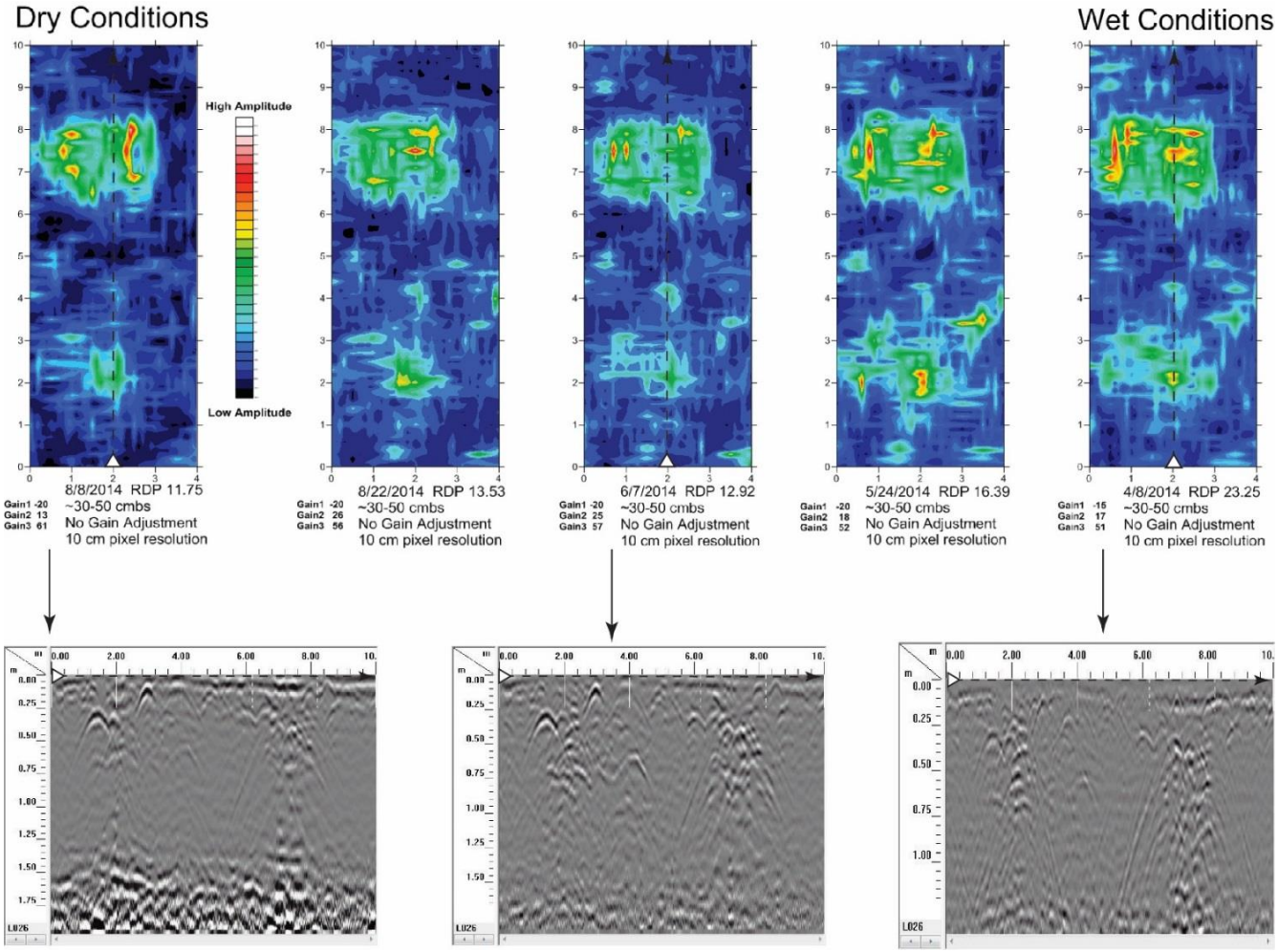

Figure 3.6. All Survey Dates at .50 m Beneath the Surface, GPR Profiles Traverse the Short Axis of the Pit

expressed with higher amplitudes at the interface, and less overall length and definition. On the wettest survey date in Figure 3.5, (April 8th) the scorched surface does not appear at all, and the transition is not apparent in the three perpendicularly intersecting profiles shown in Figure 3.6.

Cast iron cookware (frying pan base and waffle iron grid) uncovered during the excavation produced the reflections visible in the June 7th survey profile at 0.6 m in depth and 2.4 m from the transect origin in Figure 3.5. Reflections from these objects may be weakly visible in the profile collected on April 8th (the wettest survey conditions) in Figure 3.5, but are only very weakly visible under the driest conditions of August 8th of the same figure. There are similar iron cookware related reflections, moderate to high in amplitude, visible for the same dates/soil moisture conditions in Figure 6, and again with the driest conditions displaying only very weak contrasts.

3.5.4 GPR Soil Moisture Estimation

Table 3.2 is a summary of results from the entire block for each survey date. The mean RDP of all reflections used in the velocity analysis for a given date was used to calculate a single soil moisture estimate down to 0.30 m using the Topp equation. The GPR estimate of VSM for the entire block is then compared to the mean of all directly measured VSM values for each date, and also down to the depth of the deepest reflectors used (0-0.3 m). Minimum and maximum VSM differences refer to the best fitting (Θ Min diff) and most deviant (Θ Max diff) observations when comparing singular GPR/Topp VSM estimates to the soil column sample mean VSM down to the compared reflectors depth. The average directly sampled VSM value down to each individual reflector's depth

was used as the reference, and VSM calculated using GPR/Topp equation as the predicted value to derive the RMSE for the entire survey block. The RMSE is interpreted as the average squared distance of the predicted value from the directly observed value. It is reported in unsigned values of m^3m^{-3}, and is intended to offer an additional, however general, guide to the goodness of fit between direct measurement and VSM estimated by GPR. The observed VSM values of the soil core sample are not coincident with the reflectors used to estimate soil moisture, so the RMSE applies to the entire study area, and does *not* describe the fit of each reflection with a direct sample taken from within the radar footprint, as it has in previous works.

Table 3.3 represents a more detailed look at all values in the RMSE, allowing a view of all differences, including the minimum and maximum difference observations included in Table 2. Showing all differences between estimation and observation allowed the distance to the directly sampled column to be examined in the analysis, and the range of variation for all differences to be viewed.

Most noteworthy of the Table 2 summary are the differences in mean VSM estimates for the entire block using the Topp equation compared with the mean VSM of the entire soil core sample (0-1.6 m). The difference observed on 5/24 is 0.007 m^3m^{-3}, with the next lowest difference between methods falling on 6/7 at 0.013 m^3m^{-3} which also displays the lowest RMSE (0.058 m^3m^{-3}) of the study. Other observed differences in average occur at soil moisture extremes over a short range (.046 m^3m^{-3} to .059 m^3m^{-3}).

Table 3.3. Difference in Topp VSM and Directly Measured Average to Depth VSM with Distance From Reflector to Soil Sample

4/8/2014 Θ Difference	Distance (m)	5/24/2014 Θ Difference	Distance (m)	6/7/2014 Θ Difference	Distance (m)	8/8/2014 Θ Difference	Distance (m)	8/22/2014 Θ Difference	Distance (m)
-0.052	1.35	-0.006	0.51	-0.069	2.5	-0.067	1.25	-0.066	2.48
-0.023	1.74	-0.106	0.53	0.029	3.27	-0.102	3.52	0.076	3.45
-0.105	2.00	-0.064	2.87	-0.042	3.55	-0.108	3.80	0.041	3.90
-0.102	2.63	-0.085	3.23	-0.031	3.87	-0.083	4.32	-0.126	3.96
0.046	3.00	-0.078	5.24	-0.107	4.69	-0.140	4.71	-0.205	4.02
-0.072	3.21	-0.064	5.25	-0.028	5.02	-0.074	4.85	-0.050	4.47
-0.020	4.64	-0.057	6.02	-0.058	5.6			-0.139	4.52
-0.038	5.08	0.053	6.13					-0.031	5.00
		-0.106	6.26					-0.088	5.45
		-0.019	6.74						

The difference in average VSM values for the block are interestingly dissimilar when comparing the single VSM estimates using the Topp formula and the direct sample average down to the deepest reflector observed (0-0.30 m). The range of difference in averages for all five dates (0.053 to 0.103) is larger, with the dates trending from field capacity toward saturation showing a five to six percent difference in average, with the GPR estimating higher values than the soil column. The two driest dates show the greatest difference in average VSM using the two methods (8/8 diff 0.103 m^3m^{-3}, 8/22 diff 0.076 m^3m^{-3}). It appears that in Masada fine sandy loam two to eight percent slopes, the GPR predicts average volumetric soil moisture better when the soils are at field capacity or slightly wetter and when using point source object reflections as a RDP/ velocity source. Further, this dataset suggests, somewhat counterintuitively, that VSM estimates using GPR may be indicative of average VSM to a greater depth than the depth of the reflections used to estimate velocity, RDP and VSM using the Topp equation.

In 87.5 percent of comparisons between VSM over a single reflector and the average VSM from the column sample to the reflectors depth, GPR/Topp equation overestimated the volume of moisture compared to soil column measurements (Table 3.3). While their antennae arrangement, dielectric calculation process and soils were different from this study, Weihermüller et al. (2007) also noted the tendency of GPR to overpredict VSM. GPR soil moisture estimates from House in the Horseshoe do not seem to support a case for over prediction in connection to antecedent soil conditions. The survey with the lowest RMSE (June 7th Table 3.2) is also the wettest of the five dates, but does not have the lowest observed residual difference (referenced in Table 3.3). The lowest residual difference value between the GPR/Topp equation soil moisture estimate and the directly measured volume occurs May 24th, with the GPR over predicting the directly sampled measurement by approximately half of a cubic centimeter, or a 0.6 percent volumetric difference (Table 3.3). The highest residual difference when comparing column sampled moisture with radar estimates (-0.205 on August 22nd Table 3) did correspond with the highest observed RMSE, but the next highest RMSE date (0.099 August 8th Table 3.2) differed from the highest number only by a small fraction (0.007) but had a large difference between maximum value differences observed (-0.205 versus 0.140, a difference of 0.065 or 6.5 cubic centimeters).

The results from the wettest survey date, April 8th, and the two dates that follow in progressively drier conditions, May 24th and June 7th, show very little variation in minimum, maximum or RMSE values, despite the large difference in water content of the soils between dates. However, higher RMSE (~0.10 in Table 3.2) minimum and

maximum values appear to be associated with the driest dates, August 8th and 22nd. It may be the case that when soils contain large amounts of water, soil water is more evenly distributed if the soil texture is the same within a given area, especially as they approach saturation. Conversely, as a soil drains and dries, its water content becomes less homogenous spatially (Western and Grayson 1998). Considering that the soil beneath the antenna footprint is more homogenously wet when between field capacity and saturation, it will be more likely to be closer to the directly sampled value, which will be much smaller in size, but close in value to the estimate. As the soils dry and the water content is less homogenous throughout the survey area, the likelihood of the small direct sample having a different actual soil moisture content from the larger area coverage of the GPR footprint increases.

There is no apparent pattern in observed measurement differences as the distance between direct sample location and GPR estimate location increases. As an example, the first two observations on May 24th are both approximately half of a meter away from the soil sample location, but display drastically different results, the lower showing only a 0.006 m^3m^{-3} overestimation in volumetric soil moisture, the higher overestimating by 0.106 m^3m^{-3} (Table 3.3). On the same date, another pairing indicates a similar variability even at a distance (6.26 m, -0.106 difference versus 6.74 m, -.019 difference). These variations are likely due to the difference in samples compared (GPR footprint versus 1 cc soil sample) discussed in the last section, the possibility that soil moisture content may vary across space even at a short distance, and the imprecise nature of measuring soil

velocity and RDP using the hyperbolic arc fitting method of measuring the dielectric value above each reflector.

3.6 Discussion

The work at House in the Horseshoe interprets survey conditions within the wilting point- field capacity- saturation continuum. It has been said, informally and generally, that GPR surveys are ideally conducted when the soils common to the central Carolina Piedmont are not overly dry, but slightly wet (Roy Stine, Associate Professor of Remote Sensing, Department of Geography at The University of North Carolina at Greensboro 2013, personal communication: conversation). This study generally places this idea into a measured context within the aforementioned continuum.

3.6.1 Different Moisture Conditions and Effects Upon Feature Appearance in Slice Maps

Of the three survey dates, June 7th offers the most optimal soil moisture conditions for imaging large, multi-layered pits with the soils, groundcover and flat topography present at House in the Horseshoe. On that date, the upper 0.30 m of soil was just below field capacity, with the region beneath exactly at field capacity for fine sandy loam soils. Under these conditions, there was still plenty of water in the intergranular pore space of the soil matrix, but it was highly likely that most downward gravitational drainage had occurred in the upper 0.30 m, and the soils were drying out.

A vertical radar profile from June 7th indicates that the transition from the fire reddened soil cap to the charcoal lens of the historic pit/basement is best articulated on this date (Figure3.5). Excavation Level 3 soils were reddened and compact, overlying the

charcoal layer, feature Zone 1. The soil transition is visible at a greater amplitude, but shorter and with much less detail in the driest survey conditions, and not at all in the other profiles from the survey.

The shape of the feature as it appears in the slice maps surveyed in different soil moisture conditions changes very little. The most obvious change in shape between survey dates is during the driest soil conditions, on August 8th (Figure 3.5 and Figure 3.6). Under the driest conditions, the basement fill is no longer visible around the western edges of the large pit, and it now appears to have a rounded end. The areas of moderate to high amplitudes visible within the fill could potentially be objects, but are more than likely portions of the baked soils associated with the burning episode discovered in the excavation. They appear as individual objects due to the actual unevenness of the buried surface in reality, and the cross cutting effect of slice thickness (0.20 m) imposed during processing and export. The changing shape of the pit under these dry conditions has implications for smaller features that have a soil fill dissimilar from the soil matrix in Masada fine sandy loam soils. As the soil approaches wilting point, smaller pit features with no or small objects within them may not be visible to the GPR. This is consistent with the assertion of Conyers (2012), who demonstrated that the RDP of dissimilar dry soils produces very low or nonexistent dielectric contrasts, rendering features with these characteristics invisible, or weakly so, to GPR.

3.6.2 Study Limitations and Issues to Overcome for Future Work

While GPR system elements vary between studies, as well as dielectric calculation methods, and different vadose zone areas (surface soils versus subsurface), many observations within them offer insight toward interpreting the results of the House in the Horseshoe study. While all studies use RMSE to compare soil sampling or probe-based reference measurements to the GPR footprint estimate of VSM, the sample sizes of previous works are much higher than the low number of observations in this study. Further, comparable reference measurements for the calculation of RMSE are optimally made within the GPR footprint. VSM reference measurements at House in the Horseshoe came from a single column within approximately 6 m of the reflectors used for VSM estimation- they were not coincident with the GPR footprint- which must be considered when assessing the RMSE values reported in this study. Previous works also note difference in scale/volume between single point reference measurements and the GPR footprint as a potential source of error (Charlton 2000, Weihermüller et al. 2007), despite a mostly tight correlation in VSM estimates between the footprint and direct samples in off ground antenna/surface water studies (Weihermüller et al. 2007, Jadoon et al. 2010, Jonard et al. 2011). The variation in measurement scale means that the GPR estimates of VSM are affected by water holding capabilities of other objects in the soil, such as rocks (Charlton 2000) which reference measurements do not record, and variation of water distribution over a broader measurement area, in general than the reference point.

In fact, the horizontal distribution of shallow vadose zone soil water is not perfectly homogeneous whether wet or dry, and likely is the dominant factor affecting the

observed differences and RMSE values reported in this study. Lunt et al. (2005) note the work of Western and Grayson (1998) who indicate that VSM (measured by TDR probe) down to 0.3 meters can vary as much as 0.15 m^3m^{-3} at a horizontal distance scale of tens of meters under wet conditions. They also revealed that when comparing data mapped from two collection dates, wet conditions produced more spatially homogenous VSM values that vary according to their hillslope position or are "topographically organized", and that dry conditions produce very high spatial variability of VSM when single observations are logged at 10 m intervals.

The method of measuring point source reflections for determining soil velocity, RDP and VSM calculation is imprecise and also contributes a small portion of the observed differences between measurements. While Conyers (2013a) notes that the hyperbolic arc tool can accurately measure velocity and RDP, it is easily observed that the tool can produce slightly different results when a hyperbola is measured again by the same analyst, or by a different analyst, who may also choose to include a different number and quality of reflectors. This effect is likely more visible when comparing the RDP value generated for a single reflector to the reference soil column, and less evident or possibly inconsequential when the RDP value of several reflectors is used to determine a single RDP and VSM value for the entire survey area.

The closest comparable study of those reviewed herein is Weihermüller et al. (2007), who measured soil moisture using radar energy traveling between two antennae separated by 1.2 m distance, with a RMSE of 0.10 m^3m^{-3} . The Weihermüller et al. (2007) work differs from the surveys at House in the Horseshoe in several ways. The RDP of

soils was based upon signal travel times between two separate antennae and not waves reflected from objects, the soils were finer in texture than those at Horseshoe, and the reference measurements were taken such that they appeared in the center of the antenna pair to derive the error of the estimate. The studies were similar in that they examine GPR signal travel in the shallow subsurface and similar antenna nominal frequencies, with similar or identical RMSE values under dry conditions. However, given the close match between predicted and observed *mean* VSM values under near field capacity conditions at House in the Horseshoe, this work asserts that given enough subsurface hyperbolic reflectors, a very accurate average VSM estimate can be given for a small area.

Future studies that seek to report soil moisture conditions during GPR surveys of archaeological sites should further test the results of the work presented here from Horseshoe. Future works will benefit from exploratory survey coverage prior to designing a study so that knowledge of the visibility and distribution of reflectors can be known. Additionally, following the method used by Lunt et al. (2005), if depth to a reflective, flat lying interface can be determined, velocity, RDP and average VSM down to the reflection can easily be calculated. This simple velocity determination method can either supplement values in an estimate of average soil moisture conditions with the hyperbolic reflector method, or be compared. To achieve this, the reflector positions, and optimally depth, should be determined in advance, and volumetric comparison samples taken from the center position of the arc, as well as a distance either side. To broaden the work at House in the Horseshoe, additional verifiable historic site features should be

incorporated under a variety of soil moisture conditions, along with direct measurements of their size and shape to further examine fluctuating soil moisture conditions on their expression in GPR slice maps.

3.7 Conclusion

It was observed in this study that when all levels of the entire column sample are averaged and compared to a single VSM value derived from the average RDP of all reflectors, the mean of soil moisture estimates for the four by ten meter block match very closely, almost perfectly, under the moderate or and wet trending dates. When soils are approaching saturation or wilting point, the average VSM value estimated by the GPR for the entire block overestimates slightly, about $0.05 m^3 m^{-3.}$. When the column sample is compared to each individual GPR reflector's estimate at depth, GPR overestimates the volume of moisture in 87.5 percent of cases (35 of 40) with the most extreme differences in individual estimates occurring during the two driest dates, and the smallest difference when the soils were trending toward saturation or above field capacity. While the closest single difference in measurements was very small ($0.006\ m^3 m^{-3}$) and was very close to the field sample (0.51 meters) others at the same distance on the same date showed a much larger difference ($0.106\ m^3 m^{-3}$). This pattern was generally observed throughout- distance from reflector to column sample showed no relationship at all. This is likely due to three major factors. One, the direct measurement of soils was not within the GPR footprint: they measure two different areas. For this reason, the RMSE values reported apply to the entire study area, and do not represent average squared distance of *concurrent* reference measurements. Two, the differences observed between the column

sample and the GPR VSM estimate are due to the natural horizontal variability of soil moisture even at a short distance, and three, some error is inherent in the hyperbolic fitting process.

This study also reveals that broad fluctuations in water content did not drastically affect the visibility of a large historic pit in GPR surveys within Masada fine sandy loam soils. For visual interpretation purposes, moisture conditions near field capacity show that the transition between the burned layer and its smothering cap was best articulated. It is also notable that under conditions just above the wilting point, the radar plan view of the feature's west end changes to a more rounded shape, suggesting that when the soils are drier, the burned transition is less articulate around the pit edges, and that the contrast in compactness and water holding capacity of the pit fill and the soil matrix may also be contributing to the articulation of this feature's shape.

While this work indicates that a monostatic GPR antenna commonly used for archaeological prospection is an excellent estimator of average soil moisture conditions over a small area using naturally occurring reflectors, the VSM observed at each individual reflector was not tested and only suggests how well the direct measurement and GPR estimates match. Future works that wish to further test the GPR system in this study and its ability to more precisely report the volume of moisture above a point should consider using the hyperbolic reflector method in conjunction with measuring VSM above continuous horizontal reflections where the depth to the reflective surface is precisely known.

CHAPTER IV

REPRESENTING THE HIDDEN CULTURAL LANDSCAPE AT HOUSE IN THE HORSESHOE USING GEOPHYSICAL REMOTE SENSING, SCIENTIFIC VISUALIZATION AND CARTOGRAPHIC METHODS

This chapter is a manuscript prepared for submission to *Southeastern Geographer*.

4.1 Introduction

How can historic cultural landscapes of the past be visualized when their architectural elements are no longer standing or visible on the earth's surface? Geophysical sensors offer a potential solution, and are increasingly used by scholars and site managers to map the distribution of buried cultural features on historic and prehistoric sites. While sensors such as Ground- Penetrating Radar (GPR), magnetic gradiometer, and electromagnetic induction (EMI) provide a fast, non-destructive mapping solution for finding buried objects, they also present a unique problem: what are effective ways of representing cultural features that are not visible, using subsurface contrasts in physical properties of matter that are also not visible to the unaided human eye? The results of geophysical remote sensing surveys require scientific knowledge and experience to interpret, but must eventually be effectively communicated to many audiences, including other geophysical surveyors, officials working for the State Office of Archaeology or State Historic Preservation Office, cultural resource management (CRM) and academic archaeologists, site managers, the contractors that they employ, and

those that visit a site to learn about its history. The goal of this paper is to examine effective methods of presenting the results of geophysical surveys for different audiences using House in the Horseshoe State Historic Site, in Moore County, North Carolina.

4.1.1 Geophysical Sensors

Aerial photography and satellite imagery have long been used to map the distribution of cultural landscape modifications when they are visible at the surface of the earth (Clark 2001, Avery and Berlin 2004, Giardino and Haley 2006). Cameras that enable the capture of traditional imagery respond to frequencies of electromagnetic energy that are within the visible spectrum as they reflect from surface objects, or to long wave infrared radiation that is emitted from the earth's surface (Avery and Berlin 2004; Jensen 2016). Alternatively, ground based geophysical sensors respond to contrasts in invisible electrical or magnetic properties as they vary in the shallow subsurface. GPR, magnetometers, and EMI instruments in particular have undergone significant refinements in recent years, resulting in increased use for understanding the distribution of features on culturally significant sites without disturbing the earth. Each instrument has its own strengths and weaknesses when applied toward the mapping of cultural features, and has the potential to add its own unique *supplementary* information to a map or image, or offer additional *complementary* information when an object is visible to multiple instruments (Clay 2001, Turner and Lukas 2016).

GPR detects buried objects by transmitting energy in the radio wave portion of the electromagnetic spectrum into the soil via an antenna or antenna pair. Subsurface contrasts in Relative Dielectric Permittivity (RDP) are recorded using signal two way

travel time in nanoseconds, and return wave amplitude using a high resolution digital number, typically a sixteen bit signed integer (Conyers 2013a). Central antenna frequencies are chosen to locate cultural features based upon the depth of penetration needed, with the 400 and 900 MHz antenna most typically used for surveys seeking to resolve features within the upper meter of soil (Conyers 2013a).

Cultural and natural features imaged using GPR are represented within the vertical profiles and horizontal depth slices as localized areas where the returning wave amplitudes are noticeably higher than the background values. The increase in amplitude values that identify the objects of interest in profiles and slice maps are most often registering dielectric contrasts caused by differences in the distribution of water in the soil at a given time, or by differences in the density of buried features compared to that of the surrounding soil (Conyers 2013b). On historic sites, GPR is often very successful at finding larger, structural features such chimney remnants or piers that contrast significantly in compactness and water holding capacity with the surrounding soils, in addition to large pits or cellars that contain concentrations of reflective debris and sometimes layering of backfilled soils with different levels of compactness (Stine et al. 2013). Objects or phenomena imaged with GPR are often very precisely located on the horizontal plane, and with excellent representation of actual feature shape when imaging distinct, discrete structural supports such as piers or other foundation elements that are not covered with rubble (Stine et al. 2013).

A gradiometer is a specially configured magnetometer that measures shallow subsurface variations in magnetism (measured in nanotesla, or nT, 10^{-9} T) (Clay 2001,

Aspinall et al. 2009). The instrument's sensitivity to ferromagnetism enables the detection of a large number of historic and prehistoric cultural features that contain iron or iron compounds (Kvamme 2008, Aspinall et al. 2009). This includes iron objects, or pit or trench features that are visible due to their infilling with soils that contrast in magnetic susceptibility with the surrounding matrix (Clark 2001, Dalan 2006, Aspinall et al. 2009). Soils containing iron compounds in which individual grains express weak and randomly oriented magnetic fields can become collectively oriented, strengthened, and made permanent by exposure to fire- a characteristic known as thermoremnance (Clark 2001, Aspinall et al. 2009). Thermoremnance is observable in conjunction with underpinnings of structures that have been burned to the ground on historic sites, or have incorporated fire as a part of their normal functioning. Additionally, bricks express dipolar characteristics (visible positive and negative magnetic field components) due to thermoremnance (Aspinall et al. 2009). While the independent polar characteristics of single bricks cancel themselves or are weakened when intentionally arranged in structural supports (Aspinall et al. 2009), shallowly buried bricks can appear as isolated objects or as scatters of rubble (Stine et al. 2013). The physical boundaries of objects imaged with magnetometers and gradiometers are generalized, and likely only provide a suggestion as to the actual shape of larger features as they appear in the ground (Hargrave 2006). Isolated objects comprised of very different materials, such as bricks or pieces of iron in soils, often display similar dipolar characteristics, making it difficult to positively identify an anomaly's source by image interpretation alone

EMI instruments are used in the agricultural and soil sciences to rapidly characterize soils (Doolittle and Brevick 2014), and have a record of successful identification of features on historic sites (Bevan 1998, Clay 2001, Kvamme 2006). The latest generation of EMI instruments with close coil spacing (~1 m) are able to measure soil conductivity (in milisiemens per meter) and magnetic susceptibility (in parts per thousand) simultaneously at different depths (Doolittle and Brevick 2014). Historic and prehistoric human activities associated with fire, bricks, or ferrous metal are known to enhance the magnetic susceptibility of soil. (Dalan 2006, Kvamme 2008, Aspinall et al. 2009). While natural processes also and often contribute to increased magnetic susceptibility (especially in upper soil horizons), general regions of human activity can be made visible in changing background trends of magnetic susceptibility data (Horsley et al. 2014). Additionally, individual cultural features may be expressed in magnetic susceptibility images, displayed as localized anomalies where soils have been heated, where enhanced topsoil is backfilled into trenches, cellars, or pits carved into a less susceptible matrix, or where other magnetically enhanced objects are decomposing in the topsoil, such as bricks and metal objects (Dalan 2006, Aspinall et al. 2009). While there is some overlap in what is visible in magnetic susceptibility data from EMI and magnetometer images, EMI instruments that measure magnetic susceptibility are active sensors that register only the induced or temporary magnetic component, and do not respond to the permanently magnetized component of objects or soils. Magnetometers and gradiometers are passive and respond to both (Dalan 2006, Kvamme 2008).

Variations in soil conductivity are primarily related to the distribution of soil water content, which is directly related to pore space and particle size among other factors, allowing spatial variations in soil texture to be visualized (Grisso et al. 2009, Doolittle and Brevick 2014). Sites that contain soil features such as pits, mounds, trenches or other forms of earthworks where such features contrast with the undisturbed surrounding soils are good candidates for conductivity survey, as well as sites with features that are low in conductivity, such as brick or stone underpinnings (Clay 2006). EMI meters also function as standard metal detectors do, but with separate, widely spaced coils, and are sensitive to many types of metals (Bevan 1998; Clay 2006). While metal objects may be the targets of interest, many sites have modern metal refuse within the topsoil, which potentially complicates pattern recognition of features in conductivity images of historic sites (Clay 2006).

Most frequently, geophysical surveys are conducted within a georeferenced data collection grid or from a baseline established before the actual survey begins, although instruments equipped with Global Positioning Systems (GPS) are now becoming more common. Grid data collection utilizes square data collection units laid out by tape measure or total station. Grids provide a framework for systematic random sampling, are a convenient way of organizing and communicating about the area to be covered and processed in the field and in the lab, and also insure that instrument reading positions closely correspond to one another when multiple instruments are to be compared. Within the grid squares, baseline tapes establish the start and stop points for survey transect tape lines, which are then laid out at a particular interval that in part determines the density of

data collection points and the minimum pixel resolution possible for the raster output. After conducting set up routines for each instrument, each is either pushed along the transect lines or carried at a sampling pace that is set according to the comfort level of the instrument operator. Survey grids can be georeferenced a number of ways, with the most accurate methods including working from pre-established state or national geodetic survey benchmarks, static data collection with survey grade GPS used in conjunction with total station, or simultaneous stake out and georeferencing using Real Time Kinematic (RTK) GPS.

4.1.2 Scientific Visualization and Cartographic Representation of Survey Data

Following field surveys, the raw data must be converted to spatial information, and in the final step, be presented in a way that effectively communicates the study results (Jensen 2016). The connection between these two steps in the Remote Sensing Process is represented by a continuum of visual thinking followed by visual communication in which spatial patterns within the raw data are sought, hypotheses about the patterns are tested, and information is synthesized as different lines of evidence are consolidated. The explanation of the final results are represented in a map or a series of maps and charts (DiBiase 1990; MacEachren 1994; Jensen 2016).

In the conceptual model described by DiBiase (1990) (Figure 4.1), scientific visualization has a private and public viewing side, depending upon the audience. Visual thinking occurs in the mostly private viewing realm of the analyst who has specialized knowledge. When considered within the scope of the Remote Sensing Process (Jensen 2016), visual exploration and pattern confirmation is the process of interpreting images

that are not yet classified or symbolized, as a final graphic or map might appear (MacEachren 1994).

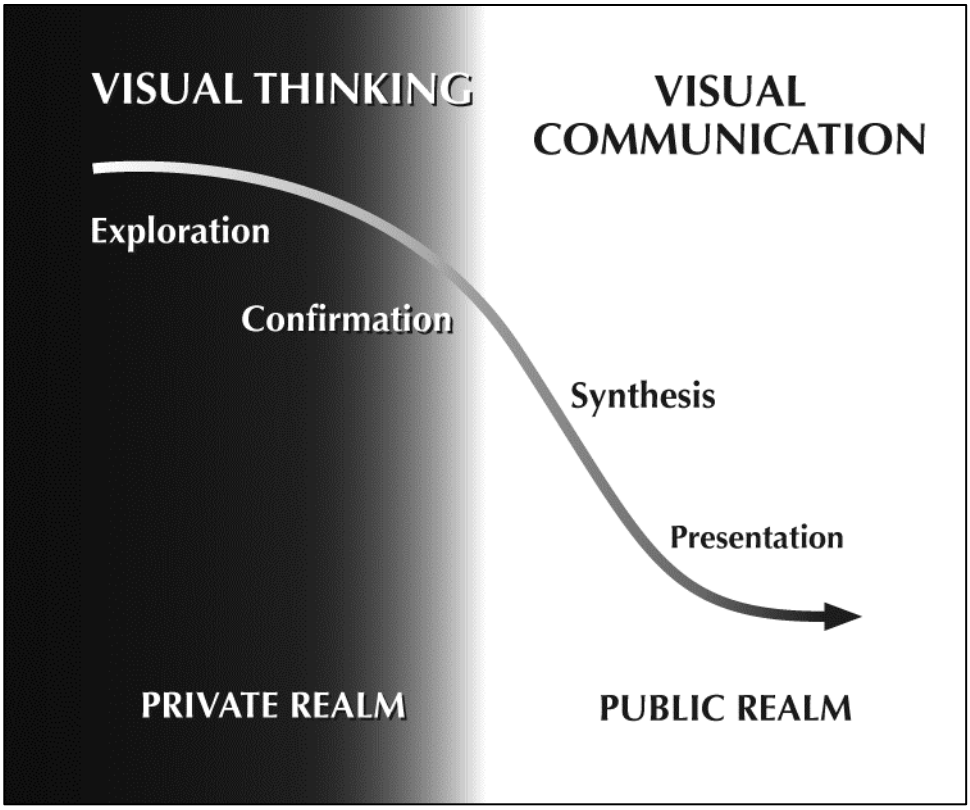

Figure 4.1. The Range of Functions of Visual Methods in an Idealized Research Sequence. From Visualization in the Earth Sciences. David DiBiase 1990. Reproduced by permission of the author

At this stage, experts determine what patterns exist, if any, and explore different methods of confirming or disproving data interpretations. In Figure 4.1, synthesis and presentation of data trend toward the public realm, where the analyst must explain the case that they are trying to make, but with a reduced version of the data that displays only the most important information symbolized on a map. The curve in the diagram represents the amount of data present in the map or image, the degree of interaction with data, and also

according to DiBiase (1990), the reduction of higher order thinking as one moves from the private view of the experts realm of knowledge into the public realm of the results presented to the interested layperson.

Kvamme's (2006) work pertaining to scientific visualization of multiple geophysical instrument surveys states that results are often interpreted as images placed side by side, and can benefit from being visualized simultaneously via data fusion methods. He divides fusion techniques into three broad categories: graphical, discrete and continuous. Fusion may allow the researcher to see patterns that are not visible with a single instrument, gain more complete information pertaining to the shape, position and condition of buried features, and may also help those who use the sensors gain a better scientific understanding of how the electrical or magnetic properties are related. This pioneering data fusion work establishes the need for improved representations of historic features within a single *image*, and also indirectly suggests a method of extracting cartographic objects from imagery by using a binary classification system. The reduction of geophysical data to the essential hidden structural elements for viewing in a traditional map offer an effective way of visually communicating survey results that can be understood by the general public.

4.2 Previous Work

House in the Horseshoe, located west of Sanford North Carolina, is a historic site managed by the North Carolina Department of Natural and Cultural Resources Historic Sites Division (North Carolina Historic Sites 2017). The house was built in 1772 or 1773 for Whig Colonel Philip Alston, and is most notable due to an armed conflict between rival militia groups that occurred there during the American Revolution in Moore County, North Carolina. In July of 1781, Alston was attacked while inside the house with his wife and children by Tory Colonel David Fanning and a small group of militia men. The house and surrounding grounds were also owned by North Carolina Governor Benjamin Williams from around 1798 to 1814, who named the plantation "Retreat" (Willcox 1999:296).

The house was the center of a slave managed agricultural plantation, from the time that it was built, and likely up to the time of the American Civil War (Willcox 1999). Plantation landscapes have been the subject of detailed studies and are usually characterized by a main house accompanied by buildings designed for a particular purpose (Vlatch 1993, Olmert 2009). While the Alston house remains in the same place where it was built (Wilcox 1999), most of its early historic outbuildings have been removed and are no longer visible at the surface. In his exhaustive research of the sites history, Willcox (1999:298) reprinted a letter written by Governor Williams, detailing the improvements to the house and grounds that made his Retreat a "tolerable" place to live, such as large extension wings on two sides of the house itself, a smokehouse, granary, dairy and barns. While Willcox reports the presence and destruction of other buildings

throughout the houses history of owners, little is known about the arrangement of outbuildings during the earliest decades of the houses existence (Harper 1984), or the precise locations of many constructions reported in later years. Baroody (1978) conducted a traditional archaeological survey at House in the Horseshoe, using a powered auger and steel probe, in conjunction with oblique infrared aerial photography in an attempt to locate building remnants onsite. Probe and auger methods were successful in revealing the location of a buried walkway leading to the house, the possible location of two granaries, and possibly the location of an external kitchen on the west side of the house that is reported by Baroody (1978) to have burned in 1804, but with no supporting documentation.

While the geophysical surveys presented here were designed to answer specific questions at House in the Horseshoe, the scope of the geovisualization study in this paper is dedicated to expanding the work of Baroody (1978) that sought the locations of historic outbuildings within the state managed House in the Horseshoe property boundary. The work commenced following the invitation to conduct surveys by Deputy State Archaeologist John Mintz and Marty Matthews of North Carolina State Historic Sites. The areas covered were recommended by the site manager at the time when surveys began, John Hairr (2013, personal communication: conversation).

4.3 Methods

A georeferenced data collection grid with ten meter square sections was as established in the northeast yard at House in the Horseshoe, with a single detached four by ten meter section, totaling 2,840 square meters in total survey area (Figure 4.2).

Figure 4.2. House in the Horseshoe Geophysical Survey Area

Three sensors were used to survey the open flat area shown in Figure 2: A GSSI SIR 3000 GPR equipped with a three wheel survey cart, distance encoder and 400 MHz antenna, A Bartington 601 dual sensor magnetic gradiometer, and a Geonics EM38 MK2 EMI instrument that recorded conductivity and magnetic susceptibility simultaneously in vertical dipole mode, using the one meter coil separation. Survey transects traversed by

all instruments were placed at half meter intervals, with eight samples per meter for EMI and gradiometer datasets, and fifty traces per meter for GPR.

In the laboratory, data from each sensor was initially processed using specialized programs dedicated to handling the data collection issues associated with each instrument. These included TerraSurveyor (v3.0.29.1 DW Consulting, Barneveld, The Netherlands) for destaggering gradiometer data, RADAN (v7.3.13.1227 Geophysical Survey Systems Inc. Nashua, New Hampshire) for GPR vertical profile processing into horizontal depth slices, and DAT38MK2 (v1.12 Geonics Limited, Mississauga, Ontario, Canada) for processing raw EMI transect data into separate magnetic susceptibility and conductivity images. Except for the gradiometer images, all data were then imported to Surfer (v 10.7.972 Golden Software Inc. Golden, Colorado) so that each could be interpolated to a common resolution and ASCII raster format. Finally, all images were imported into ArcGIS (v 10.3.1 Environmental Systems Research Institute, Redlands California) for georeferencing, interpretation, image fusion, , and cartographic work.

Following initial processing, interpretation and fusions, geophysical features of interest that were deemed cultural in origin were confirmed via direct observation using several methods: metal detection, bucket auger, probe, soil coring tool, shovel tests, and excavation units. These methods allowed the analyst to confirm the source of most anomalies in the images, and to determine a cultural association and potential date (Turner and Lukas 2016). The historical record (Willcox 1999), previous archaeological research (Baroody 1978; Harper 1984) and historic aerial photography (Moore Maps 2017) were also used to inform the interpretation of patterns observed in each dataset.

The private process of scientific visualization as it applies to the manipulation of geophysical survey data toward meaningful public view of structural representations was detailed, and as a final stage, a series of maps were created that communicate various types of information to different audiences: side by side interpreted images from each instrument, graphical and discrete fusions representing data reductions, and a traditional map combining spatial data from different sources showing hidden and visible architectural elements at House in the Horseshoe.

4.4 Results/Discussion

The exploration and interpretation of individual instrument data began during the private viewing stages of image processing (Figure 4.3). The specialized software packages offered the first on-screen visualizations and were visible only to the analyst with no classification or symbolization. During this stage, anomalies likely to be structural remains or at least of cultural origin were first identified. Each layer was enhanced according to the processes indicated in Figure 3, with the goal of allowing the greatest number of shapes or patterns to be visible at once, and so that more subtly expressed anomalies were not accidentally removed. The processing stage required constant data interaction and visual re-assessment focused solely on clarifying the images, without the benefit of other spatial data sources. After the stages of initial processing, the resolution of 0.125 m was applied for interpolation to the ASCII raster format in order to match the eight samples per meter established by the gradiometer's maximum density settings. The images were then imported into a GIS for final co-registration.

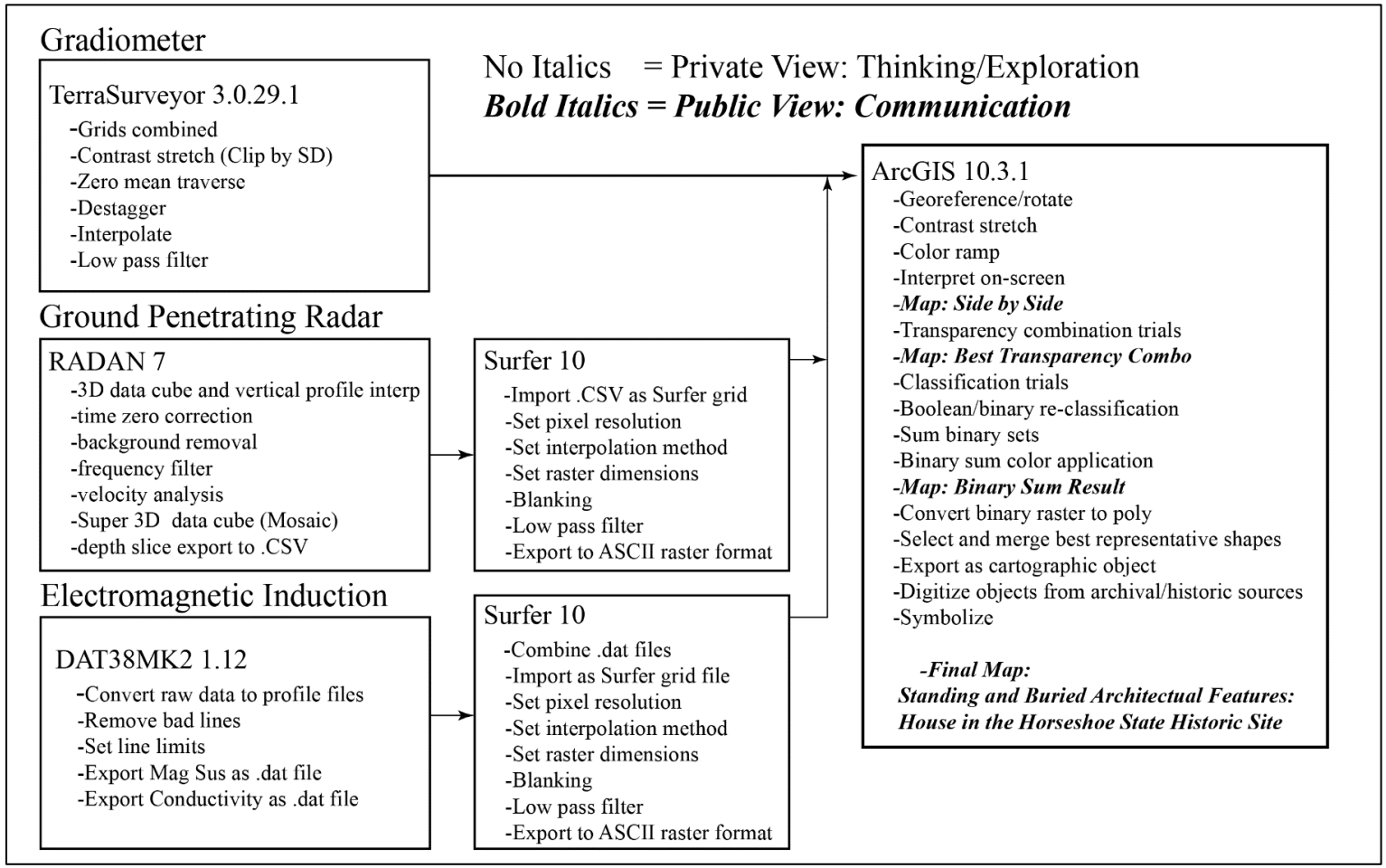

Figure 4.3. Stages in the Scientific Visualization Process

Once imported into a GIS, the visualization task at hand shifted from image processing to determining the source and significance of the objects visible within them, and the relationships between sensors. In the on-screen view of images, a grayscale color scheme and standard deviation contrast stretch were applied, so that the features visible in the processing stage were also visible when co-registered and displayed together at the same resolution. Grayscale is most frequently used by professionals for viewing magnetometer and gradiometer data, and is a preferred choice for viewing conductivity data (Clay 2006). While the application of different multi-color ramps enabled objects and trends to be more visually distinct in some cases, the application of too many colors in a single ramp made positive and negative features, or the intensity of readings difficult to visually identify.

The annotated maps from each sensor are displayed side by side in Figure 4.4, with the focus placed upon presentation of processed images to explain interpretations and sensor response**.** Four possible structures or structure areas were initially noted in the 4 data sets based on distinctive square foundation shape (Structure One), patterns and shape associated with underpinnings and rectangular fill zone (Structure Two), vertical profile pattern and rectangular shape in horizontal slice map as a large pit/cellar/privy filled with reflective objects (Structure Three, and as localized but random patterns caused by metal debris scattered close to the surface in the plow zone (Structure Four area). While all of the structural anomalies were ground truthed in the field to identify association with a cultural period and anomaly source, GIS allowed the private visualization of other relevant spatial data to aid in confirmation. Historic aerial

photography was used to determine when Structure One was removed from the landscape. Georeferenced excavation maps of Baroody were also consulted to determine generally how probe survey maps and auger tests coincide with the geophysical data, and what artifacts were observed in association with Structure Four area.

The geophysical interpretation maps of Figure 4.4 represent the first public facing view of the data, intended for a small but growing audience of subject matter experts and those with potential interpretive input. The primary audience for these maps include archaeological geophysics professionals, Geography and Archaeology Remote Sensing students, and more traditionally trained professional and academic archaeologists who want to learn how common historic site features are detected by different instruments. Even for the trained expert, a major challenge of side by side presentation in maps is in the difficulty of seeing the spatial relationships between the anomalies or patterns that appear in separate images. The reader is left in an awkward situation in which they must mentally superimpose each survey. Data fusion techniques were employed to view all features of interest at once without heads-up digitization.

Of the fusion methods, a graphical two layer overlay (semitransparent conductivity over GPR, Figure 4.5) presented all of the structures together in the same image with the greatest clarity. The conductivity transparent overlay for this particular site also allowed the visualization of areas in the northern yard where the topsoil has mostly been removed (Baroody 1978), and that the hillside in the central western most portion of the grid has many large rocks, arranged in a push-pile like shape, as indicated in the non-transparent GPR.

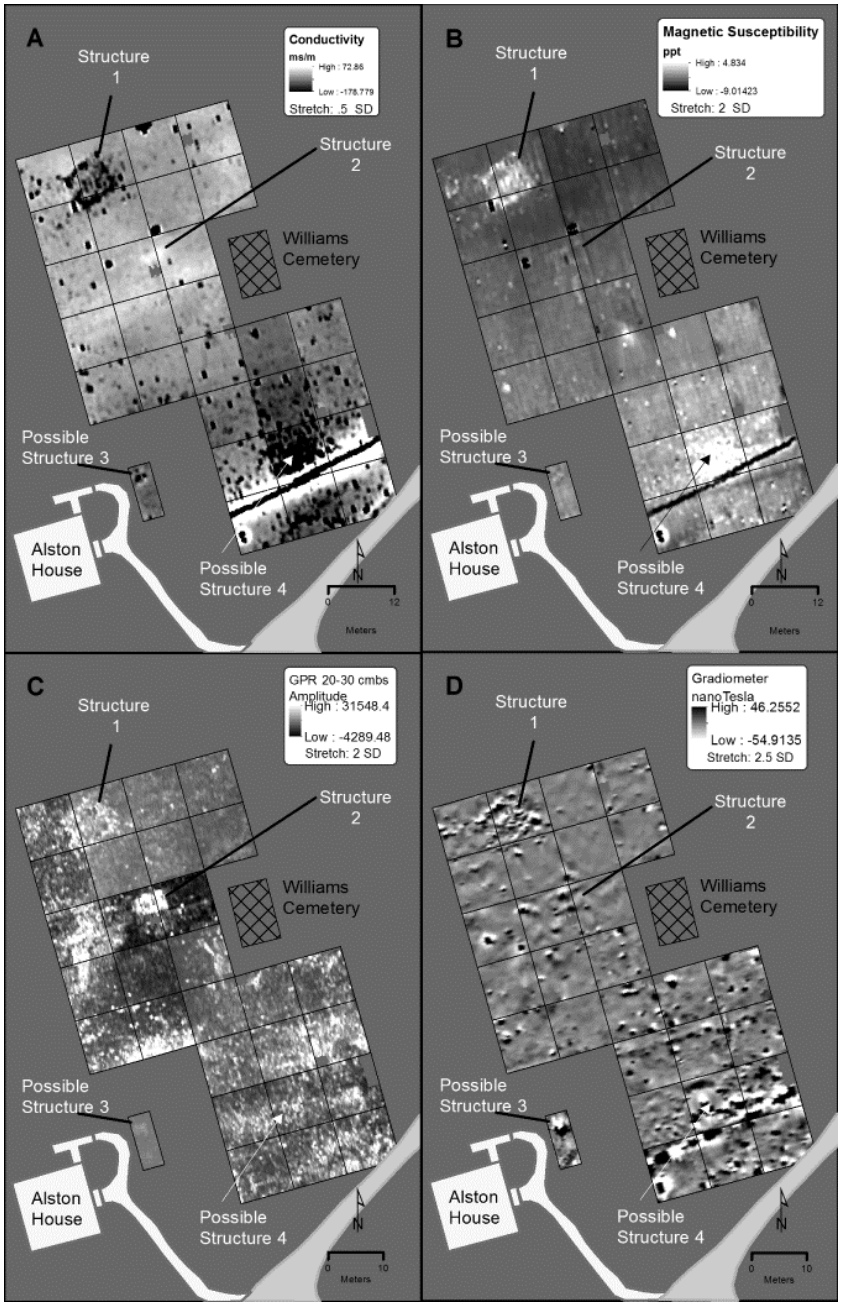

Figure 4.4. Geophysical Survey Results.
A. Conductivity B. Magnetic Susceptibility C. GPR D. Magnetic Gradiometer

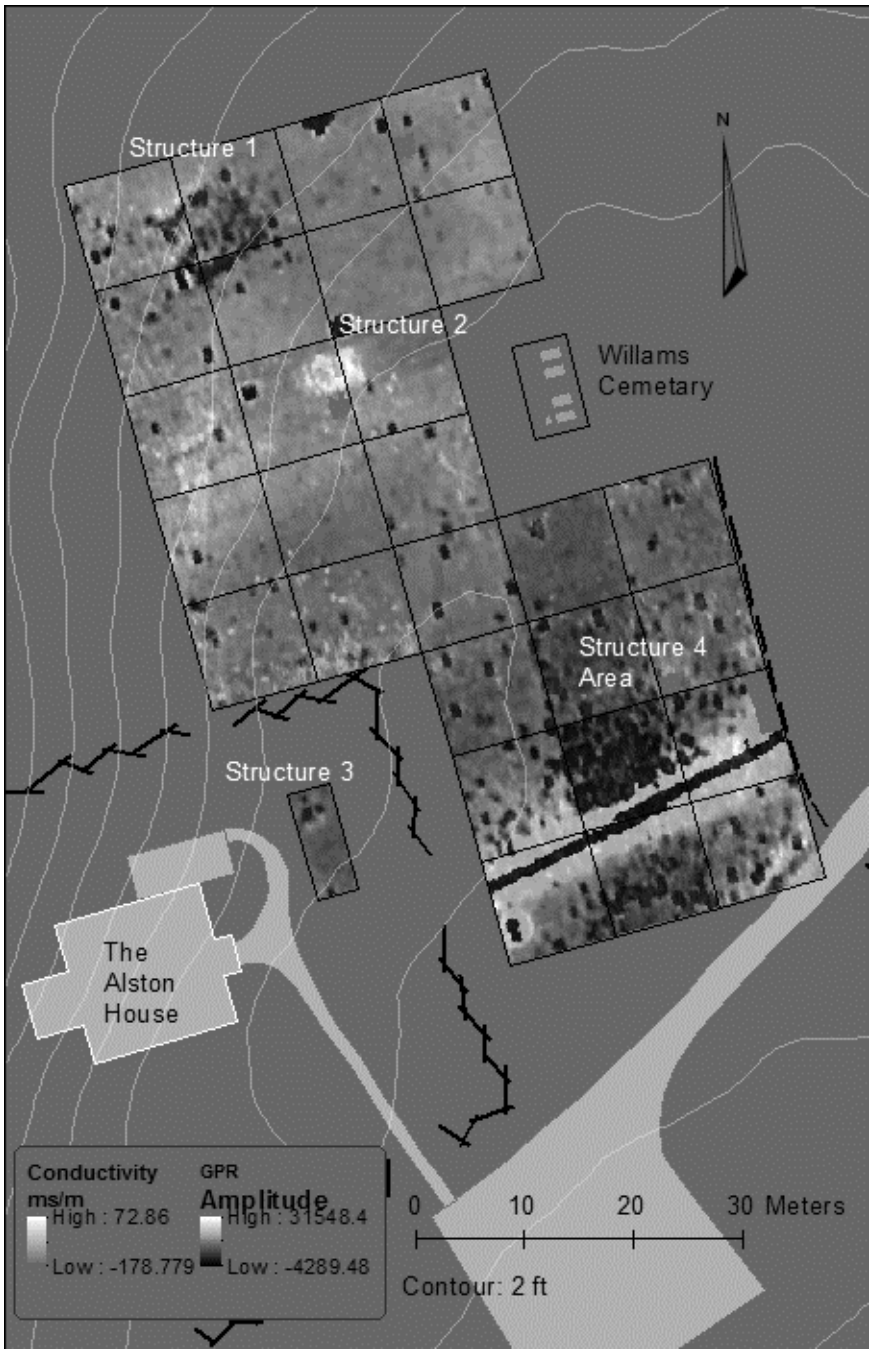

Figure 4.5. House in the Horseshoe Graphical Fusion, Semitransparent Conductivity Over GPR

These observations are important to a site manager or archaeologist, who are interested in knowing where soils have been disturbed. Disturbance indicates a higher likelihood that cultural features are also partially disturbed or destroyed in those areas, and that artifacts recovered in these zones are not likely in their original context. While this visual combination is useful for the trained analyst to explain the spatial extent of disturbance and the arrangement of structures onsite, it is not readily interpretable by most audiences without an explanation. In order to tie the geophysical image fusion to the landscape for improved interpretation and explanation to non-experts, the public facing image fusion map includes traditional map elements, such as cartographic representations of the sites central architectural feature, and contours.

Discrete fusion methods reduce the amount of data present, placing the raw continuous instrument data into hard categories that indicate where features exist. Kvamme (2006) noted that many features within geophysical data sets can be identified in the tails of the distribution curve, and that isolating those extreme values is a potentially effective method of determining what is detectable by each individual sensor. Using this method, continuous data from each survey were classified into binary categories (1= anomaly present, 0 = no anomaly present) shown in Table 4.1, which effectively separated the strongest anomalies from background values. The binary data was then added together to create a binary sum image of all instruments, which resulted in pixels fitting in a range from zero (no anomaly present) up to the total number of instruments (four) used in the study (Figure4.6A and Figure 4.6B

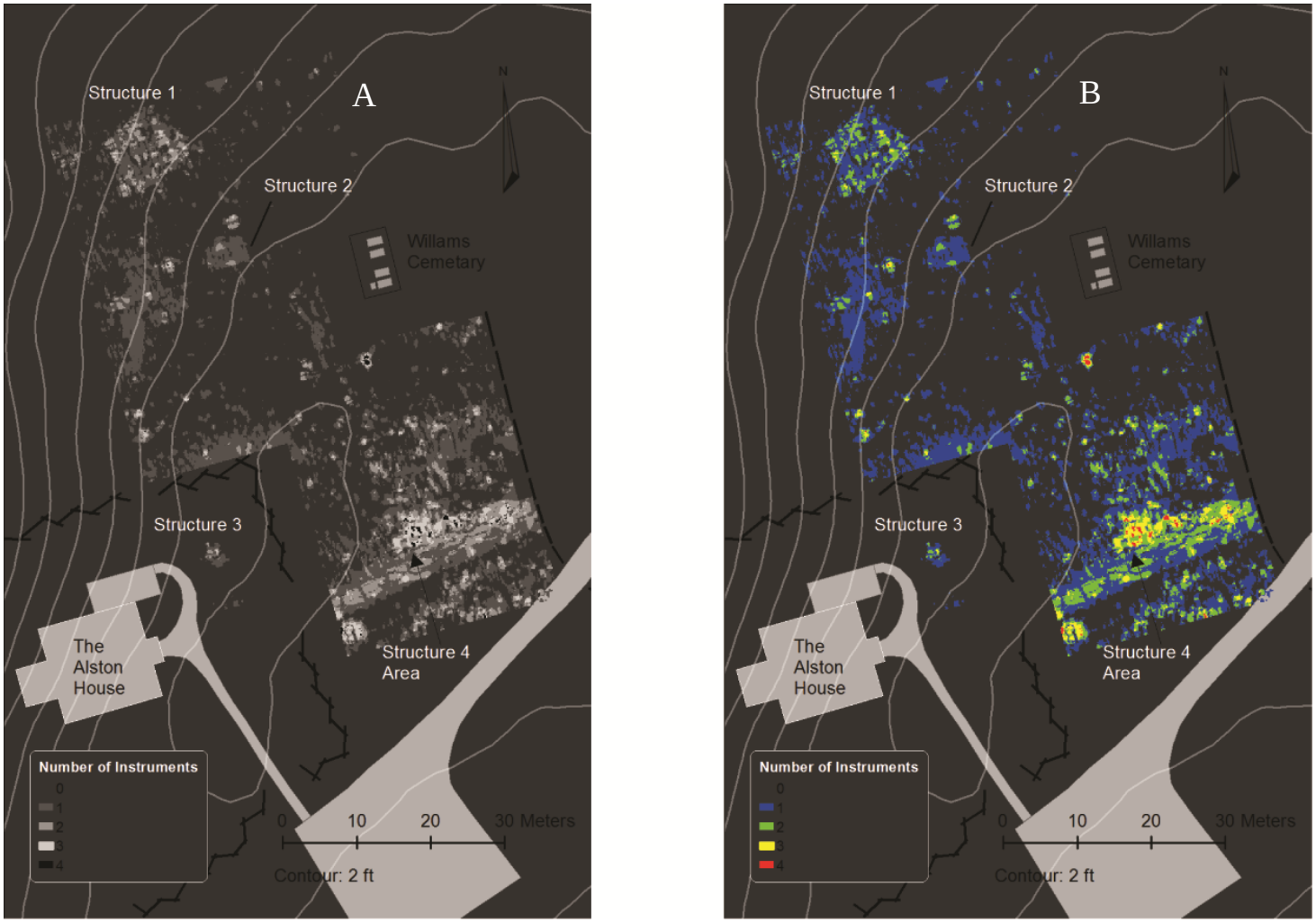

Figure 4.6. Discrete Fusion Example, Binary Sum. A. Grayscale Color Scheme B. Color Blue Green Yellow Red

Table 4.1. Threshold Values Denoting Anomaly Ranges for Each Sensor

Image	Min	Max	Expression for Values Reclassified as 1
Magnetic Susceptibility (ppt)	-9.01	4.83	Value < 0 OR Value > 2
Conductivity (ms/m)	-178.78	72.86	Value < 0 OR Value > 10
Gradiometer (nT)	-54.91	46.26	Value <-20 OR Value > 20
GPR (amplitude)	-4289	31548	Value > 1000

The results of binary sum in Figure 4.6 show how many sensors indicate that anomalous values are present. This approach to fusion does not allow the identifying instrument to be known, only that there is a higher likelihood that feature exists in a given area (Ogden et al. 2010). Additionally, not all positive values within the binary sets actually indicate the presence of an archaeological feature of interest. In the original version of Figure 4.6 (see Figure 4.6B), color was applied to the values for rapid identification of features, which indicated in the Structure Four area that a post or pier pattern may exist. Metal detection and bucket auger tests during ground truthing revealed that both magnetic surveys and conductivity data were responding to concentrations of small metal objects in the plow zone. This is corroborated by the work of Baroody (1978), who illustrates that nails were recovered in the area. Additionally, no piers or other intact foundation is evident in GPR vertical profiles or slice maps corresponding with the area (Turner and Lukas 2016). While difficult to convey here due to scale and color restrictions, if an analyst or site manager had only the benefit of the binary sum map, they might assume that piers are present just beneath the soil. While color maps may create the illusion of structural features in this instance, the application of color to this type of image may strengthen the interpretability of features in other circumstances,

especially when intact structural features exist, and there are fewer small metal objects present in the soil. This result indicates that care must be taken when ground truthing and interpreting the original images, and the need for more than one method of visualizing survey results. In this example of binary sum, the maps are best kept within the private view of the analyst to avoid incorrect assumptions about hidden cultural landscape features, or at least presented to the public alongside other clarifying maps and explanations.

The on-screen, side by side and image fusion presentation methods of visualizing structural features demonstrated thus far are not easily understood by most viewers. A more traditional map is needed to visualize the results for those only interested in the architectural layout of the site. The creation of layers for the binary sum image revealed an effective method of simplifying raw instrument readings to cartographic objects for this purpose. The reasoning and binary classification process is explained here, using soil conductivity as an example.

In order to isolate conductivity anomalies that are potential features, the distribution curve for the image was first examined in order to determine the cutoff values for separating the main body of data from the tails (Table 4.1 and Figure 4.7). The background values shown in the center spike mostly represent the electrical conductivity of the soil matrix, which is a Masada fine sandy loam 2 to 8 percent slopes (NRCS 2017). The table in Figure 4.7 indicates that loams minimally register 5 ms/m or higher. It can be observed that the most frequently occurring pixel values from the House in the Horseshoe conductivity survey are consistent with the minimum value for a loam or slightly higher.

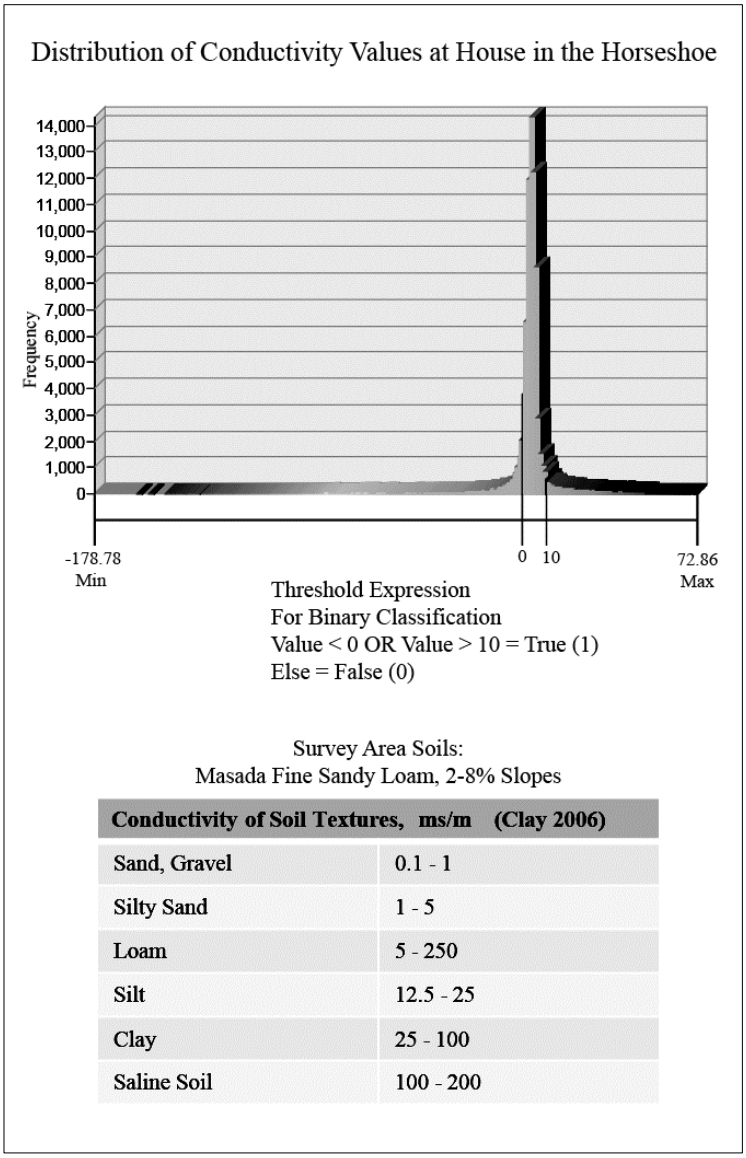

Figure 4.7. Binary Threshold Example Using Conductivity

Most of the data also have a value greater than zero, which is consistent with the minimum of possible values shown in the table. The values below zero make a reasonable threshold for the tail because they may represent low conductivity archaeological features (Clay 2006), and in the more extreme negative values, metal

objects (Bevan 1998, Geonics 2015). Metal near the surface can cause the instrument readings to spike in the positive direction as well, the direction of the erratic response to metal depending upon the orientation of the instrument relative to the object, and the objects size and shape (Geonics Limited 2015). Ten ms/ m was chosen as the positive value threshold after these considerations, by manually placing the category break at the beginning of the slope of background values, and confirming this placement after on-screen visualization of the effects of several thresholds. Boolean logic was then used to create a new image that recoded all values into binary classes that fit within the specified ranges established for the tails (1), or did not (0), as shown in the expression in Figure 4.7.

The four structure areas were examined within each of the individual binary datasets after they were first used as layers in the binary sum, in order to determine which set offered the most discrete, cleanest representation without the summing operation. The best representatives were isolated from the binary data, and combined into a single vector file to be used as cartographic objects. These subsurface architectural feature remnants were symbolized using black to separate them from surface structural elements shown in white, in the most public friendly map, which is focused solely on the architectural landscape at House in the Horseshoe (Figure 4. 8). The traditional map communicates in a concise way the geophysical survey result as it pertains to buried structures that were reasonably confirmed, without the clutter of random objects and noise shown in the raw survey data. The date and primary function for structures are also presented, which were derived following an analysis of nails and ceramic artifacts. This presentation view

contains the synthesis of the geophysical mapping effort with other subsurface structural remains from Baroody's map, and currently standing structures, offering a view of the architectural features that are known at House in the Horseshoe.

4.5 Conclusion

The roles that geophysical survey and scientific visualization played in developing information about the historic landscape at House in the Horseshoe are many. Much of the visualization involved exists within the private view of the analyst. In the initial private data exploration phase, each survey's data layer was interpreted individually as it was interactively viewed and processed, without symbolization or overlaid spatial data. While the maps that feature the initial private on-screen interpretation were published in a public forum (Turner and Lukas 2016), they require explanation to be understood; the images displayed within them are not symbolized or classified. This was done to accomplish the goal of providing examples of geophysical imagery of a historic site for a small audience, consisting of those who would like to know how such instruments detect cultural features. Also during the private exploration phase, the data layers were fused together using a variety of methods in an effort to create a comprehensive site planview of subsurface features in a single image. Two results were notable: a two layer semi-transparent overlay and survey data classified into binary categories that were added together in a binary sum. These fusions were conducted with the intent of consolidating instrument readings that indicate the presence of subsurface structural remnants.

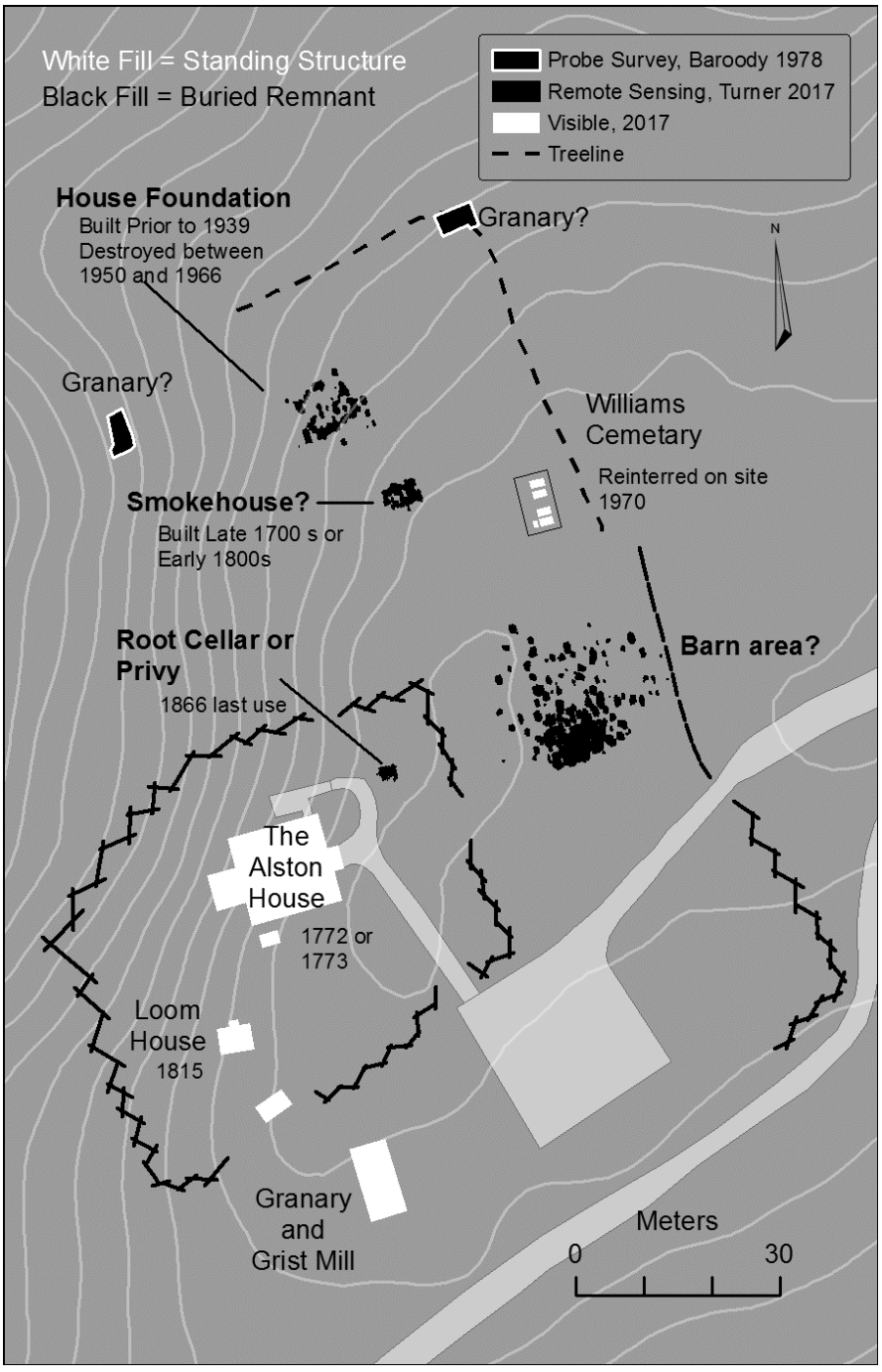

Figure 4.8. House in the Horseshoe: Standing Structures and Buried Structural Remnants

From the private vantage point of the analyst, the transparent overlay of just two data layers contained a good combination of images for structural feature visualization such that the contribution of each instrument was still somewhat evident, and allowing site disturbance to also be visible. The transparency result is still an abstract view that does not classify or symbolize the objects within them into discrete categories, and is likely better for a small audience of other geophysical surveyors and site managers. Binary segmentation and binary sum of all anomalous instrument readings had the effect of creating discrete categories, but obscured the instrument input. While this method resolved structural features in the northern survey area, areas containing metal objects in the uppermost layer of soil created the impression of post or pier like features that likely do not exist. However, this method has potential for creating site planviews where solid architectural remains exist beneath the surface, and less clutter exists.

In the public presentation phase of the Horseshoe geophysical work, a traditional map was created so that buildings currently existing on the landscape are visible with the former positions of structures, indicated by a simple black and white color scheme. The cartographic representation of each of the buried structural remnants were isolated from the continuous raster data by partitioning all data values that appear in the tails of each raster datasets distribution, and then selecting a representation for each structure based on the discreteness of its appearance from a single layer or instrument. The traditional map presents confirmed structure locations and exludes the continuous array of survey readings that make the final results difficult to interpret for those who simply want to know more about the architectural history of the site.

The work at House in the Horseshoe suggest several things in general about using scientific visualization in conjunction with GPR, magnetometer, conductivity, and magnetic susceptibility to understand the buried past. The side by side visualization of raw data presented with annotations that explain an analysts interpretations are an effective means of sharing information with other analysts and those who would like to learn more about geophysical image interpretation. Therefore while it always begins there, the single instrument or side by side display of raw geophysical data of historic sites is not always restricted to the private realm of the scientific visualization process. However, in order for the interpretations to make sense to those less accustomed to interpreting this type of image, a public facing view of raw data must be accompanied by other relevant surface objects and written annotations. These can be stylized from current orthoimagery, total station survey, historic aerial photography, and maps from previous site investigations. Data fusion allows the analyst in the private view to see the relationships between buried structural remnants and disturbances by viewing multiple datasets at once, but also has the potential to conceal the source and intensity of the contributing sensor. Fusion then, is better utilized as a tool for the trained eye seeking relationships in data as per the observations of Kvamme (2006) or at least presented with clear explanation of what is visible, and the effect that the application of data fusion has had on the image.

The theoretical model of the scientific visualization process as it applies to the use of geophysical mapping methods for understanding the architectural history of House in the Horseshoe has broader implications. While the majority of maps and images need an

explanation for the public viewer to interpret, smaller audiences comprised of specialists and site managers may benefit from visualizing geophysical data in a side by side presentation, or in a fused but still unsymbolized form. While the final map may seem to suggest that the isolation of architectural features for presentation is best, the exclusion of isolated metal, disturbed areas, and natural variations of background trends in data may be of interest to those who need to be informed about the integrity and context of historic sites. For future work, these observations indicate that when using geophysics for understanding historic sites that: the private, visual thinking side of the trained analyst plays a dominant and critical role in deriving useful patterns, that synthesis and interpretation is an ongoing process that is also largely private, and that ground truthing of detected objects is usually necessary to determine specific cultural association and for proper synthesis of information when undesired objects are present in the soil. Considering these observations, and that no site is identical to any other, it becomes clear that there is no perfect method for creating meaningful geophysics based maps of historic sites, and that experimentation is required to derive a clear fused image or map. The information illustrated during the final presentation phase depends upon the viewing audience, and understanding a site's history will be strengthened by presenting multiple views of the subsurface.

CHAPTER V
CONCLUSION

The overarching objectives of this dissertation were to connect current issues in geophysical remote sensing with the remote sensing process in the discipline of Geography. It examined the use of GPR, magnetic gradiometer, magnetic susceptibility, and the electrical conductivity of soil to detect buried structural remnants typical of historic sites, and focused on the sensitivities of a particular sensor, GPR. The images revealed structure remnants representing the buried and thus invisible portion of the cultural landscape at House in the Horseshoe, and placed them in spatial context with the house and other objects visible at the surface. The studies also presented image interpretation information pertaining to data types and the subsurface features that they represent that are new to geographic works. The ability of GPR to perform as a moisture quantifying tool as well as a subsurface mapping tool was examined for application to geomorphological and hydrology studies as well as cultural landscape research. Finally, cartographic methods for representing buried structural remnants were demonstrated, as well as GIS and image processing methods of integrating geophysical data into a single map. These topics were explored within the scope of three research articles.

The first article presented results of the multiple instrument study at House in the Horseshoe State Historic Site. The surveys captured four different structural features that exemplify the different types of outbuilding remnants that might be found beneath the soil on a historic site. These examples were investigated in the field by excavation, and in

the lab using the geophysical data together, and with other historic maps and imagery. The results visually demonstrate and discuss the relationship between sensors and how each individual sensor performed given the soil context and feature types onsite. The article also demonstrates the importance of ground truthing using traditional archaeological methods for understanding and interpreting the physical source of anomalies in geophysical rasters, and in understanding cultural associations.

The first article also found that GPR functioned with the highest degree of precision, and was able to offer highly precise estimate of both horizontal dimensions of features, and vertical depth to buried surfaces of cultural interest. As others have observed (Stine and Stine 2014, Patch 2016) it was also found that magnetic gradiometer is very effectively employed with GPR. The gradiometer resolved spatial patterns pertaining to the local magnetic disturbances created by objects such as piers and burned surfaces that were not as distinctly visible to the GPR. The gradiometer also suggested the form and condition of the features by expressing permanent magnetic dipoles, and more subtle areas associated with the increased magnetic susceptibility of heated surfaces. Magnetic susceptibility served as a complement to the gradiometer, but did not reveal patterns in the robust and distinct way that GPR and gradiometer did, and likely would not have made an effective prospection sensor on its own at House in the Horseshoe. Similarly, conductivity did identify most of the features detected by the other instruments, but only detected the most important and deeply buried intact features subtly, most crisply defining the boundaries of more shallowly buried and recent features that are not associated with the historical eras of the house. The implications of this work

are that GPR and gradiometer make a powerful combination for identifying historic features, and will likely provide sufficient results for site prospection without the inclusion of EMI. Most importantly, the structure examples serve as a geophysical image interpretation key for historical geographers, historic site officials and others who want to use the sensors to identify structures on other historic sites.

The second article examined the use of GPR to estimate soil moisture, and the effect of moisture conditions on archaeological features in GPR data. This was undertaken in an effort to develop a method of accurately describing antecedent soil moisture conditions when GPR surveys of historic sites are conducted, and to examine the accuracy and usefulness of a 400 MHz antenna to provide volumetric soil moisture measurements for non-cultural studies (soil hydrology, geomorphology) as well. The results show that when using a single direct measurement reference column to represent moisture conditions for a 4 m by 10 m area, hyperbolic reflectors used to estimate soil moisture overpredicted the volume of moisture in 87.5 percent of cases. It was generally observed that using hyperbolic reflections in conjunction with the Topp equation to estimate volumetric soil moisture (VSM) produced variable results that ranged anywhere from very close comparison (0.006 m^3m^{-3} difference in VSM estimates) to drastically different (0.20 m^3m^{-3}), with 72.5 percent of the observations less than 0.10 m^3m^{-3} in difference, and 10 percent of observations greater than 0.10 m^3m^{-3}. These results suggest that lateral variation in VSM between the GPR generated estimate and the directly sampled column may affect the observed difference, as well as measurement variability when using the hyperbolic arc fitting tool to measure the velocity of radar energy.

When the average relative dielectric permittivity of all reflectors within the total survey area was converted to VSM for a date, and then compared to the average VSM of all directly sampled levels, the results show near perfect agreement in estimation methods when soils are slightly below or at field capacity. The large historic pit feature did not change shape in the horizontal view of slice maps generated from each date except during the driest conditions. Moisture conditions just below field capacity for the upper 0.30 m of soil revealed the presence of a weak to moderate horizontal layer or transition within the vertical radar profiles that was later identified as a scorched surface layer to the pit feature. The implications of this work are that the reflector method typically used to estimate velocity and RDP for GPR surveys may offer an accurate *averaged* estimate of VSM when soils are at field capacity conditions, but is highly variable when all GPR estimates are compared with a direct sample taken within 4m of the reflector. The results also imply that Masada fine sandy loam moisture conditions just below or at field capacity may provide better resolution of zonation in pits when viewing the features in vertical profile. This suggests that surveys seeking similar historic features would maximize the interpretability of GPR data by timing the conduction of surveys according to near field capacity conditions.

Finally, the third article examined the role of scientific visualization in the process of interpreting, extracting information, and presenting geophysical survey results pertaining to the cultural historic landscape on a site. The article demonstrated that much of the processing that occurs following field surveys required interactive visualization to derive meaningful information, and was largely in the private view of the expert. It was

observed that map views designed to present results have to be prepared with interpretive annotations for the information contained within to be meaningful. Additionally, it was found that fusion methods of semitransparent overlay and binary sum of Boolean sets of House in the Horseshoe structures only slightly clarified the spatial relationships between the structure remnants visible, and that sensor knowledge was still required to interpret the fused results. The process of thresholding continuous geophysical data sets allowed the best representations of each feature to be isolated and extracted as a cartographic object, which was then used in a traditional map to present the survey results. The final map of subsurface structural remnants and visible structures presented the most public facing view. These results suggest that geophysical image presentation depends largely upon the viewing audience. The multiple views examined within also imply that geophysical remote sensors must experiment with different presentations, because site interpretations can benefit from multiple views that show different information. Additionally, each site encountered will present different conditions and features, requiring experimentation to get an optimal presentation view.

Many years ago, the development of optical sensors improved the original ground surface perspective of Sauer's landscape research paradigm by allowing a view from the sky. GPR, gradiometer and EMI methods represent advances in instrumental science that offer a view of otherwise invisible objects as they are distributed in the subsurface. The data that results from the use of these instruments are new to most historical geographers and geographic remote sensing scientists. This dissertation work presents these new data types in context, and explains what they are able to image that is of interest for historic

landscape studies. Further, the research herein contributes to GIScience and remote sensing by demonstrating many things: GIS based methods of exploring geophysical imagery for relevant content, the extraction of information from imagery, methods of presenting the image results through data fusion, and the creation of cartographic objects representing buried structural remnants. The ability of GPR to quantify soil moisture was also explored in order to expand the instrument's use beyond its normal mapping function. This demonstrates the potential utility of GPR to geomorphologists or other geographers that may not otherwise be interested in mapping the subsurface, but want to quantify the hydrologic characteristics of soil in a noninvasive way. Taken together, the articles represent a new direction in research that form a new branch of geographic remote sensing: a subfield that is concerned with the physical characteristics of the subsurface, and the objects, both cultural and natural, that exist there beyond the scope of normal human vision.

REFERENCES

Aspinall, A., C. F. Gaffney, and A. Schmidt. 2009. *Magnetometry for Archaeologists*. Lanham: AltaMira Press.

Avery, T. E., and G. L. Berlin. 2004. *Fundamentals of Remote Sensing and Airphoto Interpretation*. Upper Saddle River, N.J.; London: Prentice Hall.

Baroody, J.C. 1978. *An Archaeological Survey at the House in the Horseshoe State Historic Site Moore County, North Carolina*. Edited by Terry M Harper 1984. Site report, House in the Horseshoe folder. North Carolina Department of Natural and Cultural Resources, Historic Sites Section, Division of Archives and History. Raleigh, North Carolina.

Bevan, B. W. 1998. *Geophysical Exploration for Archaeology: an Introduction to Geophysical Exploration*. Midwest Archaeological Center Special Report No. 1. Lincoln, Nebraska: U.S. Department of the Interior, National Park Service.

Burke, E. P. 1850. *Reminiscences of Georgia*. Oberlin, OH: J.M. Fitch.

Caruthers, E. W. 1854. *Revolutionary Incidents and Sketches of Character, Chiefly in the "Old North State"*. Philadelphia: Hayes & Zell.

Clark, A. 2001. *Seeing beneath the Soil: Prospecting Methods in Archaeology*. London: Routledge

Clay, R. B. 2001. "Complementary Geophysical Survey Techniques: Why Two Ways Are Always Better Than One." *Southeastern Archaeology* 20 (1): 31–43.

Clay, R. B. 2006. "Conductivity Survey: A Survival Manual." In *Remote Sensing in Archaeology an Explicitly North American Perspective*, edited by Jay K. Johnson. University of Alabama Press.

Conyers, L. B. 2004. "Moisture and Soil Differences as Related to the Spatial Accuracy of GPR Amplitude Maps at Two Archaeological Test Sites." In *Tenth International Conference on Ground Penetrating Radar, 21-24 June, 2004, Delft, The Netherlands*.

Conyers, L. B. 2012. *Interpreting Ground-Penetrating Radar for Archaeology*. Left Coast Press, Inc

Conyers, L. B. 2013a. *Ground-Penetrating Radar for Archaeology*. Lanham: AltaMira Press, Rowman & Littlefield Publishers, Inc.

Conyers, L. B. 2013b. "Ground-Penetrating Radar Studies at the Hammer Test Bed Facility, Richland, Washington." *Journal of Northwest Anthropology* 47 (2): 153–66.

Conyers, L. B., and J. E. Lucius. 1996. "Velocity Analysis in Archaeological Ground-Penetrating Radar Studies." *Archaeological Prospection* 3 (1): 25–38. doi:10.1002/(sici)1099-0763(199603)3:13.0.co;2-u

Curry, S., R. Stine, L. Stine, J. Nave, R. Burt, and J. Turner. 2016. "Terrestrial Lidar and GPR Investigations into the Third Line of Battle at Guilford Courthouse National Military Park, Guilford County, North Carolina." In *Digital Methods and Remote Sensing in Archaeology: Archaeology in the Age of Sensing*, edited by Maurizio Forte and Stefano Campana, 53–69. Quantitative Methods in the Humanities and Social Sciences. Springer.

Dalan, R. A. 2006. "Magnetic Susceptibility." In *Remote Sensing in Archaeology an Explicitly North American Perspective*, edited by Jay K. Johnson, 161–203. University of Alabama Press.

Davis, J. L., and A. P. Annan. 1989. "Ground-Penetrating Radar for High-Resolution Mapping of Soil and Rock Stratigraphy." *Geophysical Prospecting* 37 (5): 531–51. doi:10.1111/j.1365-2478.1989.tb02221.x.

DiBiase, D. 1990. "Visualization in the Earth Sciences." *Earth and Mineral Sciences* 59 (2).

Dirksen, C. and S. Dasberg. 1993. "Improved Calibration of Time Domain Reflectometry Soil Water Content Measurements." *Soil Science Society of America Journal* 57 (3): 660–67

Doolittle, J. A., and E. C. Brevik. 2014. "The Use of Electromagnetic Induction Techniques in Soils Studies." *Geoderma* 223-225: 33–45. doi:10.1016/j.geoderma.2014.01.027.

Ernenwein, E.G. 2009. "Integration of Multidimensional Archaeogeophysical Data Using Supervised and Unsupervised Classification." *Near Surface Geophysics* 7 (662). doi:10.3997/1873-0604.2009004.

Florida Museum of Natural History 2017, March 23. *Historical Archaeology Digital Type Collections PORCELAIN, BONE CHINA - TYPE INDEX*. Retrieved from http://www.flmnh.ufl.edu/histarch/gallery_types/type_index_display.asp?type_name=PORCELAIN,%20BONE%20CHINA.

Geonics Limited. 2015. "Geonics EM38-MK2 Ground Conductivity Meter." Instrument Manual. Geonics Limited. Mississigua, Ontario, Canada

Giardino, M. J., and B. S. Haley. 2006. "Airborne Remote Sensing and Geospatial Analysis." In *Remote Sensing in Archaeology an Explicitly North American Perspective,* edited by J. K. Johnson, 47–77. University of Alabama Press.

Grisso, R., M. Alley, D. Holshouser, and W. Thomason. 2009. "Precision Farming Tools: Soil Electrical Conductivity." *Virginia Cooperative Extension Publications and Educational Resources*. https://pubs.ext.vt.edu/442/442-508/442-508.html

Hargrave, M. L. 2006. "Ground Truthing the Results of Geophysical Surveys." In *Remote Sensing in Archaeology an Explicitly North American Perspective,* edited by Jay K. Johnson, 269–304. University of Alabama Press.

Harper, T. M. 1984. *Archaeological Clearance for the Electric Lines to the Loom House, House in the Horseshoe State Historic Site, Moore County, North Carolina*. Site report, House in the Horseshoe folder. North Carolina Department of Natural and Cultural Resources, Historic Sites Section, Division of Archives and History. Raleigh, North Carolina.

HeritageQuest 2017, March 23. *1810 United States Federal Census*. Retrieved from https://www-ancestryheritagequest-com.libproxy.uncg.edu/HQA.

Evett, S. R., and C. Hignett. 2008. "Direct and Surrogate Measures of Soil Water Content." In *Field Estimation of Soil Water Content: a Practical Guide to Methods, Instrumentation and Sensor Technology*, edited by S. R. Evett, L. K. Heng, P. Moutonnet, and M. L. Nguyen, 1–22. IAEA-TCS-30. Vienna: International Atomic Energy Agency.

H in H Infrared Aerials. 1987. Color Slide Numbers 1-20. Photographer unknown. House in the Horseshoe folder. North Carolina Historic Sites Division of Archives, Raleigh North Carolina.

Horsley, T., A Wright, and C. Barrier. 2014. "Prospecting for New Questions: Integrating Geophysics to Define Anthropological Research Objectives and Inform Excavation Strategies at Monumental Sites." *Archaeological Prospection* 21 (1): 75–86. doi:10.1002/arp.1476.

Huisman, J. A., S. S. Hubbard, J. D. Redman, and A. P. Annan. 2003. "Measuring Soil Water Content with Ground Penetrating Radar." *Vadose Zone Journal* 2 (4): 476. doi:10.2136/vzj2003.4760.

Infrared Aerial House in the Horseshoe. 1978. Color slide numbers 15-20, 31MR20. Virgil Smithers and William Long. House in the Horseshoe folder. Historic Sites Division of Archives. Raleigh, North Carolina.

Jacobsen, O.H, and P. Schjønning. 1995. "Comparison of TDR Calibration Functions for Soil Water Determination.". In *Proceedings of the Symposium: Time-Domain Reflectometry Applications in Soil Science, Research Centre Foulum, September 16, 1994*, edited by L.W. Petersen and O.H. Jacobsen, 9–23. SP-Report 25-33. Lyngby: Danish Institute of Plant and Soil Science.

Jadoon, K.Z., S. Lambot, B. Scharnagl, J. Van Der Kruk, E. Slob, and H. Vereecken. 2010. "Quantifying Field-Scale Surface Soil Water Content from Proximal GPR Signal Inversion in the Time Domain." *NSG Near Surface Geophysics* 8 (1750). doi:10.3997/1873-0604.2010036.

Jensen, J. R. 2016. *Introductory Digital Image Processing: a Remote Sensing Perspective*. Glenview, IL: Pearson Education, Inc.

Johnson, J. K. 2006. "Introduction.". In *Remote Sensing in Archaeology an Explicitly North American Perspective*, edited by Jay K. Johnson. Tuscaloosa, Ala.: Univ. of Alabama Press.

Jonard, F., L. Weihermuller, K. Z. Jadoon, M. Schwank, H. Vereecken, and S. Lambot. 2011. "Mapping Field-Scale Soil Moisture with L-Band Radiometer and Ground-Penetrating Radar over Bare Soil." *IEEE Transactions on Geoscience and Remote Sensing* 49 (8): 2863–75. doi:10.1109/tgrs.2011.2114890.

Kvamme, K. L. 2006. "Integrating Multidimensional Geophysical Data." *Archaeological Prospection* 13 (1): 57–72. doi:10.1002/arp.268.

Kvamme, K. L. 2008. "Remote Sensing: Archaeological Reasoning through Physical Principles and Pattern Recognition." In *Archaeological Concepts for the Study of the Cultural Past*, edited by A. P. Sullivan, 65–84. Salt Lake City: University of Utah Press.

Lunt, I.A., S.S. Hubbard, and Y. Rubin. 2005. "Soil Moisture Content Estimation Using Ground-Penetrating Radar Reflection Data." *Journal of Hydrology* 307 (1-4): 254–69. doi:10.1016/j.jhydrol.2004.10.014.

MacEachren, A. M. 1994. *SOME Truth with Maps: a Primer on Symbolization and Design*. Washington, D.C.: Association of American Geographers.

Miller, G. L., P. Samford, E. Shlasko, and A. Madsen. 2000. "Telling Time for Archaeologists," *Northeast Historical Archaeology* 29: (1:2)

Minet, J., E. Laloy, S. Lambot, and M. Vanclooster. 2011. "Effect of High-Resolution Spatial Soil Moisture Variability on Simulated Runoff Response Using a Distributed Hydrologic Model." *Hydrology and Earth System Sciences* 15 (4): 1323–38. doi:10.5194/hess-15-1323-2011.

Moore County North Carolina GIS 2017, March 23. *Moore Maps*. Digital Airphoto Years: 1939, 1950, 1966, 1983, 1988. Retrieved from http://mooregisweb.moorecountync.gov/HistoricalImagery/MooreMaps.html

Munsell Soil-Color Charts: with Genuine Munsell Color Chips. 2013. Grand Rapids, MI: Munsell Color.

Nelson, L. H. 1968. "NAIL CHRONOLOGY: as an aid to dating old buildings". *History News*. 23 (11): 203-214.

NC Historic Sites 2017. *House in the Horseshoe*. Accessed March 23. http://www.nchistoricsites.org/horsesho/horsesho.htm

National Oceanic and Atmospheric Administration (NOAA) 2017, March 23. *National Geodetic Survey OPUS: Online Positioning User Service.* Retrieved from https://www.ngs.noaa.gov/OPUS/

Ogden, J., S. Keay, G. Earl, K. Strutt, and S. Kay. 2010. "Geophysical Prospection at Portus: An Evaluation of an Integrated Approach to the Interpretation of Subsurface Archaeological Features." In *Making History Interactive. Computer Applications and Quantitative Methods in Archaeology: Proceedings of the 37th International Conference, Williamsburg, Virginia, United States of America, March 22-26 (BAR International Series S2079)*, edited by B. Frischer, J. Webb Crawford, and D. Koller, 273–84. Oxford: Archaeopress.

Olmert, M. 2009. *Kitchens, Smokehouses, and Privies: Outbuildings and the Architecture of Daily Life in the Eighteenth-Century Mid-Atlantic*. Ithaca: Cornell University Press.

Phillips, L. 2014. Geologist and Director, Office of Undergraduate Research, The University of North Carolina at Greensboro. Personal communication: conversation.

Patch, S. M. 2016. "Geophysical Survey of Large Mississippian Villages in the South Appalachian Region." North Carolina Archaeology 65: 140–52.

Rogers, M., J. F. Leon, K. D. Fisher, S. W. Manning, and D. Sewell. 2012. "Comparing Similar Ground-Penetrating Radar Surveys under Different Moisture Conditions at Kalavasos-Ayios Dhimitrios, Cyprus." *Archaeological Prospection* 19 (4): 297–305. doi:10.1002/arp.1435.

Scarborough, Q. 1984. "Connecticut Influence on North Carolina Stoneware: The Webster School of Potters." *Journal of Early Southern Decorative Arts* 10 (1): 14–74.

Słowik, M. 2012. "Influence of Measurement Conditions on Depth Range and Resolution of GPR Images: The Example of Lowland Valley Alluvial Fill (the Obra River, Poland)." *Journal of Applied Geophysics* 85: 1–14. doi:10.1016/j.jappgeo.2012.06.007.

South, S. A. 2002. *Method and Theory in Historical Archeology*. Clinton Corners, NY: Percheron Press.

Sternberg, B. K., and J. W. Mcgill. 1995. "Archaeology Studies in Southern Arizona Using Ground Penetrating Radar." *Journal of Applied Geophysics* 33 (1-3): 209–25. doi:10.1016/0926-9851(95)90042-x.

Stine, L. F., R. S. Stine, J. R. Turner, E. S. Nelson, and D. Shumate. 2013. "Archaeological and Geophysical Research at Guilford Courthouse National Military Park (GUCO) (31GF44**) Greensboro, North Carolina." Report: SEAC-02347. National Park Service

Stine, L. F., and R. S. Stine. 2014. "Public Archaeology in the National Park Service: A Brief Overview and Case Study." American Anthropologist 116 (4): 843–49. doi:10.1111/aman.12156.

Tarantino, A, E. Romero, and Y. J. Cui. 2009. "Laboratory and Field Testing of Unsaturated Soils." *Laboratory and Field Testing of Unsaturated Soils*. http://public.eblib.com/choice/publicfullrecord.aspx?p=417119.

Thompson, V. D., C. B. Depratter, and A. D. Roberts-Thompson. 2016. "A Preliminary Exploration of Santa Elena's Sixteenth Century Colonial Landscape through Shallow Geophysics." *Journal of Archaeological Science: Reports* 9: 178–90. doi:10.1016/j.jasrep.2016.06.055.

Topp, G. C., J. L. Davis, and A. P. Annan. 1980. "Electromagnetic Determination of Soil Water Content: Measurements in Coaxial Transmission Lines." *Water Resources Research Water Resour. Res.* 16 (3): 574–82. doi:10.1029/wr016i003p00574.

Turner, J. R. "Using Geophysical Remote Sensing to Image the Cultural Landscape: The Effects of Soil Moisture upon Ground Penetrating Radar Surveys at House in the Horseshoe, Moore County North Carolina." Paper presented at the Association of American Geographers (AAG) Annual Conference, Chicago, IL. April 21-25, 2015.

Turner, J. R, and A. D. Lukas. 2016. "An Overview of Geophysical Surveys and Ground Truthing Excavations at House in the Horseshoe (31MR20), Moore County, North Carolina." *North Carolina Archaeology* 65: 108–16.

United States Department of Agriculture (USDA) Natural Resources Conservation Service (NRCS) 2017, March 23. *Web Soil Survey.* Retrieved from http://websoilsurvey.nrcs.usda.gov/

Vellidis, G., M. C. Smith, D. L. Thomas, and L. E. Asmussen. 1990. "Detecting Wetting Front Movement in a Sandy Soil with Ground-Penetrating Radar." *Transactions of the ASAE* 33 (6): 1867–74. doi:10.13031/2013.31551.

Vlach, J. M. 1993. *Back of the Big House: the Architecture of Plantation Slavery*. Chapel Hill: University of North Carolina Press.

Watters, M. 2012. "Geophysical and Laser Scan Surveys at the Longfellow House – Washington's Headquarters National Historic Site: Archaeology Survey Technology, Data Integration, and Applications Workshop, August 15-20th, 2011". Report. National Center for Preservation Technology and Training. https://www.ncptt.nps.gov/blog/archaeological-survey-technologies-data-integration-and-applications-workshop-and-seminar-longfellow-house-washingtons-national-headquarters-national-historic-site-cambridge-2012-05/

Weihermüller, L., J.A. Huisman, S. Lambot, M. Herbst, and H. Vereecken. 2007. "Mapping the Spatial Variation of Soil Water Content at the Field Scale with Different Ground Penetrating Radar Techniques." *Journal of Hydrology* 340 (3-4): 205–16. doi:10.1016/j.jhydrol.2007.04.013.

Western, A. W., and R. B. Grayson. 1998. "The Tarrawarra Data Set: Soil Moisture Patterns, Soil Characteristics, and Hydrological Flux Measurements." *Water Resources Research* 34 (10): 2765–68. doi:10.1029/98wr01833.

Willcox, G. W. 1999. *A History of the House in the Horseshoe: Her People and Her Deep River Neighbors*. Wilmington, NC: Historical Research Services.

Wyatt, P. W. 1995. *Soil Survey of Moore County, North Carolina*. Washington, D.C.: Natural Resources Conservation Service.